PREPARATION OF CROSSLINKED POLYPROPYLENE FUMARATE PARTICLES LOADED WITH MAGNETIC NANOPARTICLES AND PACLITAXEL VIA PHOTO INITIATED MINIEMULSION POLYMERIZATION

by

Gizem Karakaş

Submitted to Graduate School of Natural and Applied Sciences

in Partial Fulfillment of the Requirements

for the Degree of Master of Science in

Chemical Engineering

Yeditepe University

2016

PREPARATION OF CROSSLINKED POLYPROPYLENE FUMARATE PARTICLES
LOADED WITH MAGNETIC NANOPARTICLES AND PACLITAXEL VIA PHOTO
INITIATED MINIEMULSION POLYMERIZATION

APPROVED BY:

Prof. Dr. Seyda Malta
(Thesis Supervisor)

Assist. Prof. Dr. Erde Can
(Thesis Co-Advisor)

Prof. Dr. Gamze Köse

Prof. Dr. Nurcan Baç

Assoc. Prof. Ali Demir Sezer

DATE OF APPROVAL: ... / ... / 2016

ACKNOWLEDGEMENTS

I owe thanks to many people who helped in the accomplishment of this project. First and foremost, I would like to thank my supervisor, Prof. Dr. Seyda Malta for all of her help and support throughout this whole process and for her patience, motivation and immense knowledge. It is a pleasure working with her and I am honored to have been able to spend time with her. I also appreciate my co-advisor, Assist. Prof Dr. Erde Can for her significant comments and support throughout this work.

I would like to thank Assist. Dr. Cem Levent Altan, because he always helps me and his contributions make me better equipped to overcome the problems. In addition, I am heartily thankful to Görkem Cemali for her friendship, patience, sincere support during the study. And I would like to thank Elçin Yenigül for her kind helps. Special thanks to my dear friend, Berna Gürten for her endless support in every possible way. I am thankful for all the fun we have had in the last six years. It would not have been possible for me to be successful without her friendship.

I would like to thank Sera Erkeçoğlu, Ece Atlan, Şelale Gülyuva, Hande Duru, İlayda Acaroğlu for their kind helps and support.

Sincere thanks to my family for their love, patience, understanding and psychological support throughout this study. Without their encouragements this dissertation would not be possible. They always believe in me and support me in every situation.

ABSTRACT

PREPARATION OF CROSSLINKED POLYPROPYLENE FUMARATE PARTICLES LOADED WITH MAGNETIC NANOPARTICLES AND PACLITAXEL VIA PHOTO INITIATED MINIEMULSION POLYMERIZATION

Cancer is the deadliest disease of human beings in worldwide. For cancer treatment chemotherapy is highly preferred but most chemotherapeutic agents are non-specific. The cytotoxic drug attacks healthy cells in addition to the target tumor cells. Magnetic drug delivery with using drug carriers is a very efficient method to target a localized disease site of the body. Biodegradable nanoparticles which are produced by biodegradable polymers can be used as carriers for drug.

The aim of this project is to develop a new drug delivery system. Biocompatible polymer namely Polypropylene fumarate (PPF) is used to produce biodegradable nanoparticles to be used as drug carriers and magnetic nanoparticles are added to target a localized disease site within the body. In this project, firstly magnetic nanoparticles are incorporated in PPF which is crosslinked with a N-vinyl pyrrolidone (NVP) using photo initiated miniemulsion polymerization method. FTIR spectroscopy was used to confirm the crosslinking of poly propylene fumarate (PPF) with N-vinyl pyrrolidone (NVP) by photo initiated mini emulsion polymerization. Then the morphology and size of crosslinked polymer particles with and without magnetite were determined by SEM. FTIR confirmed the crosslinking and swelling tests were used to determine the percentage of crosslinking.

Crosslinked polymer nanoparticles with embedded magnetic nanoparticles were loaded with Paclitaxel (anticancer drug). The amount of drug release from crosslinked polymer nanoparticles with and without magnetite was determined by HPLC and these carriers are found to release all the encapsulated drug in less than one month. The degradation studies are carried out by pH and weight measurements. The release of drug is found to be complete before the polymer nanoparticles are degraded suggesting the drug release to be diffusion controlled.

ÖZET

FOTOBAŞLATICI MİNİEMÜLSİYON POLİMERİZASYONU İLE MANYETİK NANOPARÇACIKLI VE PAKLİTAKSEL İLE YÜKLÜ ÇAPRAZ BAĞLI POLİPROPİLEN FUMARAT'IN HAZIRLANMASI

Kanser ölümcül bir hastalıktır. Kanser tedavisinde kemoterapi sıklıkla kullanılır ama çoğu kemoterapötikler nonspesifiktir. Zehirli ilaçlar tümörlü hücrelerin yanında sağlıklı hücreleri de etkiler. İlacı vücudun hastalıklı bölgesine hedeflemek için, ilaç taşıyıcılar ile manyetik ilaç taşınım etkili bir yöntemdir. İlaç taşıyıcılar için biyolojik olarak parçalanabilir polimeler ile üretilen biyolojik olarak parçalanabilir nanoparçacıklar kullanılabilir.

Bu projenin amacı yeni bir ilaç taşıyıcı sistemi geliştirmektir. İlaç taşıyıcılar olarak kullanılan biyolojik olarak parçalanabilen nanoparçacıklar üretmek için biyouyumlu polimer, yani polipropilen fumarat (PPF) kullanılır ve vücudun hastalıklı bölgesine hedeflenmesi için manyetik nanoparçacıklar eklenilir. Bu projede, öncelikle manyetik nanoparçacıklar vinipirolidon (VP) ile çapraz bağlanan PPF ile fotobaşlatıcı miniemülsiyon tekniği kullanarak birleştirilir. Polipropilen fumarat (PPF) ın vinipirolidon (VP) ile fotobaşlatıcı miniemülsiyon tekniğini kullanarak çapraz bağlanmasını doğrulamak için FTIR spektroskopi kullanıldı. Daha sonra manyetik nanoparacıklı ve manyetik nanoparçacıksız çapraz bağlı polimer parçacıkların morfolojisi ve büyüklüğü SEM ile belirlendi. FTIR çapraz bağlamayı doğruladı ve çapraz bağlanma oranını belirlemek için şişme testleri kullanıldı.

Çapraz bağlı ve manyetik nanopartiküller ile gömülü polimer nanoparçacıklar Paklitaksel (anti-kanser ilacı) ile yüklenildi. Çapraz bağlı manyetik nanoparacıklı ve manyetik nanoparçacıksız polimer nanopartiküllerden ilaç salınım miktarı HPLC ile belirlendi ve bu taşıyıcılar kapsüllenmiş ilacın bir aydan daha kısa bir sürede salınmasını sağlar. Degradasyon çalışmaları pH ve ağırlık ölçümleri yürütülmektedir. İlaç salınımı polimer nanoparçacıkların degradasyondan önce kontrollü difüzyon ile tamamen gerçekleştiği bulundu.

TABLE OF CONTENTS

LIST OF FIGURES

LIST OF TABLES

LIST OF SYMBOLS / ABBREVIATIONS

ATR	Attenuated Total Reflectance
BAPO	Bisacylphosphine oxides
BPO	Benzoyl peroxide
DCM	Dichloromethane
DMSO	Dimethyl sulfoxide
ESD	Emulsification/solvent diffusion method
FTIR	Fourier transform infrared spectroscopy
HPLC	High performance liquid chromatography
MNPs	Magnetic nanoparticles
NP	Nanoparticle
PPF	Polypropylene fumarate
PTX	Paclitaxel
PBS	Phosphate-buffered saline
rpm	Rounds per minute
SDS	Sodium dodecyl sulfate
SEM	Scanning electron microscope
UV	Ultraviolet
VP	Vinylpyrrolidone
Wi	Initial Weight
Wf	Final Weight

1. INTRODUCTION

Cancer is a disease which is one of the most common cause of death in human worldwide [1]. Surgery, radiation and chemotherapy are the main methods to treatment of cancer. However, the high toxicity, the low water solubility, the poor oral bioavailability and non-specific distribution of an anticancer drug to both normal and cancer cells are the main shortcomings of the cancer therapies [2, 3]. In recent years, new therapeutic methods have been developed to increase the effectiveness of anti cancer drugs.

Magnetic particles encapsulating drugs with biocompatible polymers are widely used in the field of magnetic drug targeting. Magnetically controlled drug targeting improves treatment by increasing the amount of drug to tumour cells.

Biodegradable nanoparticles which are produced by biodegradable polymers are highly used for drug delivery systems due to their advantages such as sustained drug release, reducing the amount of drug and minimizing the undesirable side effects.

The aim of this project is to develop a new drug delivery system, using a biocompatible polymer, namely Polypropylene fumarate (PPF) with embedded magnetic nanoparticles. PPF can be crosslinked through carbon carbon double bonds, degraded into non toxic products and its degradability can be controlled for drug release. In this project, firstly PPF which is crosslinked with vinylpyrrolidone (VP) is incorporated with magnetic nanoparticles using photo initiated miniemulsion polymerization technique to obtain magnetic polymer nanoparticles. Method of preparation of these nanoparticles are optimized investigating morphologies using SEM. FTIR is used to show that crosslinking between PPF and VP is successful. Swelling tests are done to determine the percentage of crosslinking. Then crosslinked polymer nanoparticles with embedded magnetic nanoparticles were loaded with Paclitaxel (anti cancer drug) and the drug release profiles were investigated for one month until all the drug is released using HPLC. Degradation of these polymer beads with and without MNP's were investigated following pH and weight change over a period of time.

In this report, general information about nanocarriers systems for drug release control and related topics and drug targeting are given in theoretical background section. Chemicals that are

used in the project and techniques are presented in Chapter 3, experimental procedures are given in Chapter 4. The results of the measurements and discussions of the results can be found in Chapter 5. Finally, the conclusion of the experimental work and discussion along with future work are summarized in Chapter 6.

2. THEORETICAL BACKGROUND

2.1. DRUG DELIVERY SYSTEMS

Drug delivery systems can include the conservation of drug levels within a desired range, optimal use of the drug, the need for fewer administrations and increased patient compliance. The ideal drug delivery system should be biocompatible, mechanically strong, suitable for the patient, efficient of achieving high drug loading, reduction in toxicity, protected from any accidental release, simple to administer and remove, and easy to fabricate and sterilize [4]. In drug delivery systems, delivery of drugs in controlled rates for long period of time as known as controlled drug release, delivery of drugs to a specific site within a system is known as targeted drug delivery. Controlled and targeted drug release enhance drug efficacy and safety, and ease target specificity [5]. To achieve controlled and targeted drug release, various nanocarriers which have unique morphologies, compositions, and surface properties have been developed [6]. Advantages of drug nanocarriers include the small sizes compatible with intravenous injection and the large surface area per volume ratio to modification for targeted delivery. Nanocarriers provide spatiotemporal control of drug release to reduce toxicity, enhance therapeutic efficacy of a drug and improve patient's adherence to regimen by reducing the dose [7].

2.2. NANOCARRIERS SYSTEMS FOR DRUG RELEASE CONTROL

In general, several mechanism contributes to the controlled drug release from nanocarriers systems. Nanocarriers are modified in various ways to achieve further control over the drug release kinetics. These nanocarriers are described in the following section [8].

2.2.1. Liposomes

Liposomes have widely been used as controlled drug delivery systems since the 1960s [9]. They are small vesicles with lipid bilayers composed of amphiphilic phospholipids. Liposomes are used due to their size, biocompatibility and both hydrophilic as well as hydrophobic properties [10]. Liposomes can be classify by size and number of phospholipid bilayers. Types of liposomes are small unilamellar vesicles (SUVs; single lipid layer 25 to 50 nm in diameter), large unilamellar vesicles (LUVs), and multilamellar vesicles (MLVs with several lipid layers) [11].

Liposomes have been developed for the delivery of anticancer, vaccine, anti-HIV, toxoids and gene drugs [11]. There are generally three requirements of the liposomes as nanocarriers for effective passive targeting or sustained drug action [12]. Firstly, their blood life times have to be substantial enough for passive targeting. Secondly, The sizes must be smaller enough to extravasate and reach solid tumors and finally, the release duration of the drug from the circulating nanocarriers have to be longer than the half-life; otherwise free drug will be released and cleared quickly from the bloodstream [13]. Most studies applied surface modification approaches to liposomes to prolong their blood circulation time. Liposomes can be enhanced by attaching PEG (Poly(ethylene glycol)), dextran, poly-N vinylpyrrolidones and polyvinyl alcohol to the liposome surface [14] . The first successful liposomal nanocarrier for drug delivery systems was Doxil that used nano-sized liposomes (average size 90 nm). PEG molecules are grafted on to the surface of the liposomes. The chemotherapeutic drug, Doxorubicin, was loaded into the aqueous core of the liposome at a high concentration. This combination of properties which PEGylation, active loaded drug and small size provided some selectivity of action towards tumor, so reducing side effects of the drug [15]. Since Doxil, the combination of PEGylated liposome and doxorubincin (DOX), was accepted by the US Food and Drug Administration (FDA) in 1995, several other liposomal anticancer drugs such as DaunoXome and Myocet have been developed to reduce toxicity in comparison to free doxorubicin and approved for clinical uses [16].

However, in addition to their low drug loading efficiency, they have some other limitations, such as poor stability and problems with industrial reproducibility, difficulties in sterilization, the limited control of drug release and the oxidation of phospholipids [17-19]. Due to this problems, liposomes do not have enough market share [14].
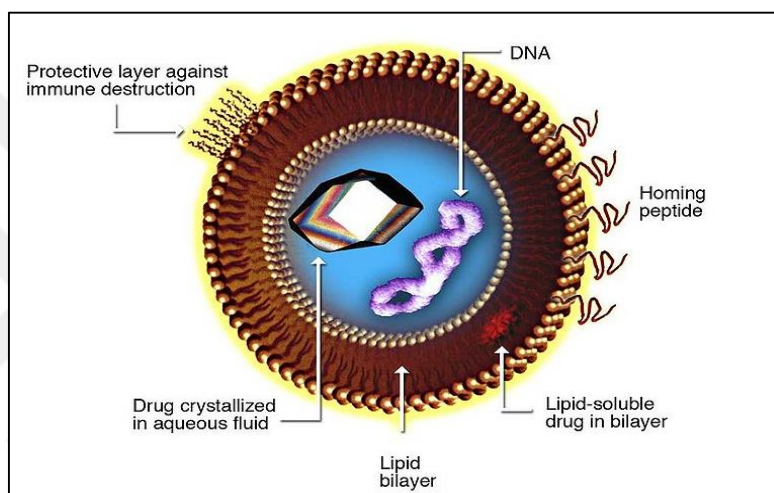
Figure 2.1. Liposome for drug delivery [20]

2.2.2. Polymeric Nanocarriers

Polymeric nanocarriers which are drug nanocarriers based on polymer. They have different possible structures such as polymeric micelles (amphiphilic core/shell), dendrimers (hyperbranched macromolecules), or polymeric nanoparticles (capsules/particles). Despite the various advantages and the developmental work on liposomes, they have shown a poor storage stability and a limited control of drug release. In addition, polymeric nanocarries offer their advantages over these liposomal limitations, because they are more stable in vivo, have higher drug circulation times and loading capacities, and show the ability to produce more controlled and targeted drug release profiles, both during prolonged periods of time and at different predetermined rates [21, 22].

2.2.2.1. Polymeric micelles

Polymeric micelles are promising vehicles for the delivery of poorly soluble toxic drugs that allow a controlled drug release [23]. They are formed by spontaneous self assembly of amphiphilic block copolymers that make core shell structure. Polymeric micelles are used as drug carriers based on simple preparation method, the ability to solubilize hydrophobic cytotoxic drugs and narrow size distribution with a diameter up to 100 nm [24]. They contain hydrophobic segments which form inner core looding poorly water soluble anticancer drugs and hydrophilic segments forming an outer shell in an aqueous solvent. Polymeric micelles have a hydrophobic shell and hydrophilic core in organic solvents and reverse polymeric micelles are formed. Reversed polymric micelles are suitable for the encapsulation of hydrophilic drugs [25]. Prolonged circulation and targeted delivery of polymeric micelles are dependent on the designing of environment responsive polymeric micelles such as pH, temperature, light [26].

2.2.2.2. Dendrimers

Dendrimers are highly branched three-dimensional macromolecules and they are synthesized from a central core. The well-defined structure, monodisperse size, compact globular shape, biodegradability and biocompability, high drug loading capacity and controllable surface functionalities of dendrimers make them excellent drug carriers [27-30]. Dendrimers have both hydrophobic core and hydrophilic surface. Drug molecules may be covalently conjugated onto surface groups or entrapped inside the core with hydrophobic linkage, hydrogen bonding or electrostatic interactions [31] [32]. Drug release from dendrimers depends on the type of interactions between a drug and a dendrimer. In early studies, dendrimers focused on encapsulating drugs. However, it was difficult for controlling the release of drugs associated with dendrimers. Polymer and dendrimer chemistry developments have provided a new molecule. It is called as dendronized polymers [33]. Their behavior provides drug delivery advantages. Dendrimers are created with polymers such as polypeptide, polyesters, carbohydrates, PEG, polyamine. Among different dendritic polymers, polyamidoamine (PAMAM) is most widely used to make dendrimer carriers due to the high density of function groups on the surface [34].

2.2.2.3. *Polymeric nanoparticles*

Over the past few decades, there has been considerable interest in developing biodegradable nanoparticles (NPs) as effective drug delivery devices [35]. The main goal in designing such devices is the controlled release of therapeutic active agents to the therapeutic moiety to optimal rate and dose [32]. Polymeric nanoparticles are the most effective carriers for controlled and prolonged anticancer targeted drug delivery. They refer to spherical nano sized biodegradable polymeric particles. Biodegradable nanoparticles are classified as nanosphere and nanocapsule. The cytotoxic drug molecules are encapsulated or physically entrapped within a polymeric matrix systems (nanospheres) or confined to a cavity surrounded by a polymer membrane (nanocapsules) [23]. These biodegradable polymeric nanoparticle-drug formulation are used to produce a hydrophobic interaction between particle and drug by increasing its solubility for insoluble drugs [36]. In addition, these carriers have many advantages in the protection properties such as reducing risk of toxicity with interaction with healthy cells, enhancement of absorption by cancer cells and long retention time. Apart from this, according to other nanoparticle systems (e.g liposomes, polymeric micelles) they show better therapeutic impact, better stability, higher drug loading, more controlled drug release with diffusion from the polymer matrix or by degradation of the particles [37]. Biodegradable polymeric nanoparticle-drug formulation depends on the choice of suitable polymeric system for having higher drug encapsulation, increasing retention time and improvement of bioavailability [38]. Polymer nanoparticles are prepared from natural or synthetic polymers that are biodegradable, biocompatible and approved by the U.S. Food and Drug Administration (FDA) for human administration. Synthetic polymers, such as polylactic acid (PLA), polyethylene glycol (PEG), poly(D,L-lactide-co-glycolic) acid (PLGA), polyaspartate (PAA) are usually used because they are easily manufactured and after use they degrade, and perform a sustained release of the active compounds over the time [39]. Among the families of synthetic polymers, the polyesters have been attractive for these applications that include drug delivery systems because of their ease of degradation by hydrolysis of ester linkage, degradation products are removed from the body with metabolic pathways [40-42]. For example, poly(propylene fumarate) (PPF) degrade by hydrolysis to individual monomers (fumaric acid and propylene glycol) [42]. However, natural

polymers, such as dextran, alginate, chitosan, albumin, gelatin, are less used because, in spite of being non-toxic, abundant in nature, inexpensive, and easily biodegraded, they present relatively fast release profiles, and they are not naturally pure and homogeneous, requiring a purification step before their use. On the other hand, natural polymers are recently gaining interest with usable options, since the production of nanocarriers with natural polymers is performed by mild methods such as ionic gelation, complex complexation, coacervation [43].
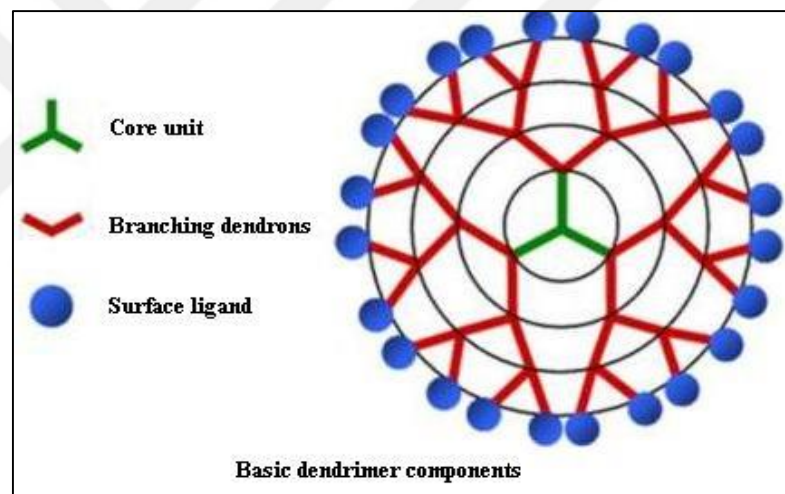
Figure 2.2. Basic dendrimer components [44]
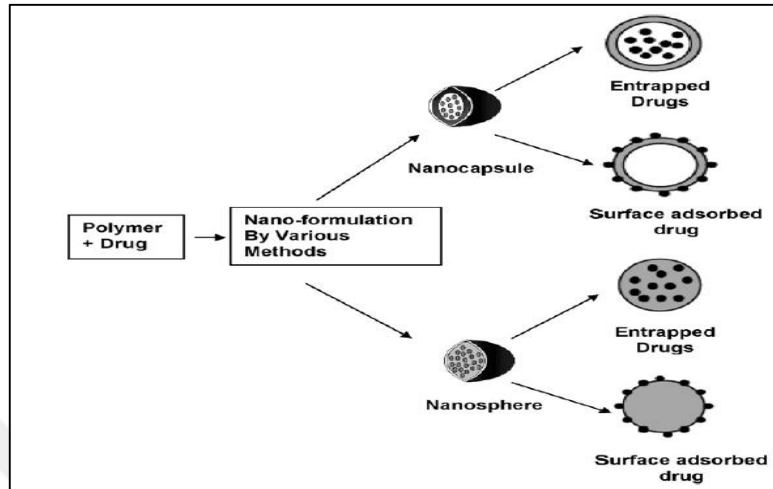
Figure 2.3. Type of biodegradable nanoparticles [45]

Methods of preparation of polimeric nanoparticles can be divided into two major classes. The first class deals with polymerization of monomers, and the secand class involves the dispersion of preformed polymers. Various methods can be used to prepare polymer nanoparticles, such as salting-out, dialysis, solvent evaporation, supercritical fluid technology, mini-emulsion, micro-emulsion, surfactant-free emulsion, and interfacial polymerization [46]. According to size of particle, size distribution and area of application, one of these methods are used [47].

Dispersion of preformed polymers: Several methods have been used to produce biodegradable polymeric nanoparticles by dispersing preformed polymers [47].

Solvent evaporation method : Solvent evaporation which was the first method developed in order to synthesize polymer nanoparticles. In this method, polymer (natural, synthetic or semi-synthetic) is dissolved in an organic solvents and emulsions are formulated. Chloroform, dichloromethane and ethyl acetate are widely used as organic solvents [48]. The emulsion is converted into a nanoparticle suspension on evaporation of the solvent for the polymer that is allowed to diffuse through the continuous phase of the emulsion [49, 50]. In this method, two

main types are used for the formation of emulsion; the preparation of single emulsions (oil-in-water) and double emulsions (water-in-oil/in-water). Ultrasonication or high speed homogenization is used in solvent evaporation. The solvent is subsequently evaporated by continuous stirring at room temperature or increasing the temperature under pressure [42]. Generally, polymer dissolved in an organic solvent constitutes the oil phase, while, the water phase with the stabilizer (surfactant) is present in an aqueous phase. This method is basically applied to liposoluble drugs. But, high energy requirements in homogenization is the main problem for a large scale pilot production [48].
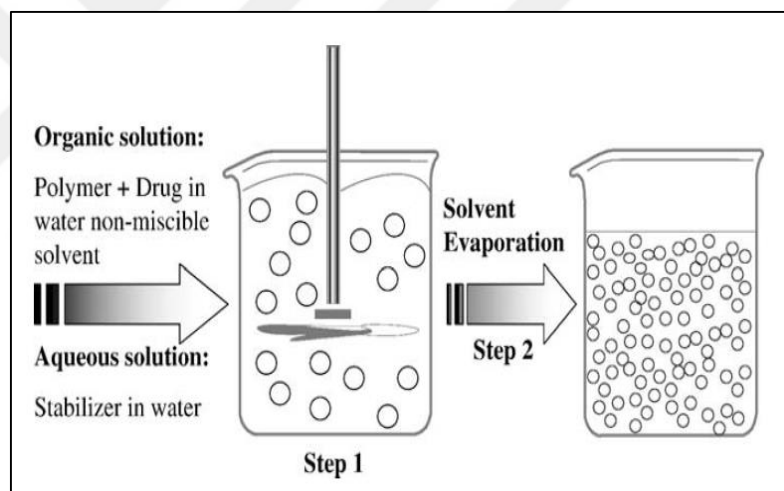
Figure 2.4. Emulsification-evaporation technique [51]

Emulsification/solvent diffusion method : Emulsification/solvent diffusion method is the modified version based on the solvent evaporation technique. The encapsulating polymer is dissolved in a partially water soluble solvent like propylene carbonate to prepare the emulsion. Then, the emulsion is prepared with water saturated with the polymer solvent to form the oil phase and with an oil phase saturated with water composing the continuous phase. The polymer-water saturated solvent phase is obtained with mixing the two liquids in equal volume. To produce the formation of nanoparticles and the precipitation of the polymer it is necessary to induce the diffusion of the solvent of the dispersed phase using dilution with an extensive

amount of pure water when the organic solvent is partly miscible with water or using another organic solvent for the opposite case. Then, solvent phase which is polymer-water saturated is emulsified in an aqueous solution with stabilizer that leads to solvent diffusion for the external phase and the formation of nanoparticles according to the oil to polymer ratio. Ultimately, solvent is eliminated using filtration or evaporation [52].
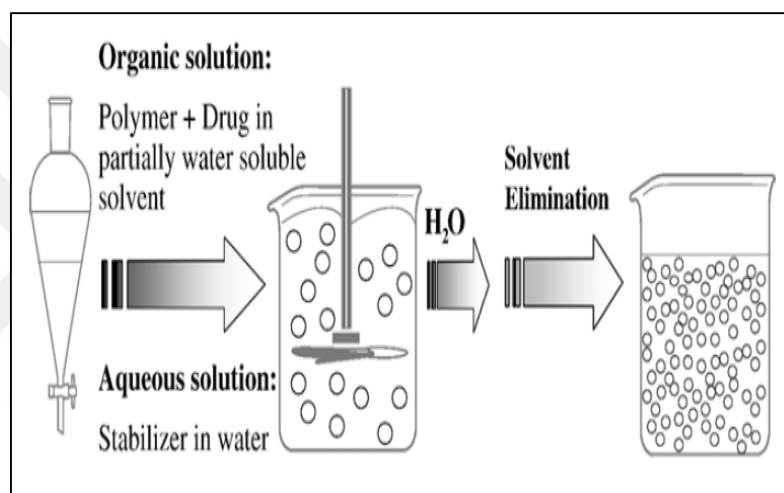
Figure 2.5. Schematic illustration of the ESD method [51]

Salting-out method : Salting out method is based on the separation of a water miscible solvent from aqueous solution with a salting out effect. This is a modified version of the emulsification/solvent diffusion. The emulsion is formulated with a polymer solvent containing a drug which is miscible with water such as acetone and emulsification of the polymer solution in the aqueous phase is achieved by containing the high concentration of salt (electrolytes) or sucrose (non-electrolyte) in the aqueous phase [52]. Calcium chloride, magnesium chloride and magnesium acetate are used suitable electrolytes [53]. When these components dissolve in the water, the miscibility properties of water with other solvents are modified. The oil/water

emulsion is diluted with a large excess of water to enhance the diffusion of acetone into the aqueous phase thus the precipitation of the polymer dissolved

in the droplets of the emulsion is formed [47]. This method provides the high drug encapsulation efficiency. The selection of the salting-out agent is important for the encapsulation efficiency of the drug [48].
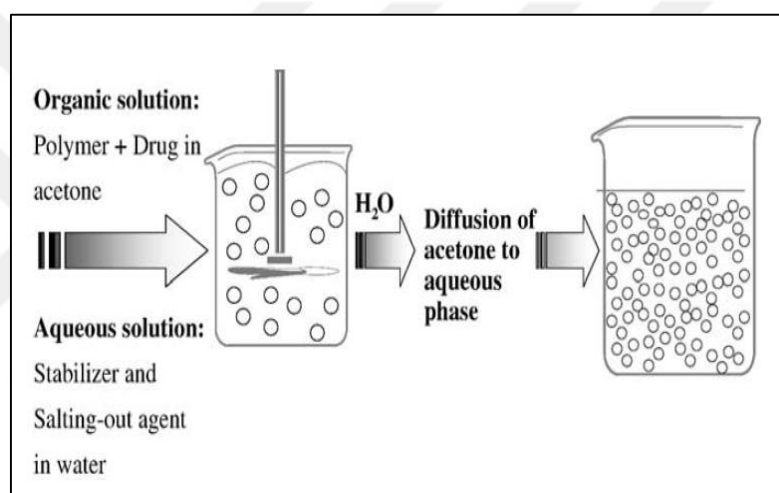
Figure 2.6. Schematic of the salting-out technique [51]

Polymerization of Monomers: In order to obtain the desired properties for a particular application, suitable polymer nanoparticles can be designed during the polymerization of monomers. For the production of polymeric nanoparticles using the polymerization of monomers, processes focus on the three major techniques as mini-, micro-, and emulsion polymerization methods [47].

Emulsion polymerization : The common method of particle synthesis in emulsion polymerization is achieved by micellar nucleation method though there is also the presence of homogenous nucleation especially in water soluble monomers. The surfactants are added which

at a concentration higher than the critical micelle concentration in the aqueous phase to form micelles. These micelles owing to their hydrophobic nature inside the inner space provide an ideal site for the radical entry as well as propagation of polymerization. The structure of surfactant is generally comprised of hydrophilic and hydrophobic. These molecules thus arrange themselves, their hydrophilic parts are in interface with water side. Every surfactant has a different critical micelle concentration (CMC) value and it should be considered while using different types of surfactants. Generally 100-200 surfactant molecules form a micelle and these micelles have a size of 10 nm. The surface tension of the solution decreases when the surfactant is added at critical micelle concentration. However, it is not only the surface tension that is affected by the surfactant [54].

When the monomer is added into aqueous solution that the surfactant forms micelle, monomer which is water insoluble enters the micelles and exist in it as droplet. These droplets are stabilized by the adsorption of surfactant molecules on the surface. The number of micelles is much larger than the number of droplets and the droplet size can fall in the desired range of size. Emulsion polymerization is performed by using soluble initiator. The polymerization is initiated by the addition of the initiator and the generated radicals in the aqueous phase reaches monomers in a micelle. When the radicals enter the micelles and start polymerizing the monomer contained in these micelles, the polymer particles form. These growing polymer particles are then supplied by the monomer molecules from the monomer droplets by diffusion through the aqueous phase. During polymerization the termination of the radicals is quite slow as at a particular time, there is rarely more than one radical per particle [54].

The conventional emulsion polymerization reaction contains three distinct intervals, labeled Intervals I, II and III. Interval I is that where particles formation phase ocur. The system consists monomer droplets, surfactants (and micelles if above the critical micelle concentration, CMC) and precursor particles. These particles are small, colloidally unstable particle and they keep on increasing in size so requiring more and more surfactant for stabilizing the increasing surface area. The adsorption of the dissolved surfactant in the aqueous phase on the surface of the particles will eventually grow to a colloidally stable 'mature' particle [55].

In the second interval, after the conclusion of the particle formation period the particles keep on growing in size and no new particles are nucleated (only mature latex particles exist). Rate of polymerization remains constant and the particles grow in size in the presence of monomer droplets. As the diffusion of monomer from the monomer droplets to a particle is rapid on the timescale of polymerization, resulting in the reduction of the size of the monomer droplets [54, 55].

After a certain conversion of the monomer is achieved, the monomer droplets also disappear and interval III commences. In this interval the remaining monomers contained within the particles keep on polymerizing. Thus, concentration of the monomer in the particles decreases, and the polymerization rate reduces. The number of particles thus also remains the same as the second interval and after the monomer has been completely depleted, the polymerization rate climbs down to zero [54]. These three intervals are shown in Figure 2.7.
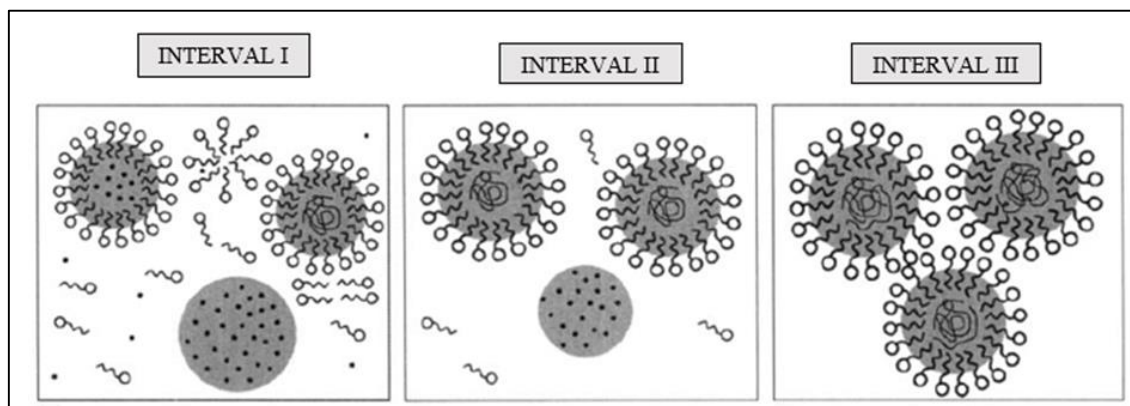
Figure 2.7. Representation of three intervals of typical emulsion polymerization[54]

Miniemulsion Polymerization : Polymerization of extremely low water soluble monomers is very difficult using conventional emulsion polymerization. The low solubility of the monomer would not allow its diffusion to the polymer particles through the aqueous medium. Because of these reasons, miniemulsion polymerization has been developed [54]. In miniemulsion polymerization, a typical formulation consists of monomer droplets, water, co-stabilizer, surfactant and initiator [47].

Miniemulsion polymerization has several advantages according to conventional emulsion polymerization. The main advantage is the elimination of the need of the monomer to diffuse through the aqueous phase from the monomer droplets to the polymer particles during the polymerization. Therefore, the monomer droplets are directly polymerized in this course of polymerization. The other key difference between miniemulsion polymerization and emulsion polymerization is the use of a high shear device such as sonicator or mechanical homogenizer and using a low molecular mass compound as the co stabilizer [47]. The application of shear breaks the bigger monomer droplets into the droplets of size range 10-500 nm that forms the range of resulting polymer particles generated by miniemulsion polymerization. Miniemulsion polymerization is the colloidal stability which is also much better as compared to the conventional emulsion polymerization and has an interfacial tension much greater than zero [54, 56].
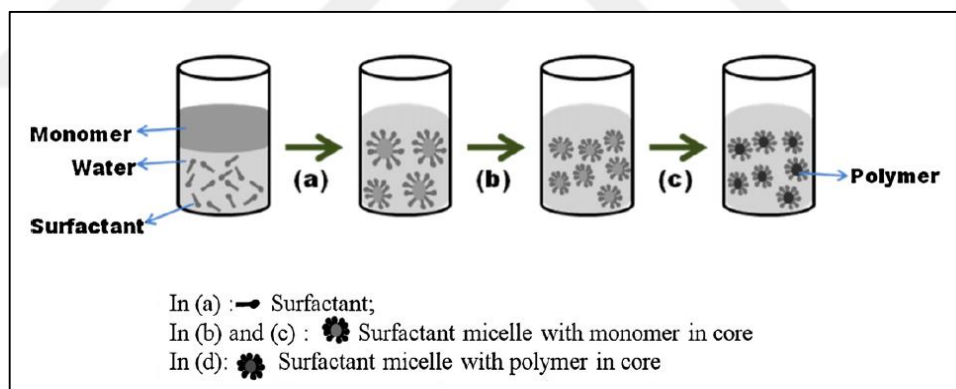
Figure 2.8. Schematic representation of miniemulsion polymerization process: (a) preemulsification, (b) high-shear emulsification and (c) polymerization [47]

Microemulsion polymerization : is a new and effective method to prepare polymeric nanoparticles. Emulsion and microemulsion polymerization appear similar method, because they produce colloidal polymer particles of high molar mass. If compared kinetically, they are different. In emulsion polymerization three reaction rate intervals are performed, however two intervals are detected in microemulsion polymerization.

An typically water soluble initiator is added to the aqueous phase of a thermodynamically stable micro emulsion with swollen micelles [57].

2.3. CONTROLLED DRUG RELEASE FOR POLYMERIC SYSTEMS

All controlled release systems are improved for the effectiveness of drug therapy. This improvement provides some advantages such as increasing therapeutic activity compared to the intensity of side effects, eliminating the need for specialized drug administration (e.g. repeated injections) or reducing the number of drug administrations required during treatment [58]. Polymers are increasingly important in the field of drug delivery systems. Controlled release of drugs from polymeric drug delivery systems is achieved by regulation of the rates of polymer biodegradation and drug diffusion out of the polymer matrix [59].

For polymeric systems, drug release typically refers to how a drug molecules which starting position in a polymeric matrix are exposed to the polymer matrix's outer surface and, how it is released into the surrounding environment. Drug molecules can be transported out of drug delivery systems with diffusion controlled release, solvent controlled release and degradation controlled release [60].

2.3.1. Diffusion Controlled Release

Polymers used for diffusion-controlled release can be produced as either polymer matrices in which the drug molecules are dispersed or as a capsule type reservoir systems in which a drug is dissoleved or dispersed in a core surrounded by polymeric mambrane [61]. Drug molecules simply diffuse out of the polymer matrix [62]. In matrix type systems, there is no membrane (diffusion barrier) therefore, this system usually shows high initial release. In capsule type reservoir systems, diffusion is the main driving force for drug release, and the drug first dissolves in the core then diffuses through the membrane [61]. Rate of release remains constant and not affected by concentration gradients. However rate of release is affected by properties of the polymeric membrane (permeability and thickness) [62].

2.3.2. Solvent Controlled Release

Solvent transport into a polymeric drug carrier can affect the drug release behavior from the carrier. The solvent controlled release includes swelling controlled release and osmosis controlled release [63]. Swelling controlled release describes the random movement of drug molecules. In degradable polymeric systems, the drug release rate is controlled by diffusion through a network of pores, with evolving structures as the polymer matrix degrades. Water is immediately absorbed by polymeric nanoparticles and is a faster process than drug release [64]. When hydrophilic polymeric nanoparticles are placed in an aqueous solution incluiding body fluids, water diffuses into the polymeric system [65]. The water that occupies the polymeric particles causes water-filled pores over time, and the size of the pores becomes larger and more numerous, fianlly leading to large enough pores to enable drug release [64].

In osmosis controlled release, carriers which control the flow of drug solutions are covered with a semi permeable polymer barriers to genetrate pressurized chambers containing aqueous solutions of the drug. Water flows from outside of the carrier (low drug concentration) to the drug loaded core (high drug concentration) [66]. Water molecules cross semipermeable membrane due to the high osmatic pressure, drug molecules dissolve in water and drug flow through pore at controlled rate [67].

2.3.3. Degradation Controlled Release

Drug carriers including biodegradable polymers such as polyesters, poly(amino acids), polyamides and polysaccharides release drugs due to hydrolytic and/or enzymatic degradation of ester, amide, and hydrazone bonds in their backbones [68, 69].

The majority of biodegradable polymers using for controlled drug delivery occur bulk degradation including the polyester materials. Matrices made of these polymers undergo bulk degradation, resulting in homogeneous degradation of the entire matrices [70]. The rate at which the water penetrates the bulk of the polymer is greater than the rate of erosion, therefore, the polymers within the bulk of the matrix are likely to be hydrolyzed and the kinetics of polymer

degradation are more complex than for surface eroding polymers. In bulk degradation mechanism, the lack of protection of drug molecules from the environment and the more limited predictability of erosion are disadvantages for controlled drug delivery [58]. On the other hand, those made of polyanhydrides and poly(orthoesters) typically undergo surface degradation [70]. In surface degradation, polymers erode from the matrix surface into the core. The size of the matrix slowly reduces from the exterior toward the interior. Polymer degradation occurs faster than the rate of water penetration in the bulk of the polymer [71]. Surface degradation is a desirable mechanism of erosion for many drug

delivery applications, as erosion kinetics and hence the rate of drug release are controllable and highly reproducible. Furthermore, the slow water permeation rate into surface eroding devices is ideal for drug delivery because water labile drugs are protected [58]. In a small dimension matrix such as nanoparticles, where the distance of water diffusion is short and the surface size of crystallization is limited, the polymer degradation is significantly accelerated. These polymers do not necessarily follow the typical surface erosion behavior however, show a sign of bulk degradation such as constant particle size during polymer degradation [72].
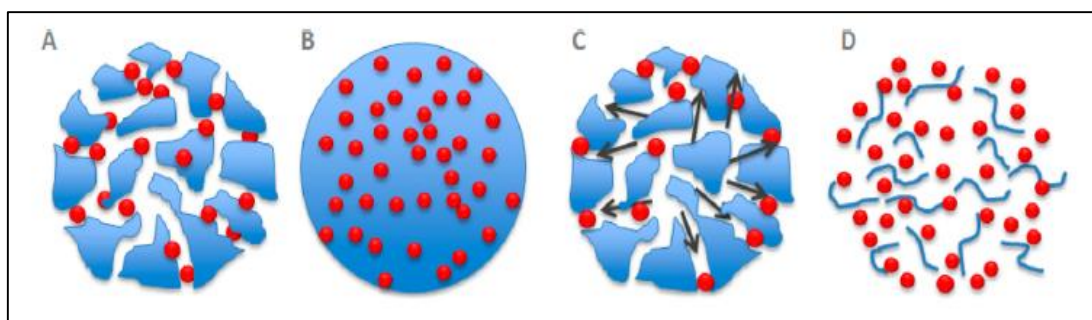

Figure 2.9. Drug release mechanisms from polymeric NPs: (A) swelling controlled release, (B) diffusion controlled release, (C) osmosis controlled release, and (D) degradation controlled release [73]

2.4. POLYMERS USED FOR CONTROLLED DRUG DELIVERY SYSTEM

Polymers are becoming increasingly important for drug delivery application. Many pharmaceutical systems are essentially made up by a polymeric carrier including the active agent (drug) inside its three-dimensional network [4]. Some of the most widely studied synthetic, degradable polymers for drug delivery applications are based upon polyesters which undergo degradation to biocompatible products through hydrolysis of the ester linkage [74].

The most widely investigated polyester is the poly propylene fumarate (PPF), which has shown to be biocompatible and biodegradable. The degradation of this polymer leads to primarily fumaric acid, a naturally occuring substance, and propylene glycol [42]. PPF has unsaturated carbon carbon bonds of the fumaric acid unit which could be used for crosslinking of the polymer into a covalent polymer network [75-77]. Crosslinked PPF based degradable polymer networks are suitable for injectable systems. Due to the injectable, biocompatible and biodegradable of PPF based polymers, they have been widely used for a number of biomedical applications, such as the fabrication of orthopaedic implants, scaffolds for tissue engineering and drug delivery systems. A variety of crosslinking agents are used in combination with PPF for the formation of crosslinked polymer networks. Crosslinking usually occurs with N-vinyl pyrrolidone which is toxic, any unreacted amount during polymerization may cause a problem [78].

The possibility of developing an alternate system for crosslinking of PPF involves ultraviolet light initiated crosslinking [79]. Biodegradable photoinitiated crosslinked polymer networks are an interesting class of materials for drug delivery applications. Polymer networks can be easily loaded with drugs during the crosslinking process. Therefore, large amounts of drug can be loaded into a polymer matrix. Moreover, drug loading crosslinked polymers are useful tool to increase the drug dissolution rate in aqueous media, so, this is particularly important for slightly water soluble drugs [80, 81]. Photo-crosslinked polymer networks are attractive for the release of sensitive drugs, because networks are formed with minimal heat generation [82] .

The ultraviolet light led to study of acylphosphine oxides as initiators for photocrosslinking of PPF [83]. Acylphosphine oxides which are a class of photoinitiators have three basic members

including monoacylphosphine oxides (MAPO), trisacylphosphine oxides (TAPO) and bisacylphosphine oxides (BAPO) [84, 85]. All of these compounds undergo α cleavage of the benzoyl-phosphinoyl bond upon irradiation. These initiators typically absorb light in the far UV to the visible region and act by homolysis to form a pair of radicals [86]. If an olefin is present, these radicals can add to its double bond and initiate crosslinking of alkenes by radical addition processes (free radical polymerization). BAPO are particulary effective crosslinking agents because it absorbs at long UV wavelengths with a high extinction coefficient ($\epsilon \sim 10^4$ at 370 nm), its excited state efficiently generates radicals that rapidly attack olefins, and the initial olefin adducts are themselves photolabile by effect of their additional acylphosphine groups [87].
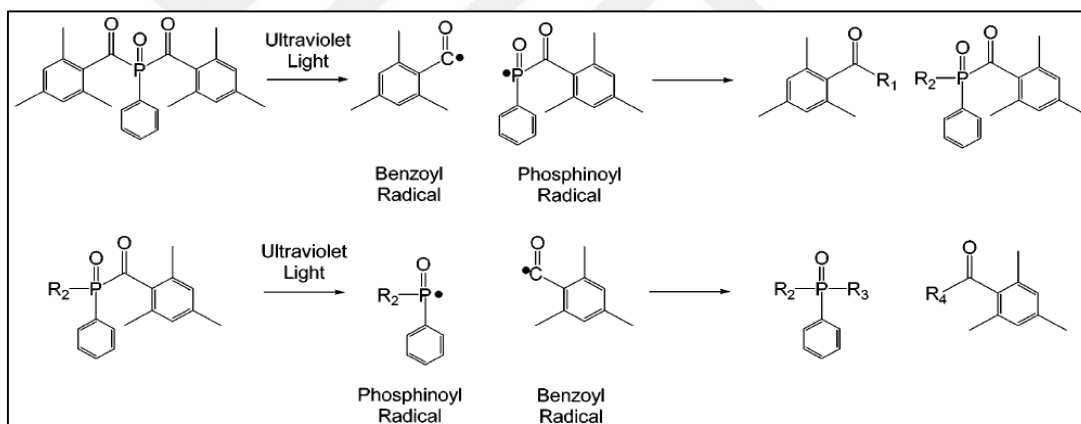
Figure 2.10. α – Cleavage of *bis*(2,4,6-trimethylbenzoyl)phenylphosphine oxide [87]

In this project, poly(propylene fumarate) was crosslinked with N-vinyl pyrrolidone using ultraviolet light and the photoinitiators bisacylphosphine oxides (BAPO). The crosslinked PPF/VP network is shown in Figure 2.11.
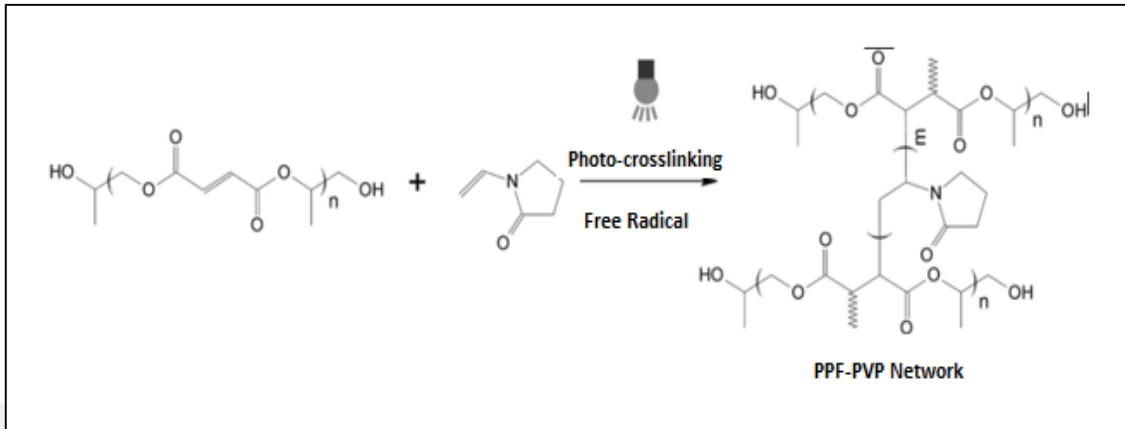
Figure 2.11. Structure of crosslinked PPF/VP network [88]

2.5. SURFACTANTS

Surfactants are organic compounds with at least one lyophobic ('solvent-fearing') group and one lyophilic ('solvent-loving') group in the molecule [89]. Surfactant is characterized by its tendency to absorb at surfaces and interfaces. Interface indicates a boundary between two immiscible phases. The main functions of surfactants are reducing surface/interfacial tension in aqueous solutions and the free energy of boundary phases. The classification of surfactants is based on their charge of polar head group and the nature of the polar head group divides surfactants into four categories such as anionics, cationics, non-ionics and zwitterionics [90].

2.5.1. Anionic Surfactants

Anionic surfactants are by far the largest surfactant class. The polar groups in anionic surfactants are carboxylate, sulfate, sulfonate and phosphate. Anionic surfactants are the most commonly surfactants because of the ease and low cost of their manufacture [90].

They include alkylbenzene sulfonates, fatty acid, lauryl sulfate, di-alkyl sulfosuccinate, lignosulfonates etc… The main usage area of anionic surfactants is detergent formulations [91].

2.5.1.1. Sodium dodecyl sulfate (SDS)

Sulfate esters are available from sulfated alcohols and alcohol ethoxylates. They form another important group of anionics. These are monoester of sulfuric acid and the ester bond is a labile linkage. Linear or branched alcohols with eight to sixteen carbon atoms are generally used as raw materials. The linear 12 carbon alcohol leads to the dodecylmonoester of sulfuric acid and after neutralization, to sodium dodecyl sulfate (SDS), which is by far the most important surfactant in this category. SDS is a common constituent of many personal hygiene and cosmetic, domestic cleaning, pharmaceutical and food products. In addition, Sulfate esters are strong wetting agents and emulsifiers applied in many fields of the industry such as house hold detergents. Due to their ability to form micelles, they are one of the most important surfactant groups in emulsion polymerization [90].
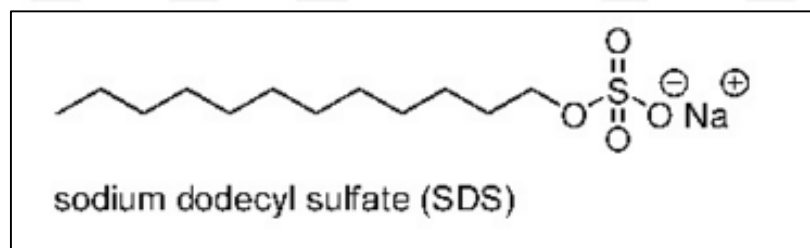
Figure 2.12. Structure of SDS [90]

2.5.2. Cationic Surfactants

A very large group of cationic surfactants corresponds to nitrogen atom carrying the cationic charge. Fatty amine salts and quaternary ammoniums are very common. Quaternary ammonium cations are not pH sensitive. On the other hand, the amines only function as a surfactant cannot be used as high pH [90]. These surfactants are generally more expensive than anionics surfactants, because of a the high pressure hydrogenation reaction to be carried out during their synthesis [91].

2.5.3. Non-ionic Surfactants

Non-ionic surfactants are the second largest surfactant class. The polar group of non-ionics surfactants have either a polyether or a polyhydroxyl unit. In a large majority of nonionic surfactants, the polar group is a polyether consisting of oxyethylene units, obtained with the polycondensation of ethylene oxide. They are called as polyethoxylated nonionics. Examples of polyhydroxyl (polyol) based surfactants are sucrose esters, sorbitan esters, polyglycerol esters and alkyl glucosides and the latter type is a combination of polyol and polyether surfactant. Polyol surfactants can also be ethoxylated. A common example is fatty acid esters of sorbitan (known as trade name of Span) and the corresponding ethoxylated products (known as Tween). The sorbitan ester surfactants are useful for food and drug applications [90].

2.5.3.1. *Polysorbate 80 (Tween 80)*

Polysorbates are a class of emulsifiers that are used in some pharmaceuticals and food preparation. Polysorbates are oily liquids derived from ethoxylatedsorbitan which is a derivative of sorbitol and esterified with fatty acids. For polysorbates, common trade names include Scattics, Canarcel, Alkest, and Tween. Polysorbate 80 is a nonionic surfactant and emulsifier. Polysorbate 80 is a polyoxyethylene ether of anhydrous sorbital and partially esterified with oleic acid. This compound is a colorless or orange yellow water soluble viscous liquid. They are used in food, cosmetic and medical applications [92].
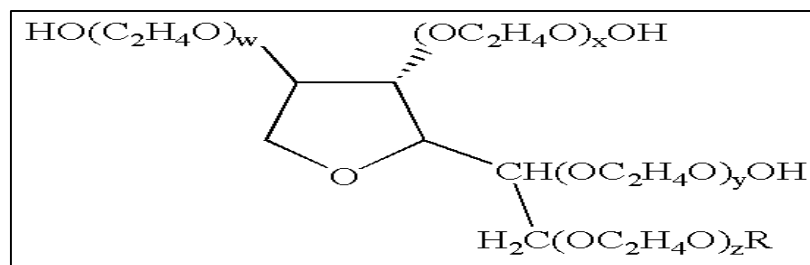

Figure 2.13. Polysorbate 80 : The sum of w,x,y and z is 20 and R = $C_{17}H_{33}CO$ [92]

In this work, both SDS and Tween 80 surfactants were employed to form miniemulsions for miniemulsion polymerization method.

2.6. DRUG TARGETING

Drug targeting technologies have been applied to drugs which clinical use is difficult such as anticancer drugs. Drug targeting research has been developed with the using of nano-sized drug carriers, therefore, nonspecific interactions with living bodies should be avoided. This case provides a new horizon for biomaterial research which is particularly related with nanotechnology [93]. Some types of nano sized drug carriers were explained in section 2.2.

Drug targeting is defined as selective drug delivery to specific sites, organs, cells, or tissues where a drug's pharmacological activities are required [93]. In drug targeting, magnetic nanoparticles have been used as therapeutic drug carriers in order to target specific sites in the body. Magnetically targeted drug delivery is an efficient method for delivering drugs to localized disease sites [94].

2.6.1. Magnetically Controlled Drug Targeting

The main disadvantage of most chemotherapeutic agents which use for cancer treatment is that they are non-specific. These therapeutic drugs (generally cytotoxic) are administered intravenously to general systemic distribution. This technique results deleterious side-effects of chemotherapy as the drug attacks normal, healthy cells in addition to the target tumour cells [95]. Magnetic drug delivery by using drug carriers is a very efficient method to target a localized disease site within the body. The two objectives of localized magnetic targeting of drug are reducing the amount of systemic distribution of the cytotoxic drug accordingly reducing the associated side-effects and reducing the dosage required by more efficient [95]. Figure 2.14 shows the comparing traditional drug therapy with magnetic drug targeting. In magnetically targeted therapy, a cytotoxic drug is bound to a biocompatible magnetic nanoparticle carrier. These drug/carrier complexes are injected into the patient's blood stream and then stopped with

an external, high-gradient magnetic field in the target area. The drug loaded carrier is concentrated at the target, then drug can be slowly released from the magnetic carriers and is taken up by the tumour cells. This system has major advantages comparing to the normal, non-targeted methods of cytotoxic drug therapy [94]. Magnetic carriers receive their magnetic responsiveness to applied magnetic field from incorporated materials such as magnetite, iron, nickel, cobalt etc. In section 2.6.1.1 iron oxides are described in detail.
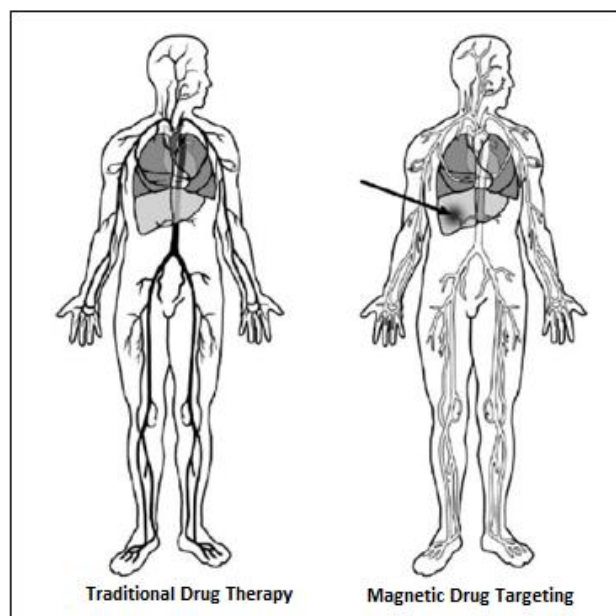
Figure 2.14. Concept of magnetic drug targeting [94]

2.6.1.1. Iron Oxides

Iron oxides exist in many forms in nature. They are easily synthesized. Almost all of them are crystalline. Their magnetic properties make them interesting for several applications.

Magnetic Behavior of Iron Oxides : The iron atom has a strong magnetic moment because of their four unpaired electrons in 3d shell. Crystals are formed from iron atoms and these crystals are classified according to their response to an externally applied magnetic field. Different forms of magnetism are identified in nature. Five basic types of magnetism can be described such as paramagnetism, ferromagnetism, antiferromagnetism, diamagnetism and ferrimagnetism [96]. These magnetic states are shown in Figure 2.1 [97].

Paramagnetic substances have an unpaired electron. The unpaired electron is free to align its magnetic moment in any direction and the crystal has a zero net magnetic moment. Paramagnetic atoms are capable of being attracted to magnetic fields and when the crystal is attracted to magnetic fields, some of these moments will align and the crystal will exhibit a small net magnetic moment. Paramagnetic crystals have a small, positive susceptibility to magnetic fields and the crystal does not protect the magnetic properties when the applied external field is removed [98]. Ferromagnetic materials have a large, positive susceptibility to an external magnetic field. They have aligned parallel magnetic moments of equal magnitude and exhibit a strong attraction to magnetic fields. Furthermore the aligned moments in ferromagnetic materials remain magnetized in the absence of an applied magnetic field [99].

In ferrimagnetic crystal, the magnetic moments in an antiparallel alignment are not equal and they do not cancel. They have a net magnetic moment. Ferrimagnetic materials are similar to ferromagnetic materials. They exhibit ferromagnetic behavior such as spontaneous magnetization but ferromagnets and ferrimagnets have very different magnetic ordering [100].

In antiferromagnetic materials, atomic magnetic moments have equal magnitude which are arranged in an antiparallel fashion [99]. Therefore, the result that the substance has no net magnetization [100].

The orbital motion of electrons respond to oppose the applied field when exposed to externally applied magnetic field. Diamagnetism know as property of all materials that display this type of weak repulsion to a magnetic field. It is very weak. Diamagnetism is observed in materials with filled orbital shells. When an applied magnetic field a negative magnetization is produced and these materials have a negative susceptibility [101].

Material's magnetic properties are based on its magnetic susceptibility which is defined by the ratio of the induced magnetization (M) to the applied magnetic field (H). When an external magnetic field is applied to ferromagnetic materials, the M increases with the H until a saturation value M_S is reached [102]. The magnetization curve of Figure 2.16 is obtained. The magnetization curve shows a hysteresis loop, since all domains do not return to their original orientations when external magnetic field is removed after the saturation magnetization value is present.

Thus, if the applied magnetic field (*H*) reduces back to zero, remnant magnetization M_R is occured. A single domain magnetic material has no hysteresis loop and it is called as superparamagnetic. Iron oxide nanoparticles which is smaller than 20 nm show superparamagnetic behavior [103].
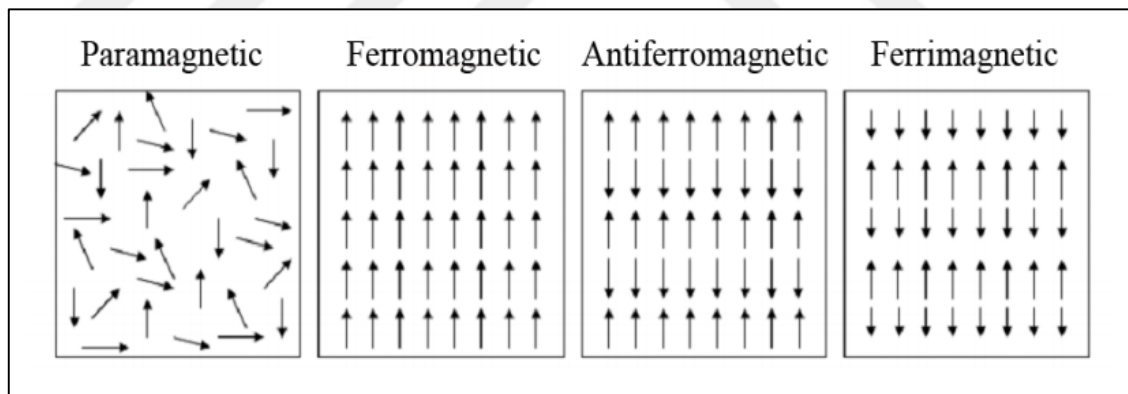

Figure 2.15. Possible alignment of individual atomic magnetic moments orientation [101]
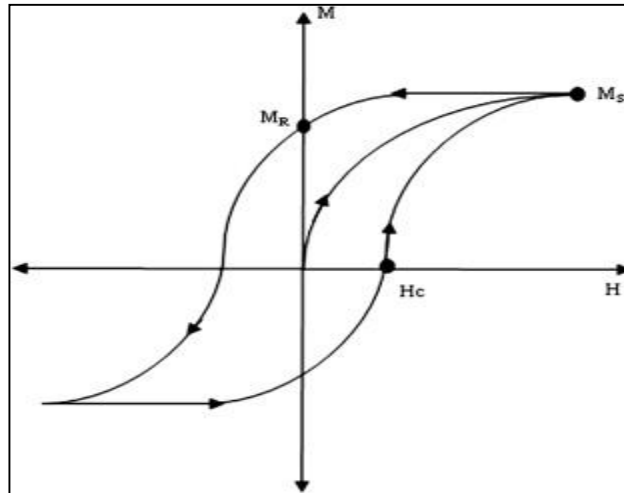
Figure 2.16. Magnetization M as a function of an applied magnetic field H [103]

Types of Iron Oxides : Several types of iron oxides are found as oxides, with magnetite (F_3O_4), maghemite (γ-Fe_2O_3), and hematite (α-Fe_2O_3) are the most common. These three oxides are very important technologically. Some of their physical and magnetic properties are shown in Table 2.1 [103].

Table 2.1. Physical and Magnetic Properties of Iron Oxides [103]

Property	Oxide		
	Hematite	**Magnetite**	**Maghemite**
Molecular formula	α-Fe_2O_3	F_3O_4	γ-Fe_2O_3
Density (g/cm^3)	5.26	5.18	4.87
Melting point (°C)	1350	1583-1597	-
Hardness	6.5	5.5	5
Type of magnetism	Weakly ferromagnetic or antiferromagnetic	Ferromagnetic	Ferrimagnetic

Hematite is the oldest known of several iron oxides and is the form of iron(III) oxide (Fe_2O_3). The color of hematite is blood-red if finely divided and black when it exist in crystalline form. It is extremely stable. It is an important pigment and is a valuable ore. Hematite exhibits weakly ferromagnetic or antiferromagnetic behavior at room temperature[103]. It is difficultly prepared single phase of iron oxide based on complex reaction and oxidation kinetics that result in phase conversion of maghemite and magnetite to hematite[104].

Maghemite occurs as a degradation product of magnetite. In addition, they form as a product of heating of other iron oxides. It is red-brown in color. The type of magnetism is ferrimagnetic. Maghemite forms continuos solid solution with magnetite [105].

Magnetite is one of the most used forms of iron oxide in nanoparticles. Magnetite is known as black iron oxide, magnetic iron ore and ferrous ferrite. It is a black, opaque, magnetic mineral. Its crystal structure contains both the ferric (Fe^{+3}) and ferrous (Fe^{+2}) iron ions. A complex pattern of electrons between the two forms of iron is the source of its magnetic nature. Although other metal oxides may match magnetite's color, specific gravity and hardness, magnetite exhibits the strongest magnetism of other transition metal oxide. It has superparamagnetic properties [105].

Magnetite nanoparticles have been applied in chemistry and biomedical applications, such as hyperthermia, drugs delivery systems, targeted drug delivery, tumor and cancer diagnosis and treatment. Most of these applications depend on particle size and shape, preparation method, size distribution and surface chemistry of the material. The particle size is the main factor for these interesting properties. The critical size should be smaller than 20 nm in order to achieve the superparamagnetic behavior. The size and shape of magnetite particles are generally controlled by the synthesis method. Several methods have been reported for the synthesis of magnetite, including co-precipitation, thermal decomposition, microemulsion, micelle synthesis, hydrothermal synthesis and laser pyrolysis techniques [106] [107] [108].

Synthesis of Nanoparticles: The preparation method plays an important role to determine the particle size and shape, size distribution, surface chemistry and therefore the applications of the material. Many synthesis techniques have been developed to produce the shape controlled,

particle size, mechanical, optical, magnetic or electronic properties, biocompatible, and mono dispersed iron oxide NPs. Synthesis methods of iron oxide nanoparticles are typically grouped into two categories: "top-down" and "bottom-up" methods.

A top–down approach corresponds to using nanofabrication tools and this approach is controlled by external experimental parameters. This method for the production of nanoscaled structures, large iron oxide materials are broken down to smaller particles with the desired shapes and characteristics. This approach may involve milling or attrition [109]. On the other hand, in bottom–up approaches molecular or atomic components are assembled into nanoparticles based on complex mechanisms and technologies. This approach involves chemical synthesis in solution or in a gas phase [110] [111]. These two strategies are schematically shown in Figure 2.17.

Synthesis of Magnetic Nanoparticles: Several methods have been developed for the preparation of iron oxide nanoparticles and these methods are employed for the preparation the shape controlled, biocompatible, stable and monodispersed iron oxide nanoparticles [101]. Some of these popular methods are co-precipitation, thermal decomposition, microemulsion synthesis.
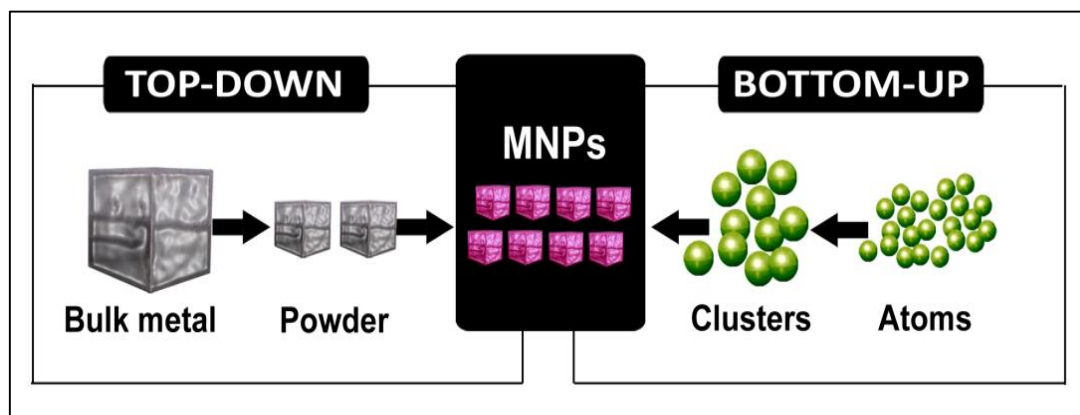

Figure 2.17. Formation mechanism of MNPs by top-down and bottom-up method [112]

Partial Oxidation and Co-precipitation method : The applications of magnetite nanoparticles depend on the preparation method which, affect particle size and shape, size distribution, the surface chemistry of the material and agglomeration.

There are two main methods to synthesise in solution of magnetite spherical particles in the nanometer range. Firstly, Partial Oxidation is used method to prepare magnetic nanoparticles. Ferrous hydroxide suspensions are partially oxidized with different oxidizing agents. For example, spherical magnetite particles which mean diameters between 30 and 100 nm can be obtained from Fe(II) salt, a base and a mild oxidant (nitrate ions) [102].

$$Fe^{2+} + OH^- \rightarrow Fe(OH)_2 \qquad\qquad (2.1)$$

$$Fe(OH)_2 \xrightarrow{NaNO_3} Fe_3O_4 \qquad\qquad (2.2)$$

Secondly, Coprecipitation is the simplest and most commonly technique for the preparation of magnetic nanoparticles. Iron oxides (Fe_3O_4 or γFe_2O_3) are usually obtained by a mixture of ferrous and ferric ions in highly basic solutions under inert atmosphere at room temperature or at increased temperature. The size, shape and composition of the magnetic nanoparticles depends on the type of the salts used, the Fe^{2+}/Fe^{3+} ratio, the reaction temperature, the pH value and ionic strength of the media.

The general size of magnetic nanoparticles can be controlled by reaction conditions and the size of magnetic nanoparticles is in the 5 to 12 nm range by co-precipitation method.

The production of large size distribution of magnetic nanoparticles is achieved by this method [113].

The chemical reaction of Fe3O4 formation can be written as Eqn 2.1

$$Fe^{2+} + 2Fe^{3+} + 8OH^- \rightarrow Fe_3O_4 + 4H_2O \qquad\qquad (2.3)$$
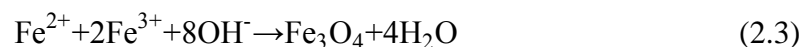
According to the this reaction, complete precipitation can be expected at a pH between 8 and 14 and this reaction is occurred with a stoichiometric ratio of 2:1 (Fe^{3+}/Fe^{2+}) in a non-oxidizing oxygen environment [114].

However, magnetite nanoparticles (Fe_3O_4) are not very stable and are sensitive to oxidation. Magnetite is formed into maghemite (γFe_2O_3) in the presence of oxygen [114].

$$Fe_3O_4 + 2H^+ \rightarrow \gamma Fe_2O_3 + Fe^{2+} + H_2O \qquad (2.4)$$
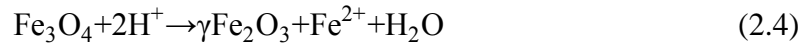
The oxidation of Fe^{+2} causes formation of maghemite which loses its susceptibility with time and decreases the magnetism of the synthesized particle. Magnetic nanoparticles have the tendency of agglomeration of particles because of hydrophobic surfaces with a large surface area to volume ratio. When the particles agglomerate and form large clusters which cause increasing particle size, particles loss the superparamagnetic properties. Therefore, in order to prevent agglomeration and increase the oxidation resistance, the surface coating of magnetite particles is desirable. In addition, the coating provides oil soluble or water-soluble nanoparticles [115].

The surface coating is required to prevent aggregation for MNPs due to their magnetic property. Several molecules have been used to coat the surface of MNPs. The biocompatible coating material, oleic acid is a commonly used surfactant to stabilize the MNPs synthesized by the co precipitation method [116] [117]. Oleic acid forms a strong chemical bond between its carboxy groups and iron cations on the magnetite surface. Oleic acid coated magnetic nanoparticles are highly dispersed, low toxicity, long term stability and providing high biocompatibility [118].

Microemulsion Method : A microemulsion method has been widely used in order to synthesize uniform sized magnetic nanoparticles (MNPs). This is an isotropic and thermodynamically stable dispersion of two immiscible liquids. This system uses an amphiphilic molecule which is called surfactant. The both liquids are stabilized by surfactant molecules. Surfactant molecules contain the hydrophilic head groups in the aqueous phase and hydrophobic tails dissolved in the oil phase. They lower an interfacial tension between oil and water resulting in the formation of a transparent solution [119]. Depending on relative concentration, surfactant molecules self assemble into a variety of structures in the solvent mixture, for example; micelles, microemulsions and lamellar phases.

Most commonly used structures in nanoparticle synthesis are reverse micelles and microemulsions. Water in oil microemulsions systems, the nanosized water droplets dispersed

in a continuous oil phase and surrounded by surfactant molecules at the water/oil interface. This method has been widely used to synthesize iron oxide nanoparticles. By mixing of two water-in-oil microemulsions containing metal salt and a reducing agent, metallic nanoparticles in w/o microemulsion have been prepared [120] [121].

Thermal Decomposition : Iron oxide nanoparticles with a higher level of monodispersity and size control can be produced by thermal decomposition of iron organic precursors, such as $Fe(Cup)_3$ (cup=N- nitrosophenylhydroxylamine), $Fe(acac)_3$ (acac = acetylacetonate), or $Fe(CO)_5$ in organic solvents, and using surfactants such as oleic acid, fatty acids and hexadecylamine [122]. Thermal decomposition of iron organic (organometallic) precursors which metal is the zerovalent in their composition (such as $Fe(CO)_5$) produces iron NPs and the following oxidation can cause a high in quality monodispersed metal oxides. Otherwise, direct decomposition of $Fe(Cup)_3$ or $Fe (acac)_3$ single precursor causes metal oxides NPs. The particle diameter can be obtained from 4 to 20 nm by using this method. The ratios of the starting reagents that include organometallic compounds, solvents, and surfactants are the significative parameters to control the morphology and size of MNPs. In addition, the rection temperature and time may be effective for the control of size and morphology. Morphology, size and magnetic properties of nanoparticles are affected with reaction times and temperatures. This effects are shown in Figure 2.18 [123].
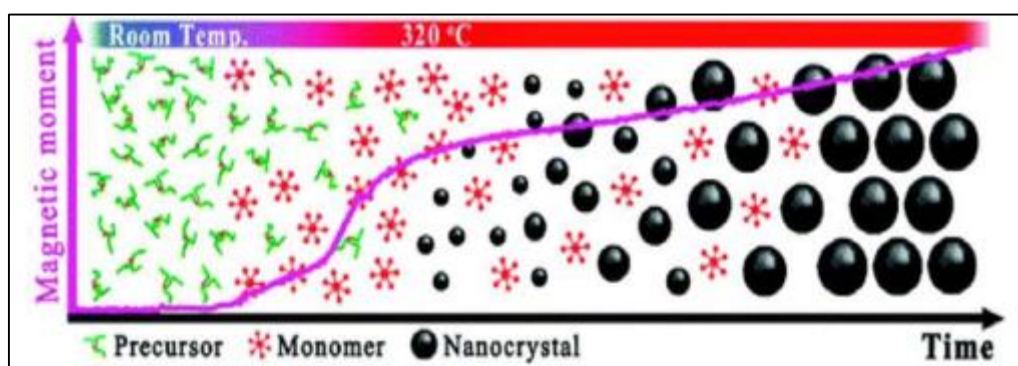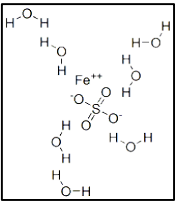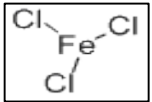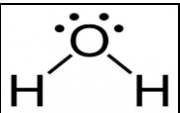

Figure 2.18. Effect of reaction times and temperatures on nanoparticles [123]

3. MATERIALS AND METHODS

3.1. CHEMICALS

Table 3.1. and 3.2 list the chemicals used for the synthesis of coated MNPs by coprecipitation and partial oxidation method. Table 3.3. and Table 3.4. list the chemicals used for the synthesis of polymer nanoparticles.

Table 3.1. Chemicals for synthesis of coated MNPs by Coprecipitation method

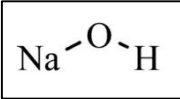| Chemical Name and Formula	Molecular Structure	Molecular Weight (g/mol)	Purity	Production Company
Iron (II) sulfate heptahydrate $FeSO_4.7H_2O$		278.01	90%	Riedel-de Haen
Iron (III) Chloride $FeCl_3$		162.2	97%	Riedel-de Haen
Water H_2O		18.02	-	-

Sodium hydroxide (NaOH)	Na—O—H	40	99%	Riedel-de Haen

Table 3.1. Chemicals for synthesis of coated MNPs by Coprecipitation method (cont.d)

Chemical Name and Formula	Molecular Structure	Molecular Weight (g/mol)	Purity	Production Company
Ammonium hydroxide (NH$_4$OH)	H:N:H:O:H	35.05		Riedel-de Haen
Oleic acid, C$_{18}$H$_{34}$O$_2$		282.47	-	Sigma Aldrich
Citric acid, C$_6$H$_8$O$_7$		192.13	%99	Sigma Aldrich

Table 3.2. Chemicals for synthesis of coated MNPs by Partial oxidation method
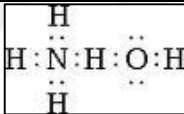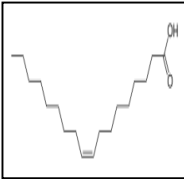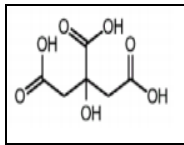
Chemical Name and Formula	Molecular Structure	Molecular Weight (g/mol)	Purity	Production Company
Potassium Nitrate (KNO$_3$)		101.1	≥99%	Sigma Aldrich
Potassium Hydroxide (KOH)		56.1	≥85%	Merck

Table 3.2. Chemicals for synthesis of coated MNPs by Partial oxidation method (cont.d)

Iron (II) sulfate heptahydrate FeSO$_4$.7H$_2$O		278.01	90%	Riedel-de Haen
Oleic acid, C$_{18}$H$_{34}$O$_2$		282.47	-	Sigma Aldrich
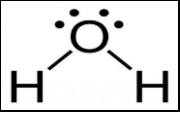
Water H_2O		18.02	-	-

Table 3.3. Chemicals used for synthesis of polymer nanoparticles at 90 ℃
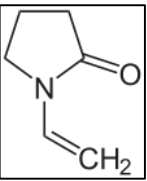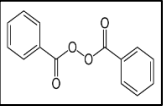
Chemical Name and Formula	Molecular Structure	Number Aver. Molecular Weight (g/mol)	Purity	Production Company
Polypropylene fumarate (PPF)		1258	-	-
Vinyl pyrrolidone (VP) C_6H_9NO		111.14	-	Santa Cruz Biotechnlogy
Benzoyl peroxide (BPO) $C_{14}H_{10}O_4$		242.23	≥97%	Fluka

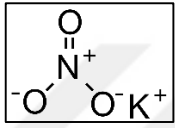Table 3.3. Chemicals used for synthesis of polymer anoparticles at 90 ℃ (cont.d)
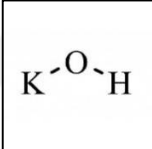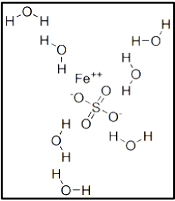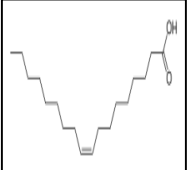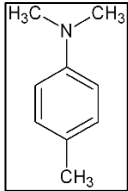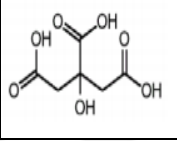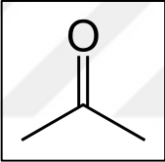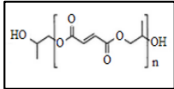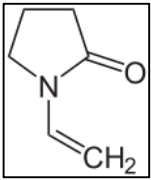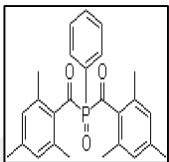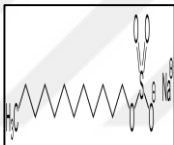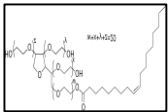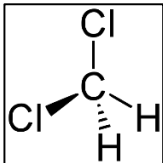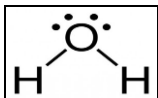
Chemical Name and Formula	Molecular Structure	Molecular Weight	Purity	Production Company
N-dimethyl-p-toluidine (DMT) $C_9H_{13}N$		135.21		Sigma Aldrich
Citric acid, $C_6H_8O_7$		192.13	%99	Sigma Aldrich
Acetone C_3H_6O		58.08		Riedel-de Haen

Table 3.4. Chemicals used for synthesis of polymer nanoparticles

Chemical Name and Formula	Molecular Structure	Number Aver. Molecular Weight (g/mol)	Purity	Production Company
Polypropylene fumarate (PPF)		1258	-	-

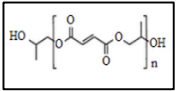| Name	Structure	Molecular Weight (g/mol)	Purity	Supplier
Vinyl pyrrolidone (VP) C_6H_9NO		111.14	-	Santa Cruz Biotechnlogy
bis(2,4,6-trimethylbenzoyl) phenylphosphine oxide (BAPO) $C_{26}H_{27}O_3P$		418.46	-	Sigma Aldrich
sodium dodecyl sulfate (SDS) $NaC_{12}H_{25}SO_4$		288.37	90%	Merck
Tween 80 $C_{64}H_{124}O_{26}$		1310	-	Sigma Aldrich
Dichloromethane (DCM) CH_2Cl_2		84.93	≥99%	Sigma Aldrich
Water H_2O		18.02	-	-

3.1.1. Paclitaxel

Paclitaxel is one of the most effective anti cancer drugs. Paclitaxel is used for the treatment of a wide range of solid tumors, such as ovarian cancer, breast canser, head and neck tumors [124]. It is a white crystalline powder and it is poorly soluble in water [125]. The chemical structure of paclitaxel is given in Figure 3.1. Its clinical use has been greatly limited due to its low water solubility and strong adverse reactions (low blood pressure and allergies). New delivery systems of Paclitaxel have been developed such as the use of polymeric nanoparticles, liposomes, protein-PTX conjugates in order to overcome these Paclitaxel related disadvantages [126].
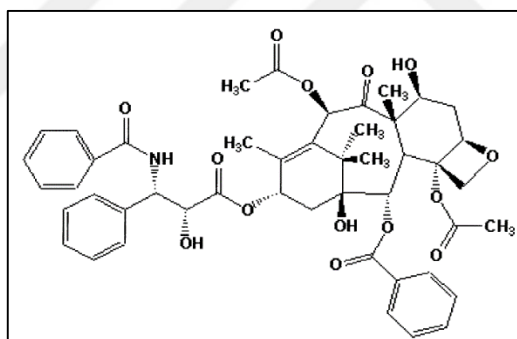
Figure 3.1. Structure of Paclitaxel [125]

3.2. METHODS

3.2.1. High Performance Liquid Chromatography (HPLC)

High performance liquid chromatography (HPLC) is one of the most used tools in analytical chemistry and biochemistry. It is used to separate, identify, purify and quantitate the compounds that are present in any sample which can be dissolved in a liquid. HPLC is widely applied in a variety of areas such as pharmaceuticals, biotechnology, food, cosmetics, environmental and polymer industries [127].

The High Performance Liquid Chromatograph system consists of following five main components:

1. UV/Visible Detector
2. Degasser
3. HPLC Pumps
4. Autosampler

The small amount of liquid analysis sample is injected into the carrier stream of liquid which is called the mobile phase. The liquid phase is pumped at a constant rate to the column paceked with particles of stationary phase. On reaching the column the sample is separated into its components and this separation depends on different degrees of retention of each component in the column. Sample component which is retained in the column is determined with its partitioning between the liquid mobile phase and the stationary phase.

Detection techniques are provided characteristic retention time of the eluted components. Retention time depends on the strength of its interactions with the stationary phase, the ratio/composition of solvent used, and the flow rate of the mobile phase [127]. An image of an HPLC is shown in Figure 3.2.
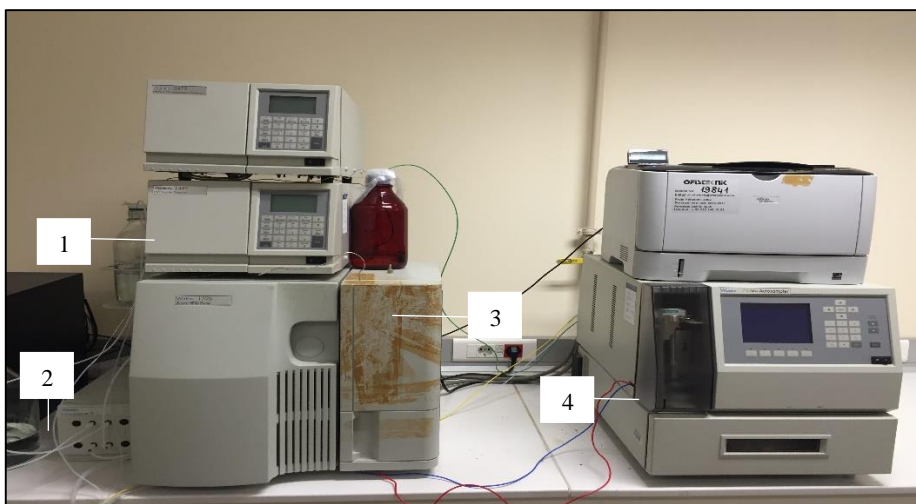
Figure 3.2. High Performance Liquid Chromatography (HPLC)

In this work, high performance liquid chromatograph was used to determine the amount of drug released from crosslinked polymer particles. Waters HPLC system used in this work was equipped with a 2487 UV-Vis Detector, 1525 Binary Pump, 717 Autosampler, Degasser. X-Bridge C-18 column (150×4.6 mm, particle size 5 μm) was used. The mobile phase was composed of solvent A (0.5% H_3PO_4 aqueous solution) and solvent B (Methanol). The flow rate was 1.0 ml/min. The gradient elution conditions are given in Table 3.5. The run time of each sample was 18.50 minutes, injection colume 50 μL and 3 injections were applied for each sample. The column temperature was 30 ℃. The UV absorbance at 227 nm for Paclitaxel was used. Five different paclitaxel concentrations were prepared in 75% ethanol aqueous solution and standard calibration curve was obtained. Measuring peak areas were compared to calibration curve that is known concentrations and the amount of drug in crosslinked polymer particles were determined.

Table 3.5.   Gradient elution condition

Time	%A	%B
0.01	94.0	6.0
3.00	94.0	6.0
3.50	35.0	65.0
16.00	35.0	65.0
16.50	94.0	6.0
18.50	94.0	6.0

3.2.2.   Scanning Electron Microscopy (SEM)

A scanning electron microscope requires an electron optical column to produce electron probe, a vacuum system, a specimen stage and software. Basic construction of a SEM is shown in Figure 3.3.
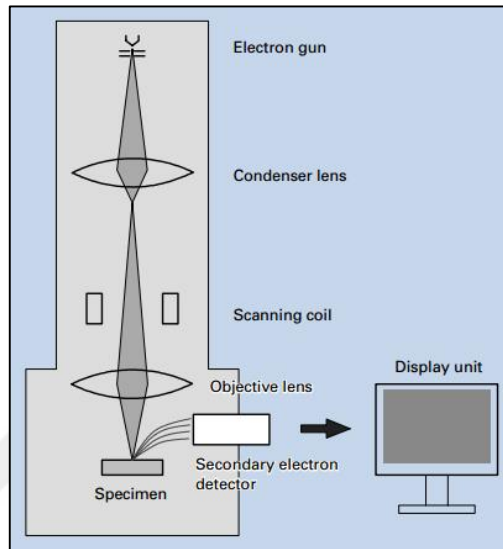
Figure 3.3. Basic construction of a SEM [128]

The electron optical column includes an electron gun, a condenser and objective lenses to control the diameter of the beam. Electron gun produces electron beam and this beam focus on the specimen and scanned over the specimen. The intensities of various signals formed by interactions between the beam electrons and the specimen are measured and stored in computer. The electron optical column and the specimen chamber are maintained at vacuum. Before the spacimen is loaded to the SEM stage, specimen is prepared. The main requrements are that specimen surface is exposed to observe, specimen is fixed to the specimen stage and the specimen has conductivity. If specimen is nonconductive, its surface is coated with a thin metal film. A noble metal such as Au, Au-Pd, Pt, Pt-Pd etc. is used as a coating material because it is highly stable and has a high secondary electron yield [128].

In this work, Scanning Electron Microscope was used to determine the morphology and size of crosslinked polymer particles with and without magnetite.

3.2.3. Attenuated Total Reflection (ATR)

Attenuated Total Reflectance (ATR) is the most widely used FTIR sampling tool. ATR is a sampling technique used in conjunction with infrared spectroscopy. It provides non-destructive measurement of samples with no sample preparation and this provides increasing speeds sample analysis. In addition, the main benefit of ATR sampling is depth of penetration of the IR beam into the sample. In traditional FTIR sampling, the sample must be prepared with IR transparent salt, pressed into a pellet, prior to analysis to prevent totally absorbing bands in the infrared spectrum [129].

In this work, IR spectroscopy was used to confirm the crosslinking of poly propylene fumarate (PPF) with N-vinyl pyrrolidone (VP) by photo initiated mini emulsion polymerization.

4. EXPERIMENTAL PROCEDURES

4.1. SYNTHESIS OF OLEIC ACID COATED MAGNETIC NANOPARTICLES BY COPRECIPITATION METHOD

Magnetic nanoparticles are synthesized using the well known co-precipitation method. 80 mL distilled water is deaerated by passing nitrogen gas through the reaction medium for 30 minutes. The water is heated to 60 ℃ and stirred mechanically at 200 rpm. Then 0.282 g $FeCl_3$, 0.242 g $FeSO_4.7H_2O$ and 2 mL oleic acid are added to water at 60 ℃ while stirring under nitrogen atmosphere. After 15 minutes, 0.514 g NaOH that is dissolved in 10 mL of water is added slowly to the reactor and nitrogen gas is immediately discontinued. The formation of a black precipitated is observed. The mixture is vigorously stirred another 30 minutes. The obtained oleic acid coated magnetite nanoparticles are washed with acetone. After washing the nanoparticles with acetone, the acetone is evaporated using a rotary evaporator to obtain dry nanoparticles.

4.2. SYNTHESIS OF OLEIC ACID COATED MAGNETIC NANOPARTICLES BY PARTIAL OXIDATION METHOD

Magnetic nanoparticles were synthesized using partial oxidation method. Firstly, 2.525 g KNO_3 and 0.974 g KOH were dissolved in 118.75 mL H_2O. Then oleic acid is added to the prepared solution in 250 mL round bottom flask. The mixture is deaerated at room temperature under magnetic stirring in a nitrogen atmosphere for 1 h. At the same time, 6.25 mL water is deaerated by nitrogen gas bubbling for 1 h. After 1 hour, 0.868 g $FeSO_4.7H_2O$ is dissolved in the 6.25 mL deaerated water with using nitrogen gas bubbling. Dissolved $FeSO_4.7H_2O$ was added with syringe to the round bottom flask and the mixture was deareted by nitrogen gas for another minute. The mixture was heated to 90 °C in an oil bath under stirring for 4 h.

4.3. SYNTHESIS OF POLYPROPYLENE FUMARATE (PPF)

Polypropylene fumarate (PPF) was synthesized from fumaric acid and propylene glycol. Hydroquinone and p-toluene sulfonic acid were used as a radical inhibitor and catalyst respectively. The synthesis reaction is shown in Figure 4.1.
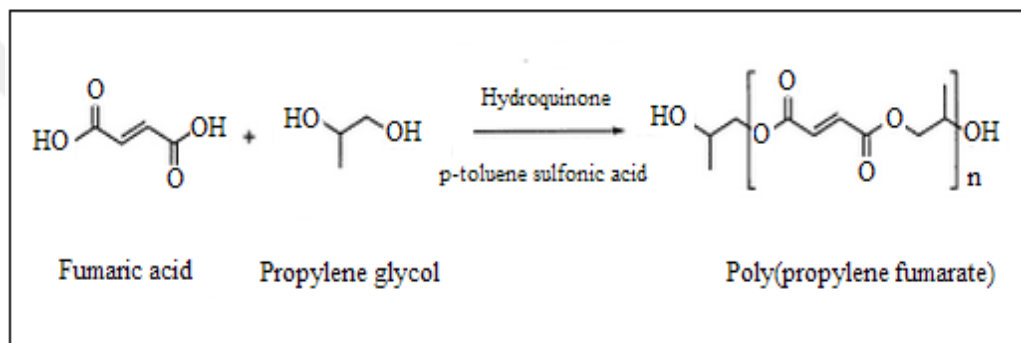
Figure 4.1. The synthesis reaction for polypropylene fumarate

In this reaction, the stoichiometric ratio of fumaric acid to propylene glycol was 1.5:1.65 moles. The radical inhibitor, hydroquinone was used as 0.1% and the catalyst, p-toluene sulfonic acid was used 0.4% of the total weight of propylene glycol and fumaric acid mixture. The reaction content was reacted for 1 hour at 145 °C and at 180 °C for 3 hours, distilling out water, the byproduct of the reaction. The PPF product was purified before use. The synthesis of PPF was carried out by Görkem Cemali and was given to us to be used in this project.

4.4. SYNTHESIS OF CROSSLINKED POLYMER PARTICLES AT 90 °C

PPF was crosslinked with 1-vinyl-2-pyrrolidinone (NVP) at 90 °C to obtain crosslinked polymer particles. 160 mL distilled water was deaerated by nitrogen gas. The water was heated to 90 °C and stirred using either a magnetic bar or a mechanical stirer. In this synthesis, 1-vinyl-2-pyrrolidinone (NVP), benzoyl peroxide (BPO) and N-dimethyl-p-toluidine (DMT) were used

as crosslinker, free radical initiator and accelerator, respectively. NVP, BPO and DMT were dissolved in 1 mL acetone in one vial and 0.24 g PPF was dissolved in 40 mL acetone in another vial. Firstly, PPF solution was added to water at 90 ℃ and after 1 minute, VP/BP/DMT mixture was added to the reactor while stirring under nitrogen atmosphere. The mixture was stirred for 24 hours. The obtained crosslinked polymer particles were precipitated by centrifugation and these particles were dried using freeze dryer. In this method, citric acid coated magnetic particles were used to synthesize the crosslinked polymer particles with magnetite. Citric acid coated MNP's were added to the water during deaeration.

4.5. SYNTHESIS OF CROSSLINKED POLYMER PARTICLES BY PHOTO INITIATED MINIEMULSION POLYMERIZATION

PPF was crosslinked with VP as a crosslinking reagent using photo initiated polymerization method. In applied the procedure, about 0.38 g of the polymer (PPF) was dissolved in dichloromethane in a glass vial. BAPO used as a photoinitiator, and VP were added in the polymer solution. Then this organic solution was added to the aqueous solution containing determined amount of surfactant (SDS or Tween80). This mixture was homogenized at different rpms and for various periods of time to optimize the production of the miniemulsion mixture. Then formed crude miniemulsions in the reactor were placed under the UV lamp (365 nm). The light beam was focused onto the reactor to cover the entire reaction mixture. During the polymerization, the mixture was continuously stirred under nitrogen atmosphere. The mixture was irradiated for 30-60 minutes. The obtained crosslinked polymer particles were washed 3 times with water to remove residual surfactant. After washing with water, crosslinked polymer particles were dried with freeze dryer. In order to prepare crosslinked polymer nanoparticles with magnetite (synthesized by either coprecipitation or partial oxidation method), two methods were developed based on the addition of magnetite. Firstly, oleic acid coated MNP's were added in the organic solution including PPF/VP/BAPO in DCM. Drug loaded crosslinked polymer nanoparticles were prepared in a similar manner. To load the drug to the particles, about 4 mg of Paclitaxel was dissolved in the organic solution in both methods. Secondly, oleic acid coated

MNP's were dissolved in DCM and then added to the rest of the solution while organic and aqueous solution were homogenized.

4.6. DRUG RELEASE OF POLYMER PARTICLES

Three series were studied to study drug release from crosslinked polymer nanoparticles with and without magnetite. PBS solution at 7.4 pH was added into the each synthesise in the test tubes. When PBS was added, the supernatant was immediately taken to determine the initial amounts of drug. Then the test tubes were placed in an orbital shaker at 37 ℃ 100 rpm. The amounts of drug in supernatant were measured by using HPLC in order to obtain drug release profiles from crosslinked polymer particles. The amounts of drug were measured through 30 days (days 1, 5, 8, 12, 15, 19, 22, 26, 30). The supernatants were refreshed after every HPLC measurements. In addition, each synthesise was washed with water 3 times to remove residual surfactant and nonencapsulated drug. After each washing processes, the supernatants were taken and the amounts of nonencapsulated drug were measured by HPLC.

4.7. DEGRADATION TEST FOR CROSSLINKED POLYMER PARTICLES

4.7.1. pH Measurements

Crosslinked polymer particles were synthesized as defined in part 4.4. The synthesized crosslinked particles were divided into 4 almost equal amounts ($\sim$ 0.15 g each) and 10 mL phosphate-buffered saline (PBS) at pH 7.4 was added to each sample. The samples were placed in an orbital shaker (LABWIT, ZWYR-240) at 37 ℃ 100 rpm. The pH values were measured daily for the first 5 days and then weekly. PBS solution was changed every week.

4.7.2. Weight Loss Measurements

The synthesized crosslinked particles were divided into 24 almost equal amounts and phosphate-buffered saline (PBS) at pH 7.4 was added to each sample. The samples were

placed in the shaker at 37 ℃ 100 rpm. Every week (weeks 1, 2, 3, 4, 5, 6,) four samples were removed from PBS solution and the samples were washed with water to remove PBS. After washing with water, these samples were freezed using liquid nitrogen and then dried using freeze dryer. The dry samples were weighed and the difference between the initial and final weight was recorded to show the weight loss of the polymer particles in the given amount of time.

4.8. CROSS-LINK DENSITY

After the synthesis of nanobeads, the cross-link density of crosslinked polymer nanoparticles was investigated. Three parallel series were studied. Crosslinked polymer nanoparticles were weighed (W_i) and then placed in 3 mL distilled water at room temperature for 2 days. The swollen crosslinked polymer nanoparticles were dehydrated using freeze dryer. The dried samples were immersed in 3 mL THF for 2 days. At the end of 2 days, samples were removed from THF and dried in a vacuum oven at 60 ℃ for 2 days. Dried samples were weighed and the final weights (W_f) were recorded. The cross-link density was calculated using equation 4.1.

$$\text{Cross} - \text{link density} \ (\%) \ = \ (\frac{W_f}{W_i}) \times 100 \qquad (4.1)$$

5. RESULTS & DISCUSSION

Polymer dissolution in solvents is an important area for many applications in industry including plastics recycling, membrane science, and drug delivery. Polymer dissolution depends on physical properties and chemical structure such as moleculer weight, polarity, and whether the polymer is cross-linked or not etc [130]. An efficiently cross-linked polymer does not dissolve but swells in solvents.

In this project, the solubility of the synthesized polymer particles was tested as a first indication of the success of crosslinking. For insoluble particles, FTIR and SEM were used to confirm crosslinking of PPF with VP.

5.1. CROSSLINKED POLYMER NANOPARTICLES SYNTHESIZED AT 90 ℃

5.1.1. Solubility of Crosslinked Polymer Nanoparticles Synthesized at 90 ℃

Firstly, this method was applied at 60 ℃ and at different reaction times. However, synthesized polymer particles were soluble in dichloromethane. Solubilities of synthesized polymer particles synthesized at 60 ℃ for different reaction time were given in Table 5.1. Therefore, temperature was increased from 60 ℃ to 90 ℃ in order to obtain crosslinked polymer particles which are not soluble in dichloromethane. The synthesis was performed at 90 ℃ for 24 h with stirring magnetic bar or mechanical stirrer. Then SEM was used to determine the morphology and size of the obtained crosslinked polymer particles which are not soluble in DCM. Parameters for the crosslinked polymer nanoparticles synthesized at 90 ℃ are given in Table 5.2.

Table 5.1. Solubility data for Polymer Nanoparticles Synthesized at 60 ℃

Sample	Solubility in DCM	Reaction time
1	Soluble	30 min
2	Soluble	60 min
3	Soluble	90 min
4	Soluble	2 h
5	Soluble	8h
6	Soluble	24h
7	Soluble	48h

Table 5.2. Parameters for the Optimization of Crosslinked Polymer Nanoparticles by Synthesis at 90 ℃

Sample	Magnetic bar	Mechanical stirrer	Initiator%	Coating of MNPs	Concentration of magnetite
1	✓		2	-	-
2	✓		3	-	-
3		✓	2	-	-
4	✓		2	citric	1%

5.1.2. SEM images of Crosslinked Polymer Nanoparticles Synthesized at 90 ℃

SEM was used to determine the morphology and size of the crosslinked polymer particles synthesized at 90 ℃. SEM images of Sample 1 showed non spherical shaped beads as shown in Figure 5.1. Beads were agglomerated and this kind of agglomeration was not desirable for formation of crosslinked polymer nanoparticles.
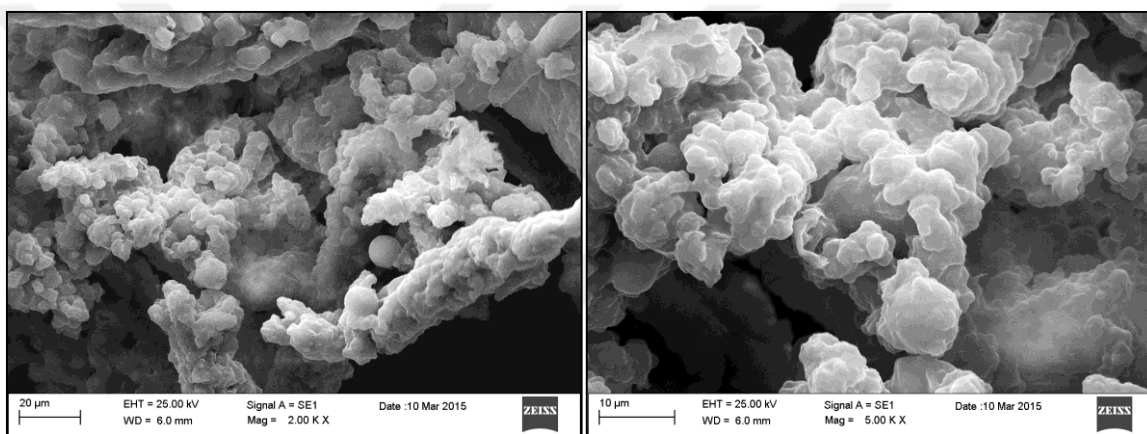
Figure 5.1. SEM images of Sample 1

Sample 2 was used to investigate the effect of the increase in BPO content. Typically, increase in BPO content may act to increase the polymerization rate. However, increasing BPO content had no effect on the crosslinked polymer particles. The SEM images of Sample 2 are shown in Figure 5.2 which exhibit similar structures to those with less initiator (Sample 1).
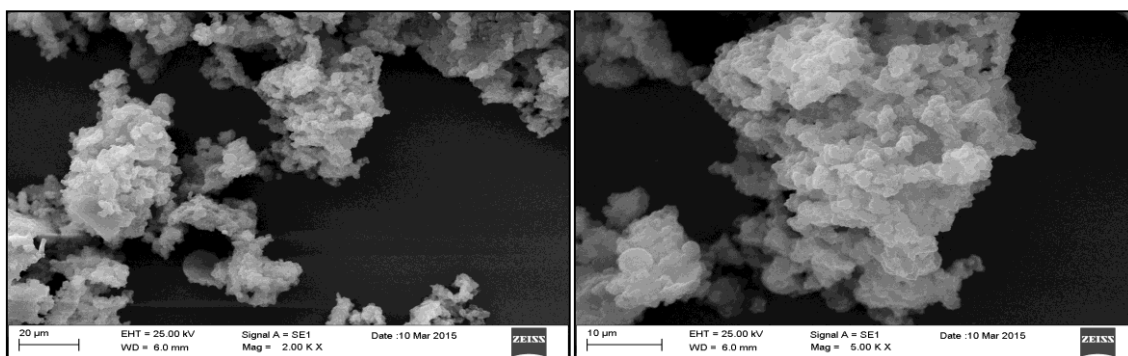
Figure 5.2. SEM images of Sample 2

For Sample 3, there was no improvement in the morpholgy of crosslinked polymer particles when the mechanical stirrer was used instead of magnetic bar. Hardly any particle formation is observed, with the occasional spherical morphologies. Figure 5.3 shows the morphlogy of Sample 3.
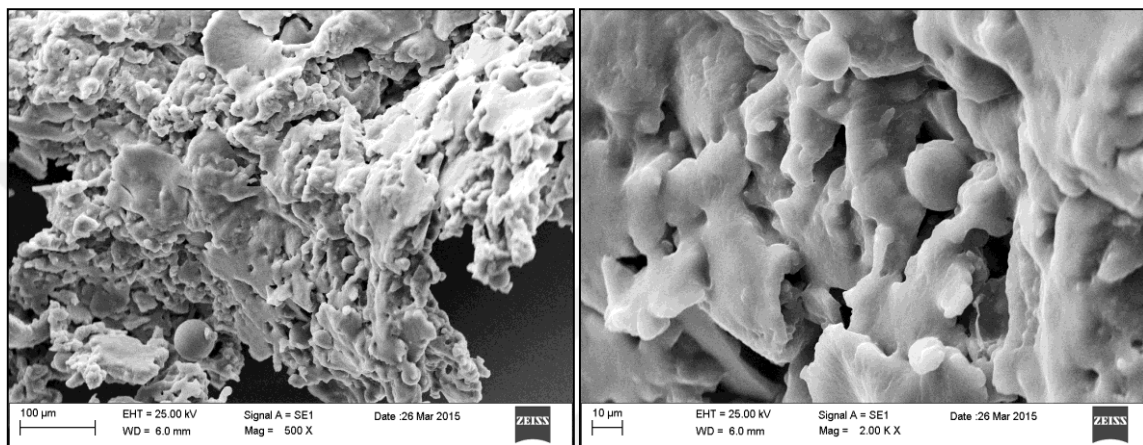
Figure 5.3. SEM images of Sample 3

Citric acid coated MNP's were added to the mixture prepared similar to Sample 1. SEM images of the Sample 4 is highly similar with Sample 1. This is also due to the presence of low amount of added magnetite (1%) as shown in Figure 5.4.

Figure 5.4. SEM images of Sample 4

In synthesis of crosslinked polymer nanoparticles at 90 ℃, the desired size and morphology of beads could not be obtained. In addition, high temperature synthesis is not suitable for drug applications. Therefore, this method was not used to produce crosslinked polymer nanoparticles which are loaded with Paclitaxel.
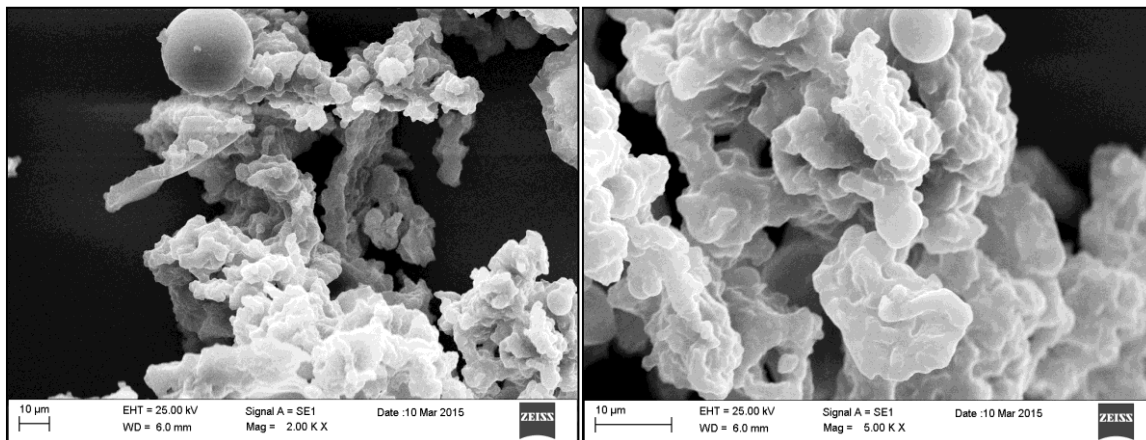
In this work, photo initiated miniemulsion polymerization method was used to synthesize PPF nanoparticles. In this method, crossliked polymer nanoparticles were formed with minimal heat generation using UV irradiation. Two different surfactants were used in photo initiated miniemulsion polymerization method. Section 5.2 includes crosslinked polymer nanoparticles synthesized using TWEEN 80 and section 5.3 includes crosslinked polymer nanoparticles synthesized using SDS.

5.2. SYNTHESIS OF CROSSLINKED POLYMER NANOPARTICLES USING TWEEN80 BY PHOTO INITIATED MINIEMULSION POLYMERIZATION METHOD

Crosslinked polymer nanoparticles were produced using Tween 80 as a surfactant by photo initiated miniemulsion polymerization method. Parameters for the crosslinked polymer nanoparticle by photo initiated miniemulsion polymerization method are given in Table 5.3.

Table 5.3. Parameters for the Optimization of Crosslinked Polymer Nanoparticles by Photo Initiated Miniemulsion Polymerization Method

Sample	Homogenizer Speed (rpm)	Homogenizer Time (min)	UV time (min)	Concentration of magnetite	Coating of MNPs
1	10000	5	30		
2	10000	5	60		
3	1000	60	60		
4	10000	5	60	%1	oleic

5	10000	5	60	%2	oleic

5.2.1. SEM Images of Crosslinked Polymer Particles Synthesized with TWEEN 80

Synthesized crosslinked polymer nanoparticles with Tween 80 (Sample 1) were produced using a homogenizer for 5 min at 10000 rpm and under UV lamp for 30 min. The morphologies of the Sample 1 are shown in Figure 5.5. As shown in the Figure 5.5, the surface of the Sample 1 is not smooth. The SEM image showed that many small beads were filled into one bead and therefore, large beads were produced. The mean diameter of all beads was approximately 100–150 μm which is much larger than desired.
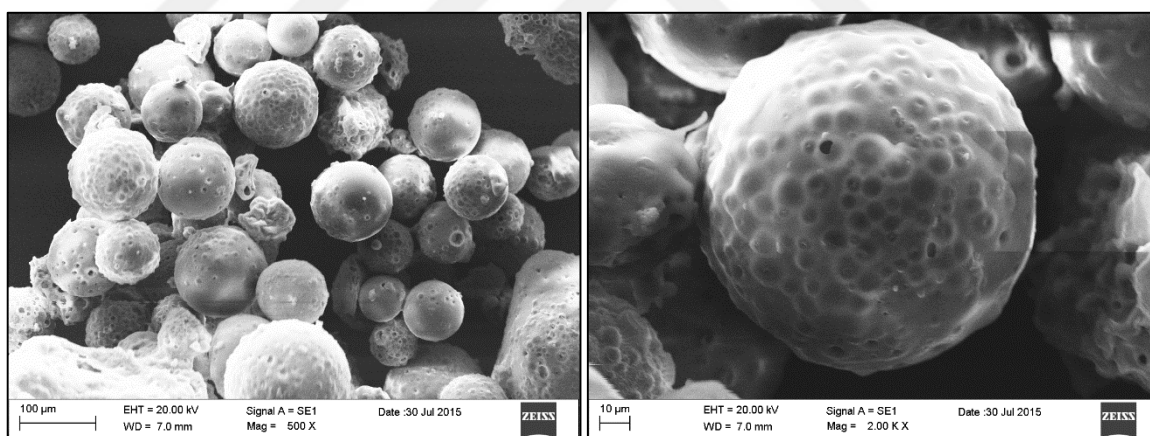
Figure 5.5. SEM images of polymer particles for Sample 1

The same procedure was applied for Sample 2. However, to obtain better samples, the UV time was increased from 30 to 60 min. With increasing the UV time, large beads that are seen in Sample 1 are divided into smaller beads now of approximately 5 μm. Sample 2 includes heterogeneous particle sizes of beads. In addition, hollow structures were seen in the beads as shown in Figure 5.6.

For Sample 3, a different procedure was applied. Sample 3 was continuously homogenized at 1000 rpm under the UV lamp for the whole duration of 60 min. The SEM images of formed

crosslinked polymer particles are given in Figure 5.7. Possibly due to extended homogenization period, this method caused the disruption of the spherical beads structure resulting in irregular morphologies. Therefore, homogenization time was kept at 5 minutes for mixing only for the rest of the work.
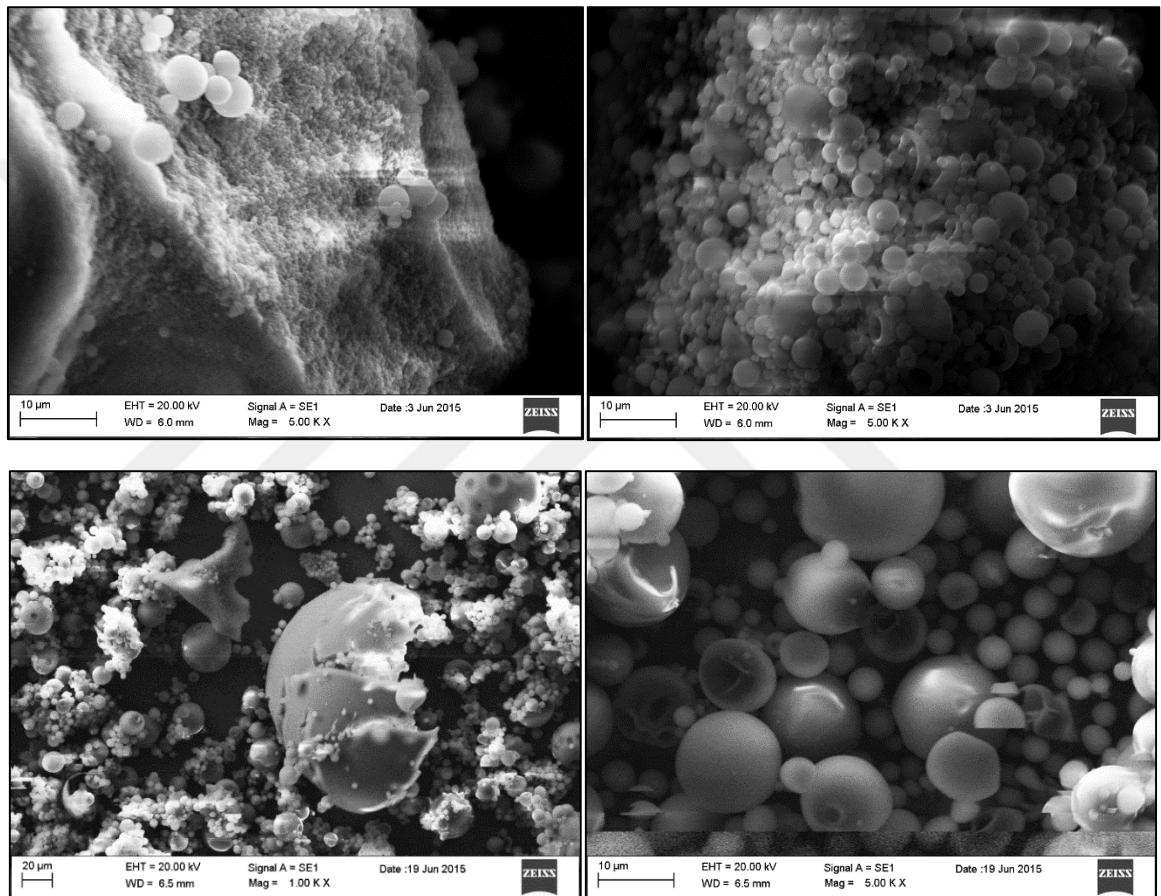
Figure 5.6. SEM images of polymer particles for Sample 2
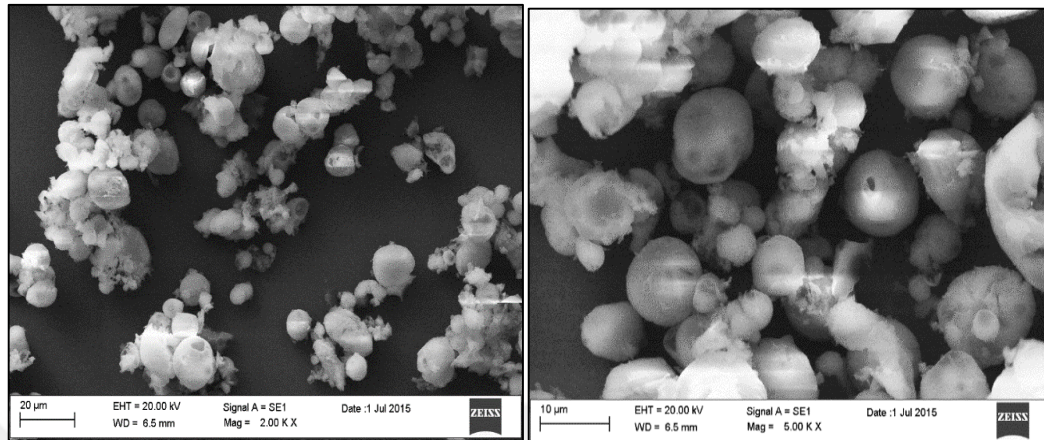
Figure 5.7. SEM images of Sample 3

The oleic acid coated magnetic nanoparticles were added in Sample 4. Sample 4 was homegenized in different mediums such as beaker, vial and graduated cylinder to provide better mixing. However, there was no specific change in the size and morphology of beads when the samples were homogenized in different mediums. The SEM images of Sample 4 are shown in Figure 5.8.
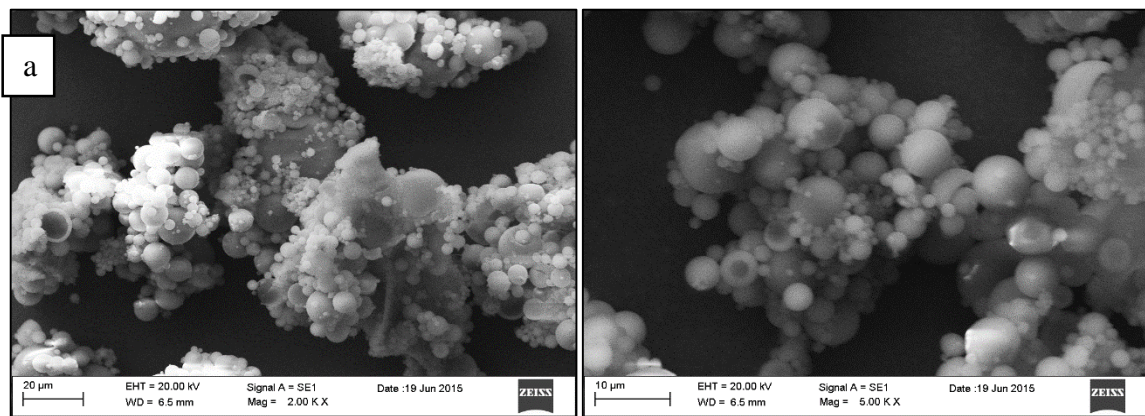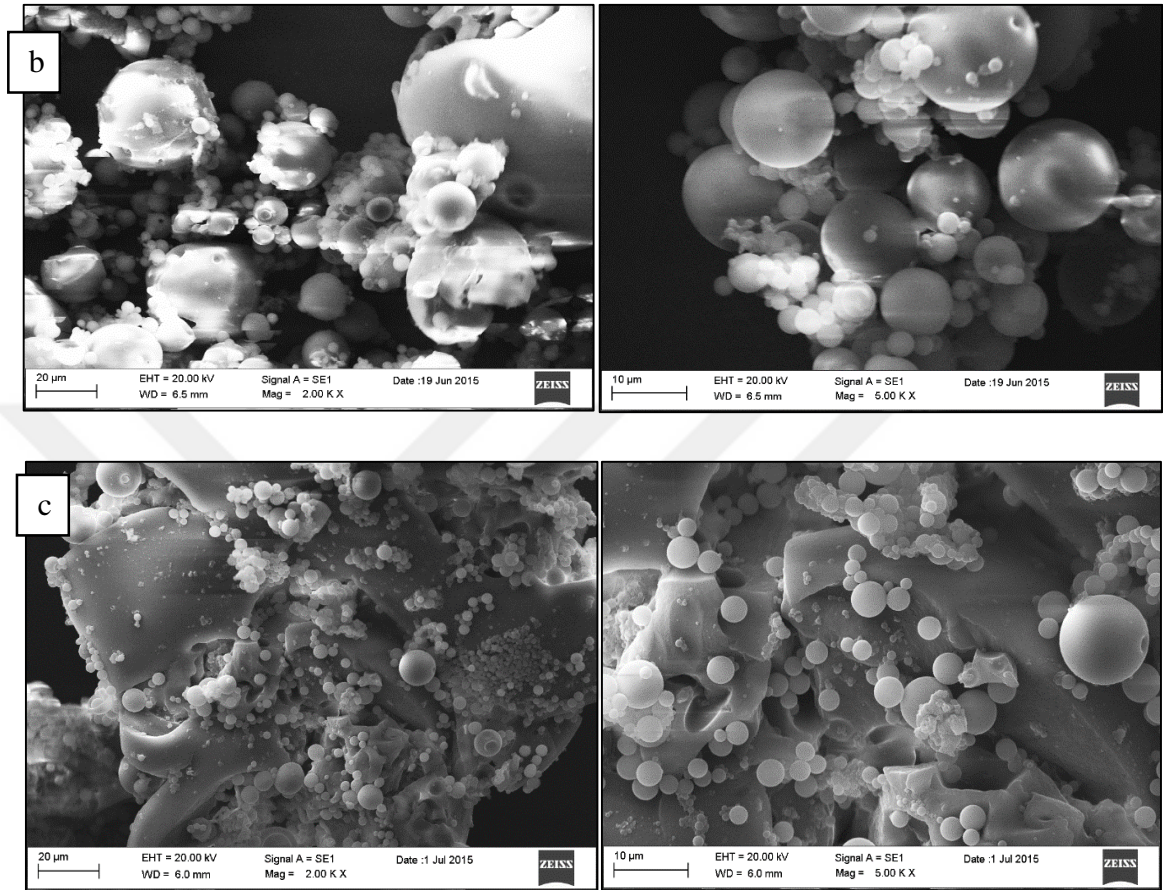
Figure 5.8. SEM images of Sample 4 (a) Sample 4 was homogenized in beaker (b) in vial and (c) in graduated cylinder

Sample 5 was prepared using graduated cylinder during homogenization. For Sample 5, the concentration of oleic acid coated magnetic nanoparticles was increased to 2%. SEM images of this sample (Figure 5.9) showed that the average size of beads was 100-150 μm. When the concentration was increased 2 times to that of Sample 5, there was no apparent change of in the structure of beads.
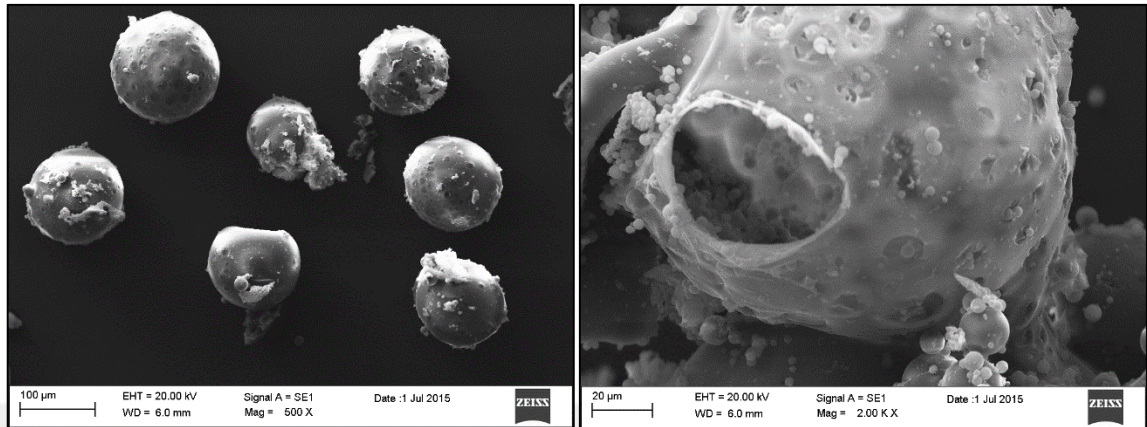
Figure 5.9. SEM images of Sample 5

Vineeth et al. [131] studied preparation of PLGA nanoparticles using Tween80 by emulsion solvent evaporation technique. The obtained nanoparticle diameter was found to be 112.1±6.4 nm. Fuchs et al. [132] studied producing the PMMA latexes using Tween80 as surfactant by photo initiated miniemulsion polymerization. The obtained latexes average particle diameter of 183 nm were measured using SEM. In our work, in forming of crosslinked polymer particles with using Tween 80, porous structures were seen in all beads. The pores of the beads were very large. Smaller beads were seen to fill the pores of the larger beads. The SEM images showed that the average size of beads were approximately 100-150 μm. As the aim was to obtain nanoparticles, crosslinked polymer particles were synthesized using SDS as a surfactant in an attempt to synthesize smaller particles.

5.3. SYNTHESIS OF CROSSLINKED POLYMER NANOPARTICLES USING SDS by PHOTO INITIATED MINIEMULSION POLYMERIZATION METHOD

5.3.1. Synthesis of Crosslinked Polymer Particles Using Magnetic Bar

To synthesise crosslinked polymer particles, an emulsion was prepared with using SDS as a surfactant. Firstly, prepared emulsion (20 mL aqueous solution containing SDS as surfactant and 5 mL organic solution containing PPF/VP/BAPO) is stirred using magnetic bar for 10 min

and then this emulsion is placed under UV lamp to obtain crosslinked polymer particles. The parameters for the optimization of crosslinked polymer particles synthesis using magnetic bar are given in Table 5.4.

Table 5.4. Parameters for the Optimization of Crosslinked Polymer Nanoparticles Synthesis Using Magnetic bar

Sample	Magnetic bar	Mixing time with magnetic bar (min)	Initiator %	UV time (min)	Concentration of magnetite	Coating of MNPs
1	✓	10	2	60		
2	✓	10	2	60	1%	oleic
3	✓	10	2	30	3%	oleic

5.3.2. SEM Images of Crosslinked Polymer Nanoparticles Synthesized Using Magnetic Bar

The UV initiated polymerization of prepared emulsion with SDS (Sample 1) produced crosslinked polymer particles with an average size of 20-40 μm as measured using SEM as seen in Figure 5.10. Although there is a slight decrease in the size when SDS is used, the obtained beads were still not in the desired size range.
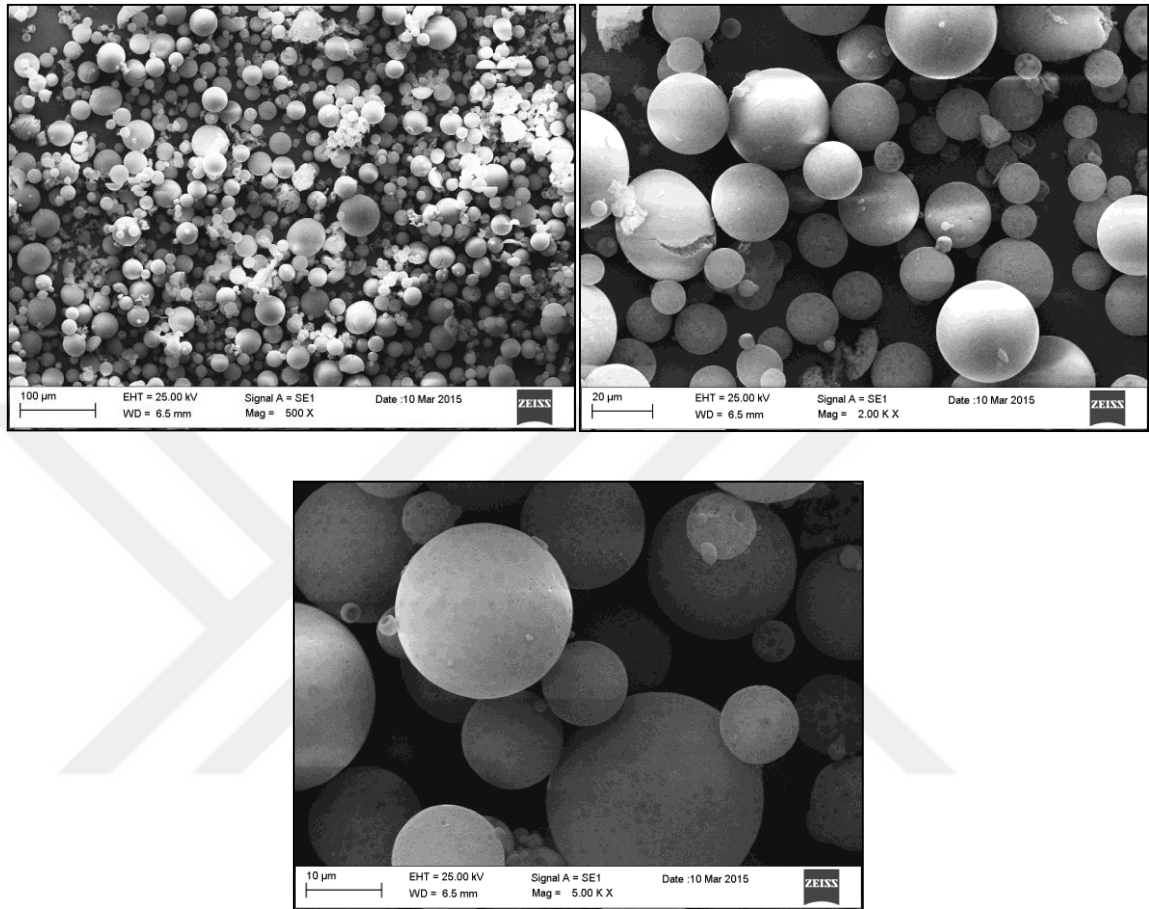
Figure 5.10. SEM images of Sample 1

In order to obtain magenetic polymeric beads, oleic acid coated MNP's were added to Sample 2. When the low concentration (1%) of magnetite is added, the size of beads appeared highly similar to Sample 1. The surface of Sample 2 had a more porous structure compared the surface of Sample 1. SEM images of Sample 2 are shown in Figure 5.11.

When the concentration of magnetite was incereased to 3% and UV time was decreased to 30 min (Sample 3), non spherical shaped beads were obtained as shown in Figure 5.12. Suggesting decreasing the irradation time to 30 minutes prevents the formation of spherical particles as was observed for Sample 1 when TWEEN80 was used. Further studies were continued with 60 minutes UV irradation time.

Crosslinked polymer particles which were prepared using SDS and stirred with magnetic bar, were obtained as smaller spherical shaped beads when compared to synthesized crosslinked polymer particles with Tween 80 (described in Section 5.2).

Crosslinked polymer particles were synthesized using homogenizer instead of using magnetic bar to obtain even smaller particles.
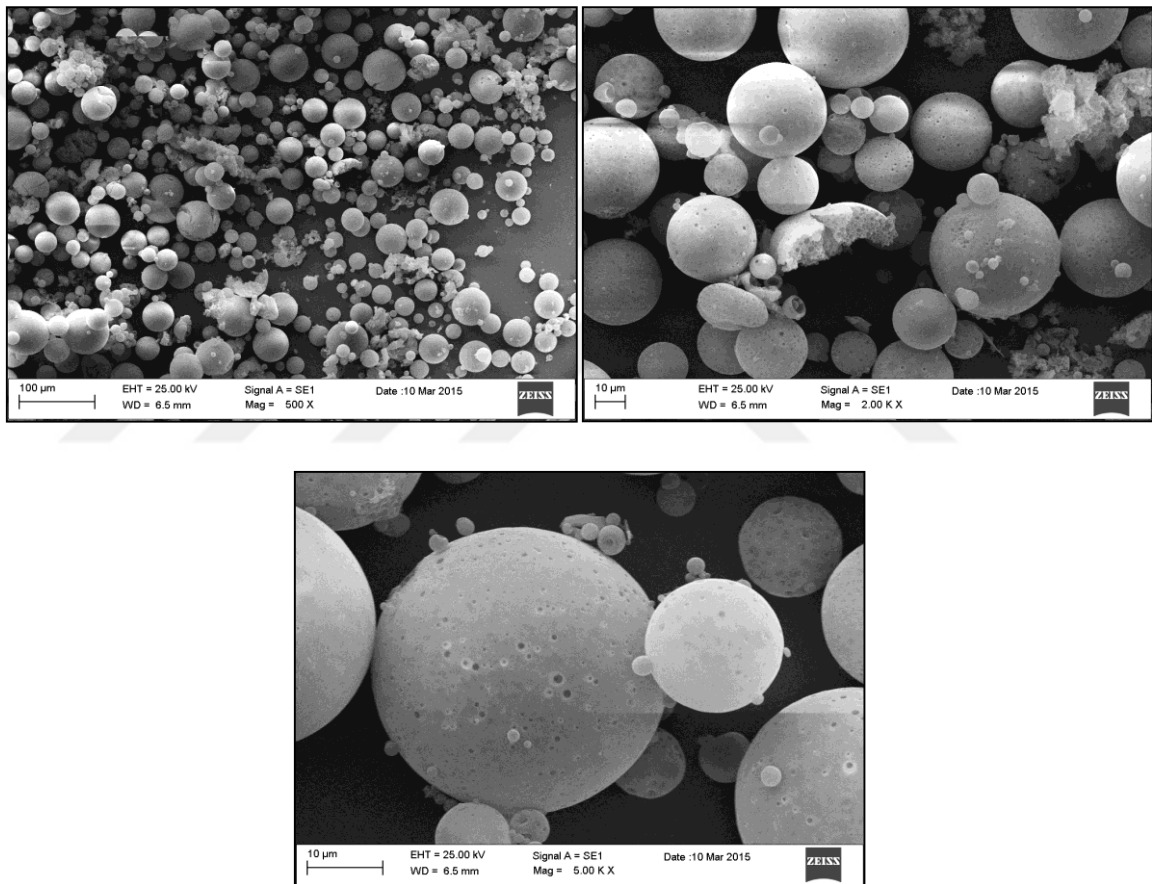
Figure 5.11. SEM images of Sample 2

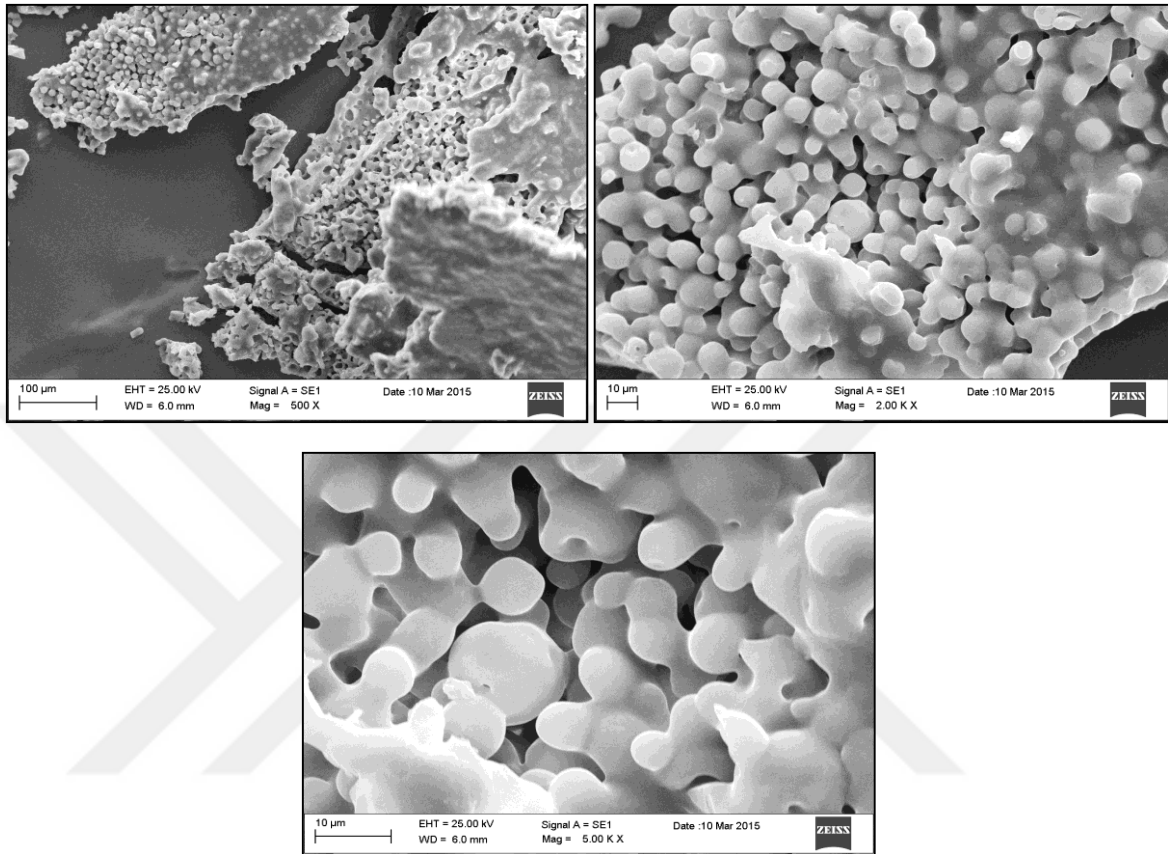Figure 5.12. SEM images of Sample 3

5.3.3. Synthesis of Crosslinked Polymer Particles Using Homogenizer

In this Section, emulsion which was prepared with SDS in water was homogenized at different rpm's then this emulsion was placed under UV lamp to obtain crosslinked polymer particles. For the optimization of crosslinked polymer particles synthesis using homogenizer, the parameters are given in Table 5.5.

Table 5.5. Parameters for the Optimization of Crosslinked Polymer Nanoparticles Synthesis Using Homogenizer

Sample	Homogenizer Speed	Initiator %	UV time (minutes)
1	2000	2	60
2	10000	2	60
3	10000	3	60

5.3.3.1. *Fourier transform infrared spectroscopy (FTIR) analysis of the crosslinked polymer particles synthesis using homogenizer*

Salarian et al. [88] showed FTIR spectra of PPF and crosslinking the synthesized PPF nanocomposites using N-VP. In this study, the peak at 1645 cm^{-1} (C=C stretching band) disappeared and the disappearance of the C=C stretching band confirmed the crosslink reaction which consumed the C=C double bond. In our study, the FTIR spectra of pure PPF, Sample 2 and Sample 3 are given in Figure 5.13.The major characteristic peaks are identified at 1715 and 1644 cm^{-1} in the spectrum of PPF as shown in Figure 5.13a, corresponding to the the C=O stretching, C=C stretching bands, respectively. In the FTIR spectra of Sample 2 and Sample 3, the peak at 1644 cm^{-1} that shows C=C double bond decreases after the crosslinking reaction between the PPF and VP. After the crosslinking reaction, the peak at 1715 cm^{-1} that belongs to C=O stretching should remain constant whereas the peak at 1644 that belongs to C=C stretching must decrease its intensity. There is no significant change on the peak at 1644 cm^{-1} of Sample 3 when the initiator (BAPO) was increased. For the synthesis of polymer nanoparticles 2% BAPO seems to suffice.
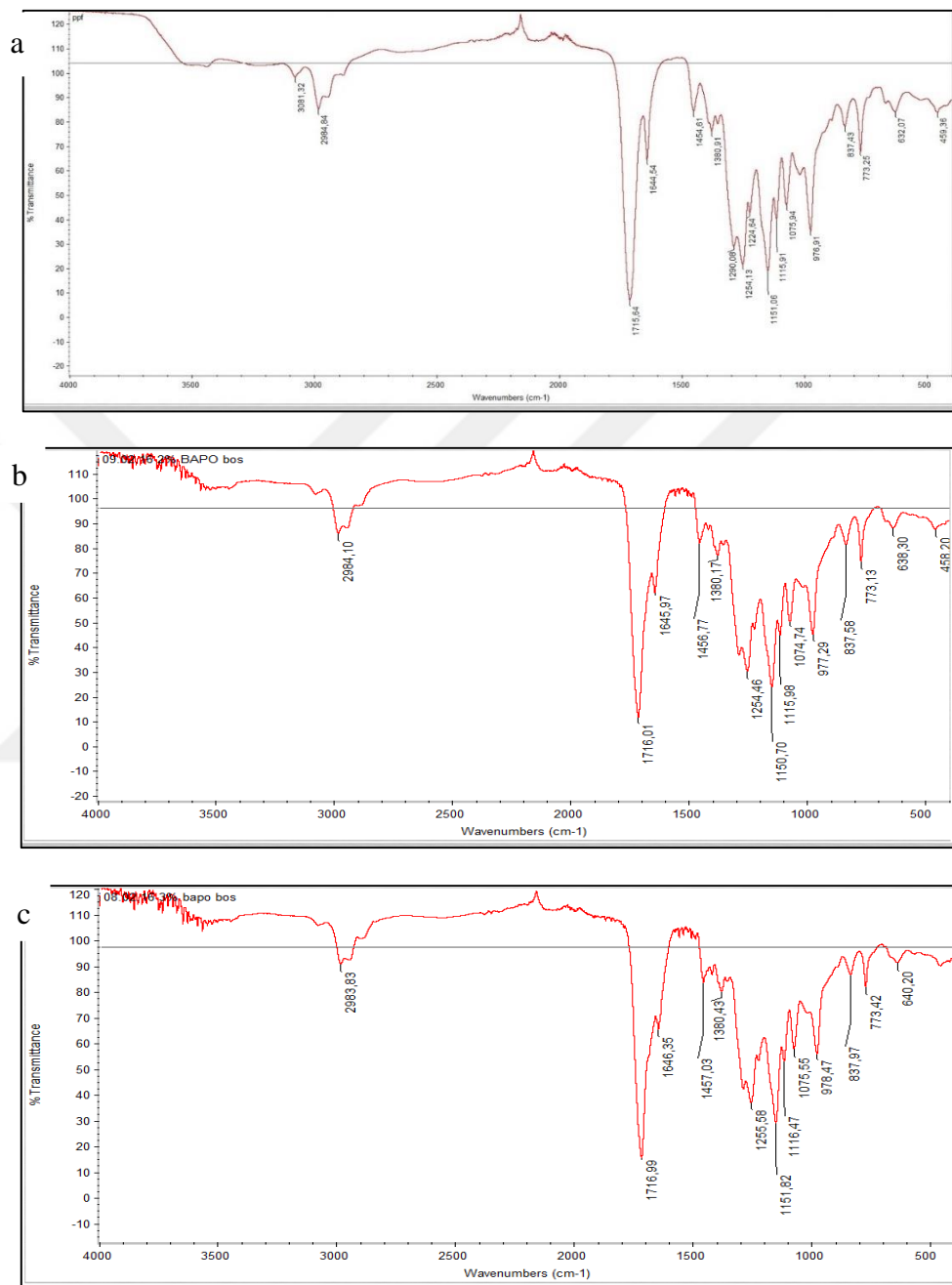
Figure 5.13. ATR spectra of (a) PPF (b) Sample 2 and (c) Sample 3

5.3.3.2. SEM images of crosslinked polymer particles synthesis using homogenizer

Sample 1 was synthesized using homogenizer at 2000 rpm and 5 min. The average size of Sample 1 was approximately 10 μm as seen in Figure 5.14. The beads appear to be porous.
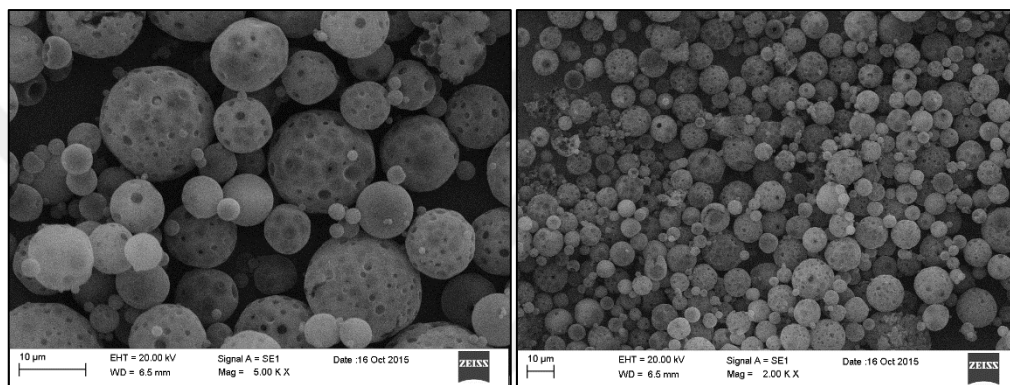
Figure 5.14. SEM images of Sample 1

Sample 2 was homogenized at 10000 rpm for 5 min. This increase in rpm lead to a decrease in the size of the beads to 500 nm as shown in Figure 5.15. The surface of the Sample 2 was smooth. SEM images showed generally homogeneous particle size distribution. A histogram showing the size distribution of crosslinked polymer nanoparticles as determined from SEM analysis is shown in Figure 5.16.

Figure 5.15. SEM images of Sample 2

Figure 5.16 shows that the diameter size range of crosslinked polymer nanoparticles are between 100 to 800 nm with an average diameter of 403 $\pm$ 128 nm.

Figure 5.16. Size distribution of crosslinked polymer particles

For Sample 3, the amount of initiator was increased compared to that used in Sample 2. Increase in BAPO initiator content had no effect on the particle size and morphology of Sample 3. SEM images of Sample 3 are given in Figure 5.17.
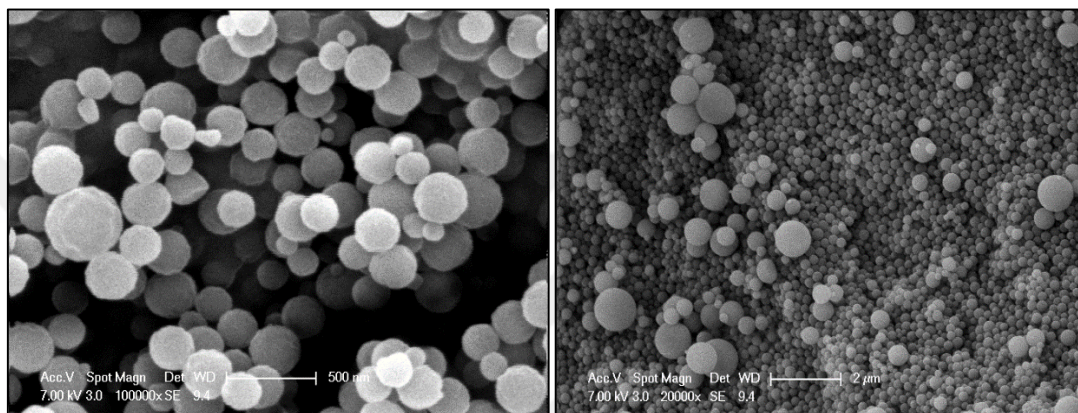
Figure 5.17. SEM images of Sample 3

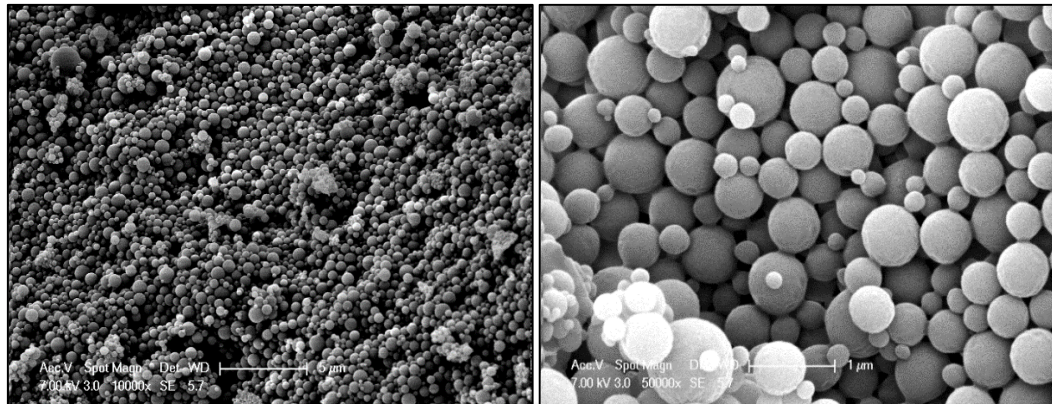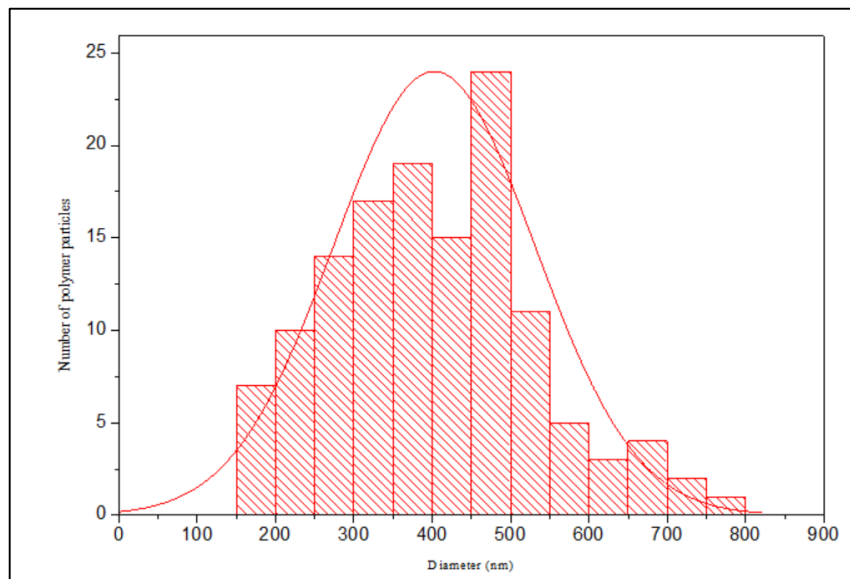Landfester et al. [133] produced polyacrylonitrile nanoparticles in the size range of 100-180 nm by miniemulsion polymerization technique using SDS as the surfactant. In our study, the size of the obtained polymer nanoparticles was 403 ± 128 nm which are larger but still in the acceptable range.

5.3.3.3. Synthesis of Crosslinked polymer nanoparticles with MNP's by photo initiated miniemulsion polymerization method

Magnetic nanoparticles were incorporated into crosslinked polymer nanoparticles using photo initiated miniemulsion polymerization technique. Magnetic nanoparticles were synthesized by coprecipitation and partial oxidation method. While the mean diameters of spherical magnetite particles can be obtained between 30 and 100 nm by partial oxidation method, the size of magnetic nanoparticles was in the 5 to 12 nm range by co-precipitation method. In addition, MNP's were coated with oleic acid or citric acid to prevent agglomeration.

Characterization of the crosslinked polymer nanoparticles loaded with MNP's that are synthesized by co precipitation method

Solubility Analysis : The solubility of the synthesized crosslinked polymer nanoparticles with oleic acid coated MNP's is tested in dichloromethane. Some particles were soluble in DCM and these samples are given in Table 5.6. Samples in Table 5.6 were all synthesized using homogenizer at 10000 rpm for 5 min. For crosslinked polymer nanoparticles with MNP's, UV time affects crosslinked density. When the UV time decreased to 30 and 45 min, crosslinking between the PPF and VP decreased and therefore, polymer particles were soluble in DCM.

Table 5.6. Solubility for Preparation of Polymer Nanoparticles with MNP's (Coprecipitation Method)

Sample	Concentration of magnetite	Number of washing cycles	UV time (min)	Inititor %
1	4%	2	30	2
2	4%	2	45	2
3	4%	3	30	2

Table 5.6. Solubility for Preparation of Polymer Nanoparticles with MNP's (Coprecipitation Method) (cont.d)

4	4%	3	45	2
5	8%	3	30	2
6	8%	3	45	2
7	4%	3	45	3

As neither of these particles was insoluble in DCM, no further analysis was carried out. Different parameters were tried to synthesise crosslinked polymer nanoparticles. The parameters that led to insoluble particles are given in Table 5.7. The initiator amount for samples in Table 5.7 was 2% except Sample 10. In Sample 10, initiator amount was increased to 3%.

Table 5.7. Parameters for Optimization of Polymer Nanoparticle Synthesis with Magnetite (oleic acid synthesis by coprecipitation method)

Sample	Homogenizer Speed	Homogenizer Time	Concentration of MNP's	Number of washing cycles	Method of magnetite addition	UV time (minutes)
1	2000	5	1%	2	Dry	60
2	2000	5	2%	2	wet	60
3	6000	5	2%	2	wet	60
4	10000	5	2%	2	wet	60
5	10000	5	2%	2	dry	60
6	10000	5	4%	2	dry	60
7	10000	5	6%	2	dry	60

8	10000	5	8%	2	dry	60

Table 5.7. Parameters for Optimization of Polymer Nanoparticle Synthesis with Magnetite (oleic acid synthesis by coprecipitation method) (cont.d)

9	10000	5	4%	2	dry	120
10	10000	5	4%	3	dry	60
11	10000	5	4%	3	dry	30

Table 5.8. Parameters for Optimization of Polymer Nanoparticle Synthesis with Magnetite (citric acid synthesis by coprecipitation method)

Sample	Homogenizer Speed	Homogenizer Time	Concentration of MNP's	Number of washing cycles	Method of MNPs addition	UV time (min)
12	10000	5	%4	2	dry	60
13	10000	5	%8	2	dry	60

FTIR spectra : The ATR spectra of crosslinked polymer nanoparticles with MNP's are shown in Figure 5.18. In ATR spectrum of Sample 6, 7, 8 and 10, the peak at 1644 cm^{-1} that shows C=C double bond is decreased compared to that of PPF. However, the peak at 1644 cm^{-1} was observed to decrease less when compared with crosslinked polymer particles without MNP's. When the magnetite concentration was increased, the decrease in the peak at 1644 cm^{-1} is not clearly observed, suggesting crosslinking either did not to take place or was minimal.
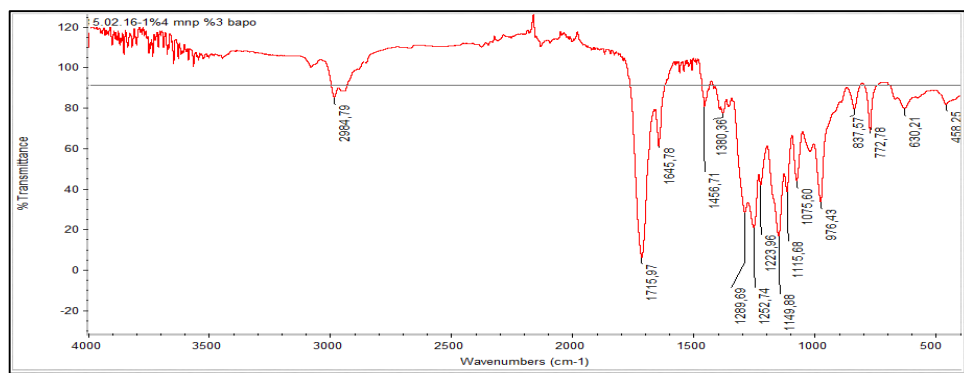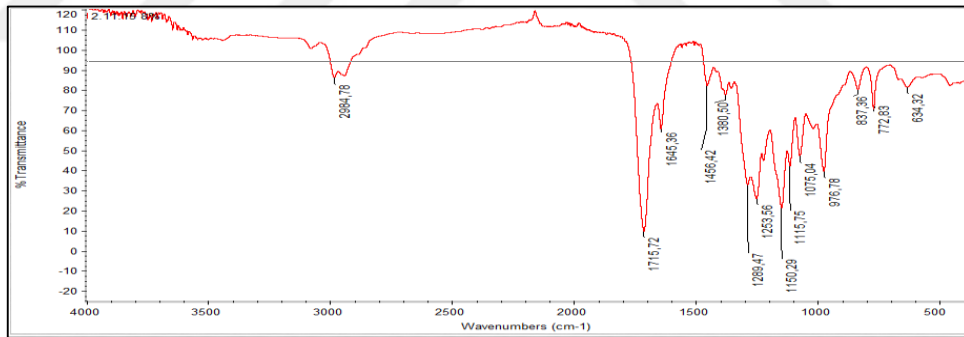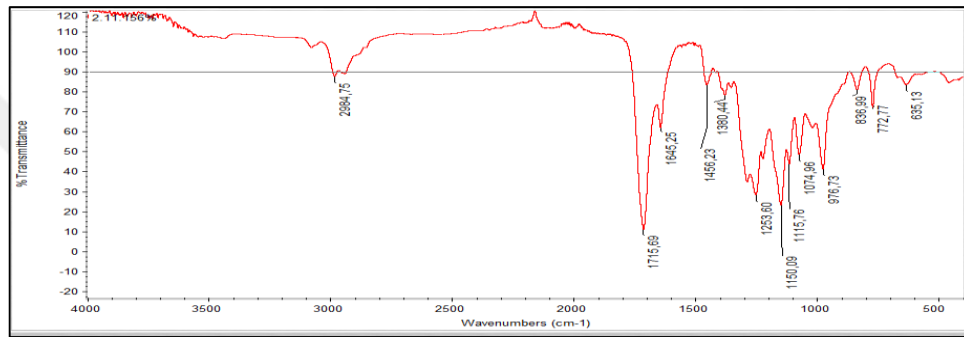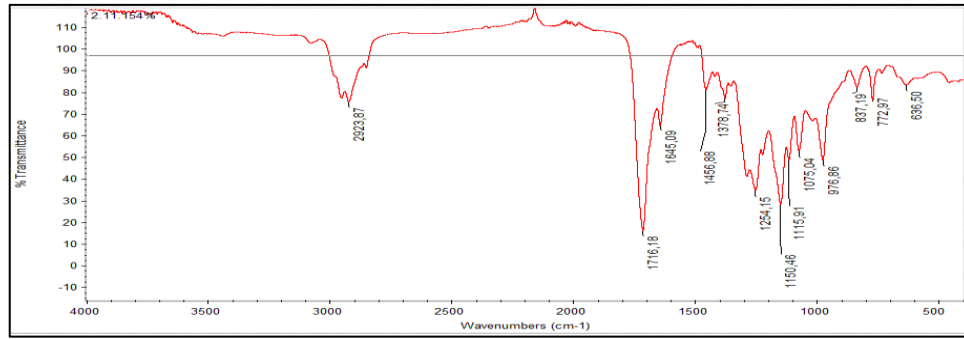
Figure 5.18. FTIR spectra of Sample 6,7,8 and 10

SEM images of crosslinked polymer nanoparticles synthesized with magnetite

Sample 1 included 1% concentration of oleic acid coated MNP's. Sample 1 was homogenized at 2000 rpm for 5 min. The mean size of the beads was measured to be approximately 5 μm according to SEM images. Some hollow structures were observed also in the beads as shown in Figure 5.19.

In Sample 1, dry magnetite was used to obtain crosslinked polymer nanoparticles with magnetite. While Sample 2, 3 and 4 were synthesized, magnetite (concentration as 2%) was dissolved in DCM and added into polymer solution. Samples were homogenized at different rpm for 5 min and the changes of the morphology are shown in Figure 5.20. It appears that as the homoganization rate is increased, the morphology of the obtained particles worsened.

This is unique to polymer particles containing magnetite. During the synthesis of polymer particles without the magnetite, increasing the homogenization speed led to the formation of smaller particles.
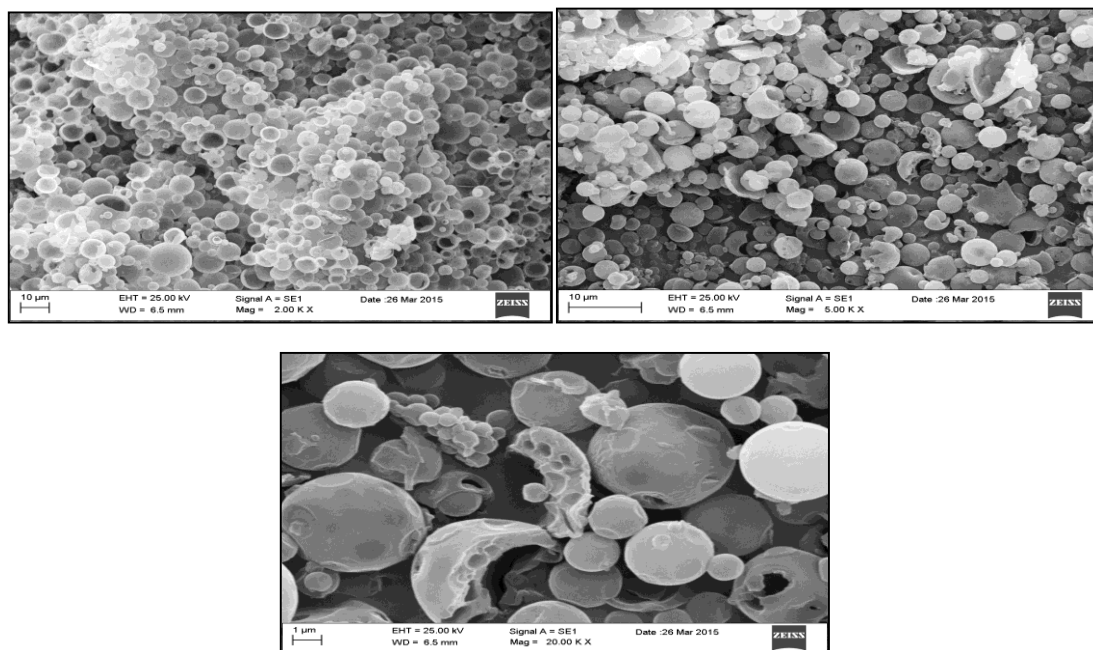
Figure 5.19. SEM images of Sample 1

Sample 5 was prepared using the same method as Sample 4. But, dry MNP's were added to the polymer solution instead of wet MNP's. SEM image of Sample 5 was observed to be similar to SEM image of Sample 4, again showing that at high homogenization speeds, particles are not even obtained although the MNP's were introduced in a different method as shown in Figure 5.21.

For Samples 6, 7 and 8, the effect of increasing of magnetite concentration was investigated. This samples were homogenized at 10000 rpm for 5 min. With increasing the oleic acid coated MNP's, the structure of the beads gradually changed. When the magnetite concentration was increased 2 times (Sample 8) with respect Sample 6, oleic acid coated MNP's covered all beads. Therefore, beads in Sample 8 did not even appear as shown in Figures 5.22, 5.23, 5.24.
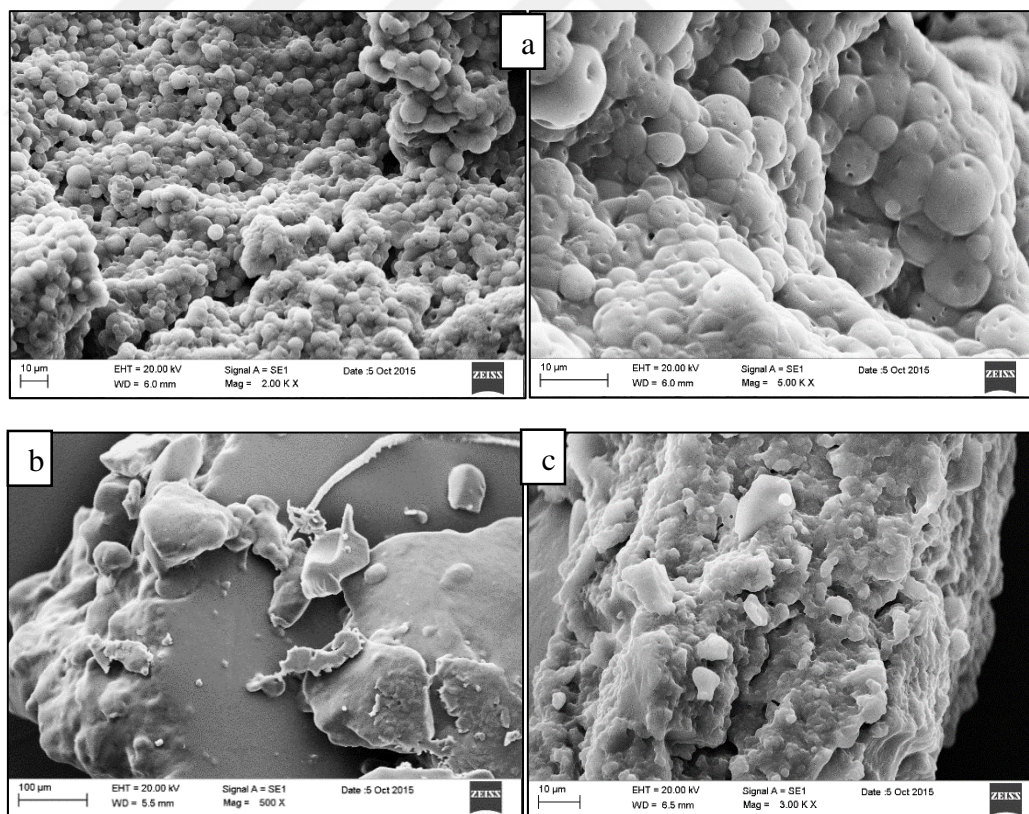
Figure 5.20. SEM images of (a) Sample 2 at 2000 rpm (b) Sample 3 at 6000 rpm and

(c) Sample 4 at 10000 rpm
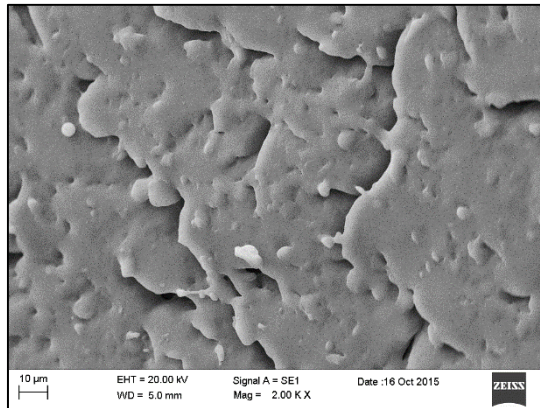
Figure 5.21. SEM images of Sample 5
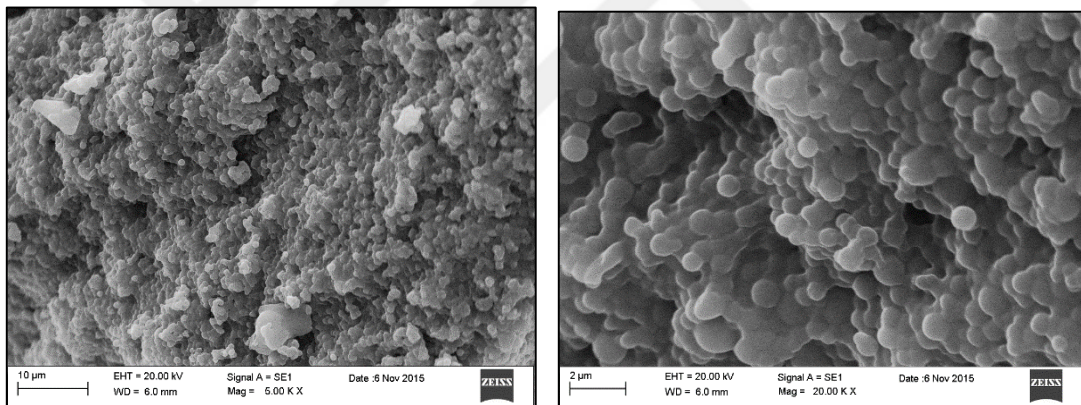
Figure 5.22. SEM images of Sample 6
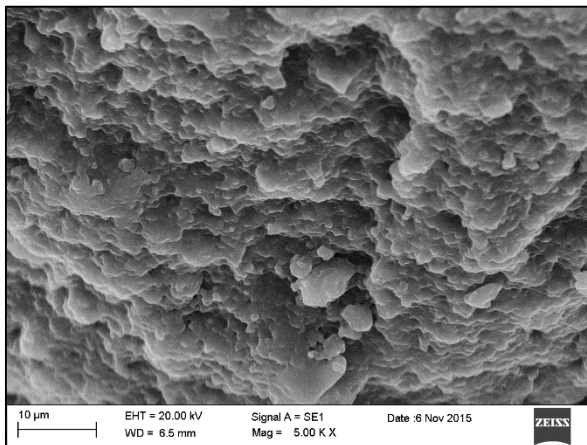
Figure 5.23. SEM images of Sample 7
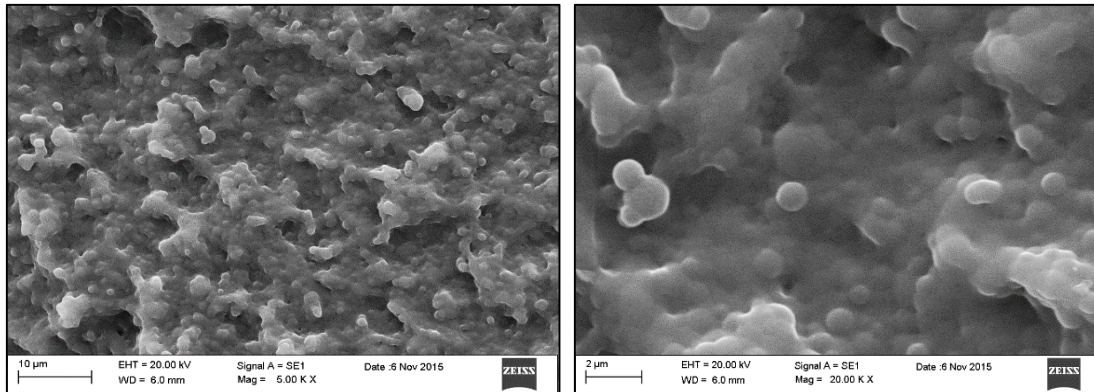
Figure 5.24. SEM images of Sample 8

To quickly check if formation of particles are hindered as a result of incomplete crosslinking due to the presence of MNP's, UV irradiation time was doubled (120 min). No improvement in the morphology was observed. SEM images of Sample 9 are shown in Figure 5.25.
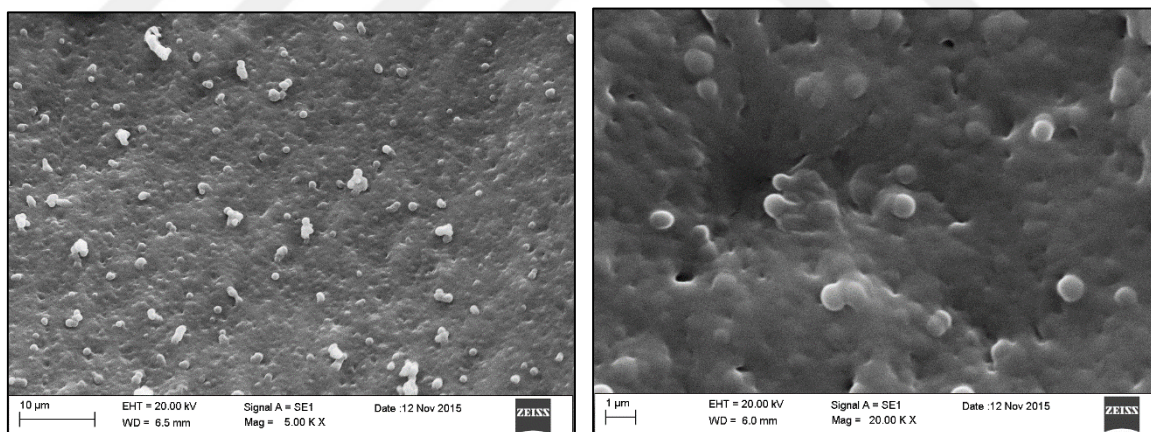
Figure 5.25. SEM images of Sample 9

Similarly, increasing the amount of initiator form 2% to 3% also did not cause any improvement in the formation of nanoparticles as shown in Figure 5.26.
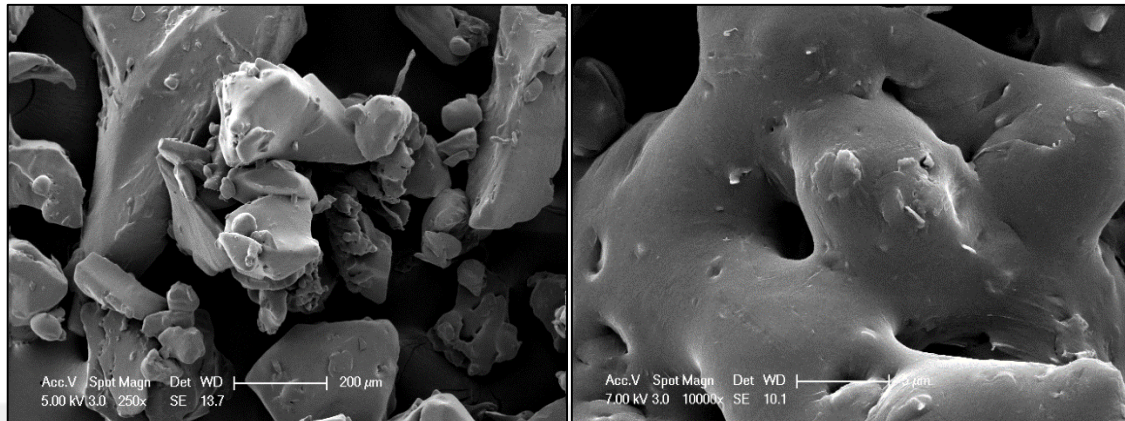
Figure 5.26. SEM images of Sample 10

The synthesized oleic acid coated magnetite nanoparticles were washed with acetone 2 times to remove excess oleic acid. However, according to the SEM images of crosslinked polymer nanoparticles with MNP's, it should be noted that excess oleic acid can cause appearance of non spherical beads. All beads were covered with oleic acid. Therefore, number of washing cycles was increased to 3.

Sample 11 was synthesized using oleic acid coated MNP's which were washed 3 times. With increasing the number of washing, the obtained beads were much more identifiable in the size range of about 500 nm as shown in Figure 5.27.

To overcome the potential problems of the pesence of oleic acid in the medium, citric acid coated MNP's were used to obtain crosslinked polymer nanoparticles with magnetite (Sample 12 and 13). Coating with citric acid provides water soluble magnetic nanoparticles. Therefore, citric acid coated MNP's were added to aqueous solution including surfactant (SDS). Addition of citric acid coated MNP's resulted in particles with undefined shapes as shown in Figure 5.28. Therefore, no further experiments were performed with citric acid.
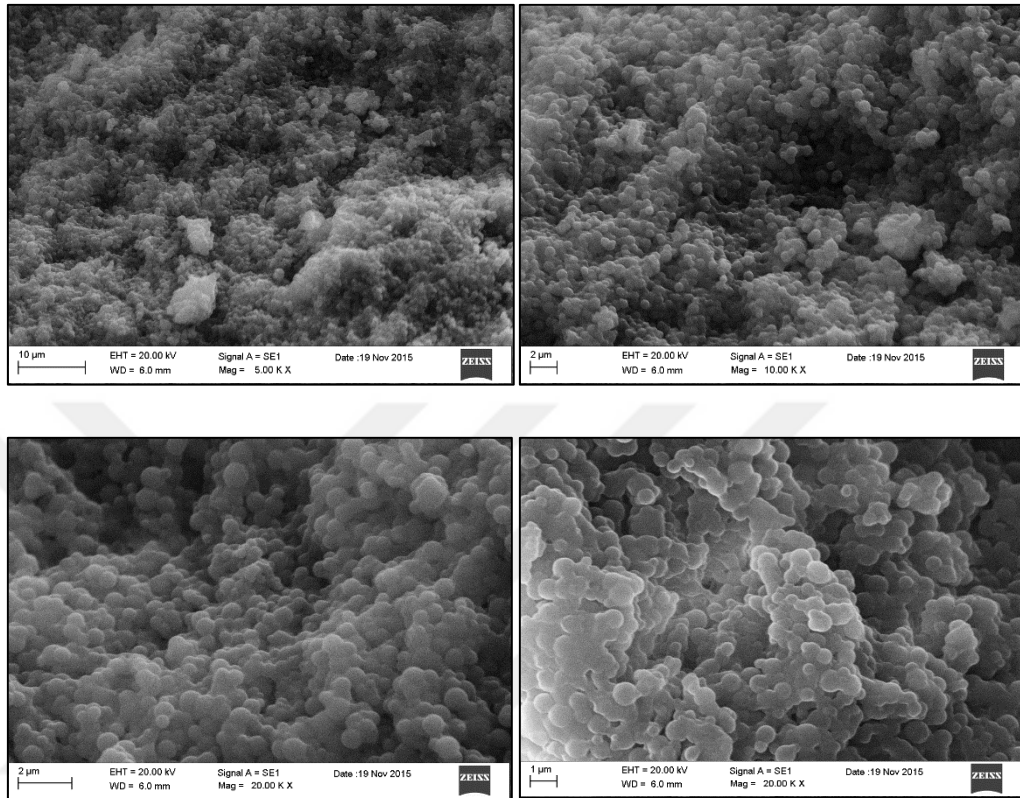
Figure 5.27. SEM images of Sample 11
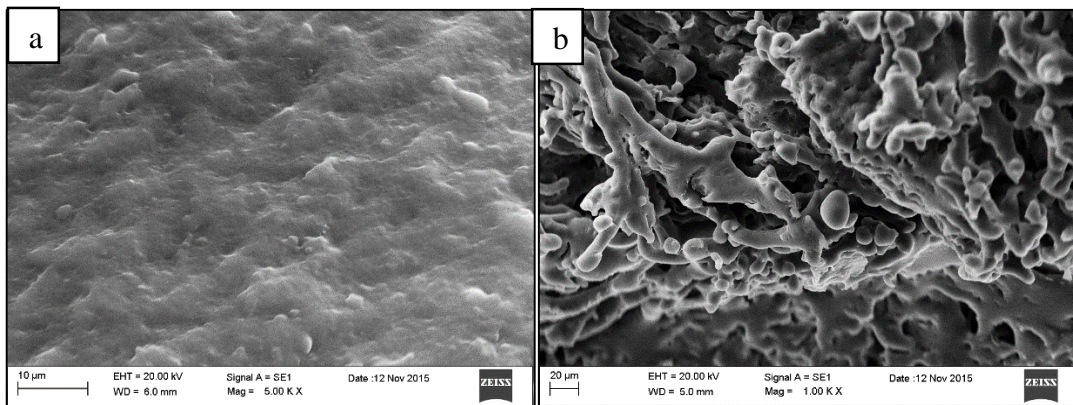
Figure 5.28. SEM images of (a) Sample 12 4% concentration and (b) Sample 13 8% concentration of citric acid

When the concentration of magnetite which are synthesized by coprecipitation method is increased, the morphology of the obtained particles worsened. Therefore, synthesized magnetic nanoparticles by partial oxidation method are used to obtain polymeric beads with higher magnetic properties using low magnetite concentration. The size of magnetic nanoparticles by partial oxidation is larger than size of synthesized magnetic nanoparticles by co precipitation method and their saturation magnetization values are higher. The parameters for the optimization of crosslinked polymer particles synthesis using MNP's by synthesized partial oxidation method are given in Table 5.9.

Table 5.9. Optimization of Crosslinked Polymer Nanoparticle Synthesis with Magnetite (partial oxidation method)

Sample	Concentration of magnetite	Method of MNP's addition	Freezing method	Number of washing cycles
1	2%	Dry	-80	-
2	4%	Dry	-80	-
3	4%	Wet (droper)	-80	-
4	4%	Wet (droper)	Liq N_2	3

FTIR spectra of crosslinked polymer nanoparticles with magnetite (partial oxidation method)

FTIR analysis of Sample 2, 3 and 4 are presented in Figure 5.29. After crosslinking reaction, the peak at 1644 cm^{-1} in the spectrum of Sample 2, 3, and 4 decreases compared to pure PPF. Decreasing the peak at 1644 cm^{-1} of Sample 2 and Sample 3 is very similar although the MNP's are added with different methods. Sample 4 was frozen using liquid nitrogen and obtained crosslinked polymer nanoparticles with MNP's were washed with water 3 times. FTIR analysis of Sample 4 showed that the peak at 1644 cm^{-1} in the spectrum was observed to decrease more when compared with Sample 3, indicating more crosslinking has taken place.

SEM images of crosslinked polymer nanoparticles with magnetite

In Sample 1, dried MNP's (2 wt%) were added and obtained crosslinked polymer nanoparticles were frozen at -80 ℃. In Sample 1 beads are not even distinguished as shown in Figure 5.30. When the magnetite concentration was increased from 2% to 4%, beads of Sample 2 appeared similar as shown in Figure 5.31.

In Sample 3, dissolved magnetite in DCM was added while organic and aqueous solution were homogenized. When the magnetite was added with this method, the obtained beads were more identifiable as shown in Figure 5.32.

The same method was used in Sample 4. But, Sample 4 was frozen using liquid nitrogen and obtained particles were washed with water 3 times. Spherical shaped beads were obtained. SEM images in Figure 5.33 showed that the average size of beads was 319 nm. Polymeric beads with magnetite that are obtained in Sample 4 are very similar to those without the magnetite. This shows that addition of magnetite prepared by partial oxidation overcomes some of the issues with the synthesis and that desired particles are now obtained.

Diz et al.[134] investigated magnetic and non-magnetic PLGA– PVA nanoparticles. PLGA–PVA nanoparticles were prepared by emulsion-solvent evaporation method and magnetite was incorporated. The nanoparticles had an average size of 50 nm. The incorporation of magnetite into the NPs did not change their size. In our study, MNP's were incorporated into crosslinked

PPF/VP nanoparticles. A histogram showing the size distribution of crosslinked polymer nanoparticles with MNP's as determined from SEM analysis is shown in Figure 5.34. Figure 5.34 shows that the size diameters range of crosslinked polymer nanoparticles with MNP's are between 100 to 900 nm with an average diameter of 319 ± 109 nm. MNP loaded polymer nanoparticles are somewhat smaller than the empty ones, however considering the large polydispersity, this is not very significant.
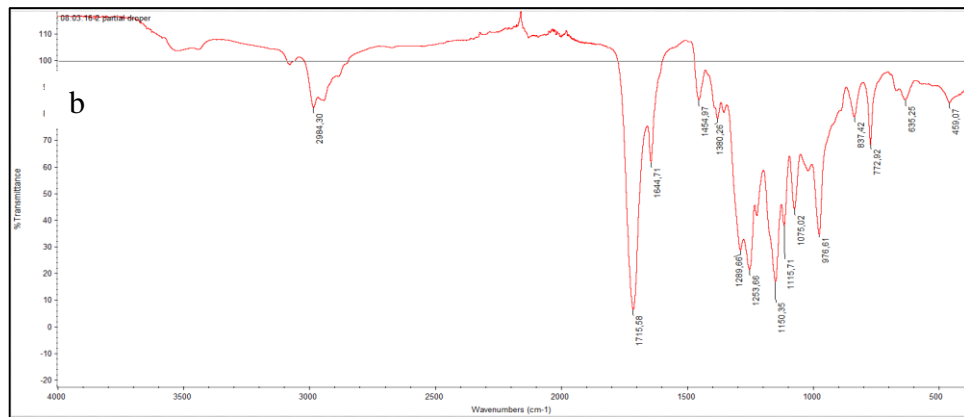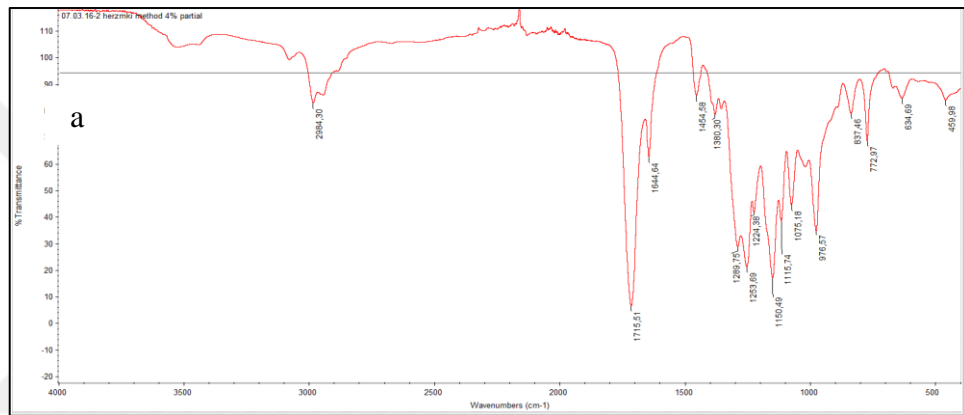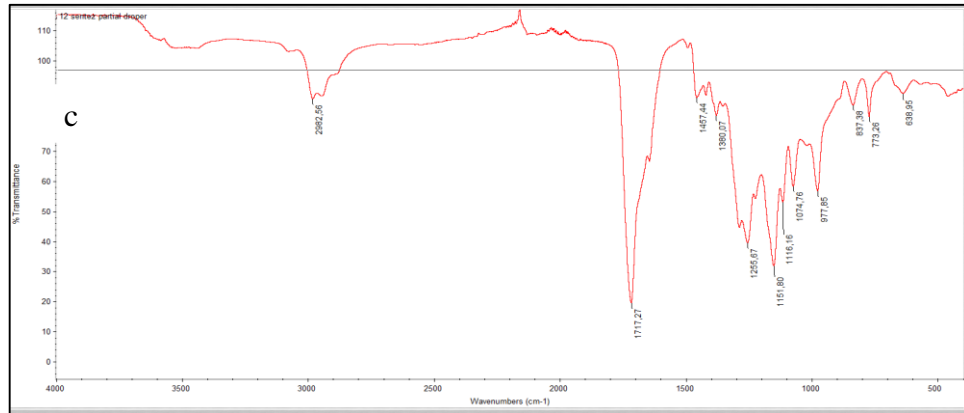
Figure 5.29. FTIR analysis of (a) Sample 2 (b) Sample 3 and (c) Sample 4
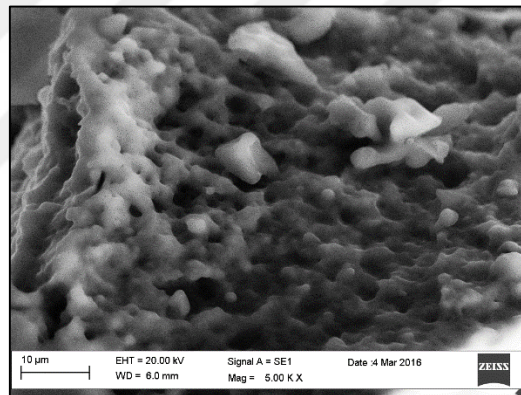
Figure 5.30. SEM images of Sample 1
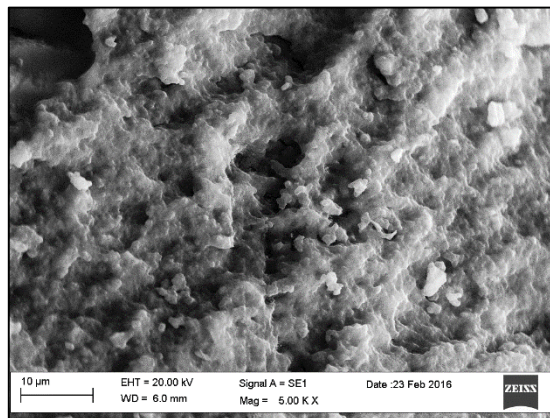
Figure 5.31. SEM images of Sample 2
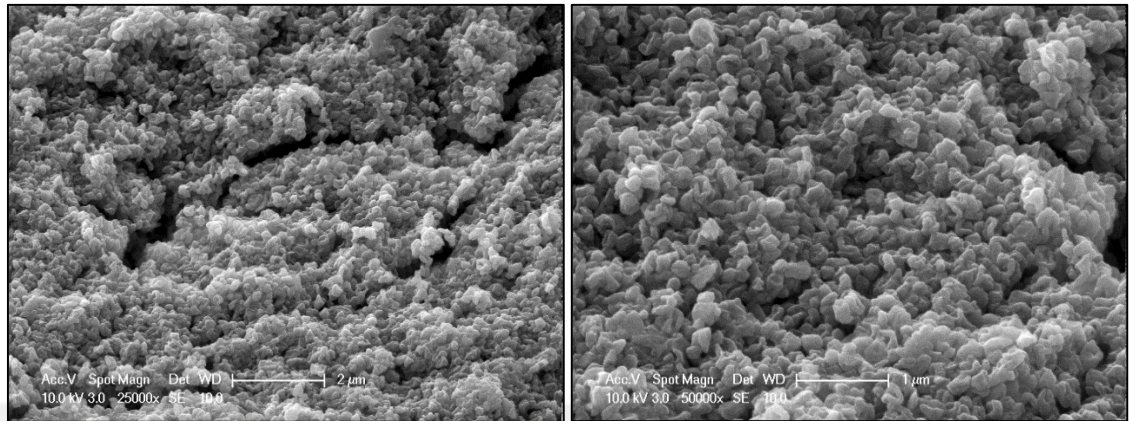
Figure 5.32. SEM images of Sample 3
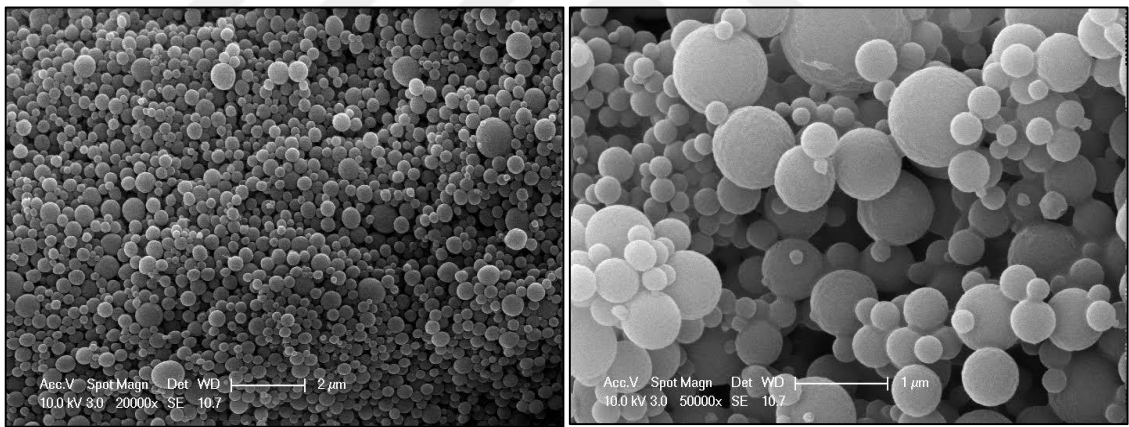
Figure 5.33. SEM images of Sample 4
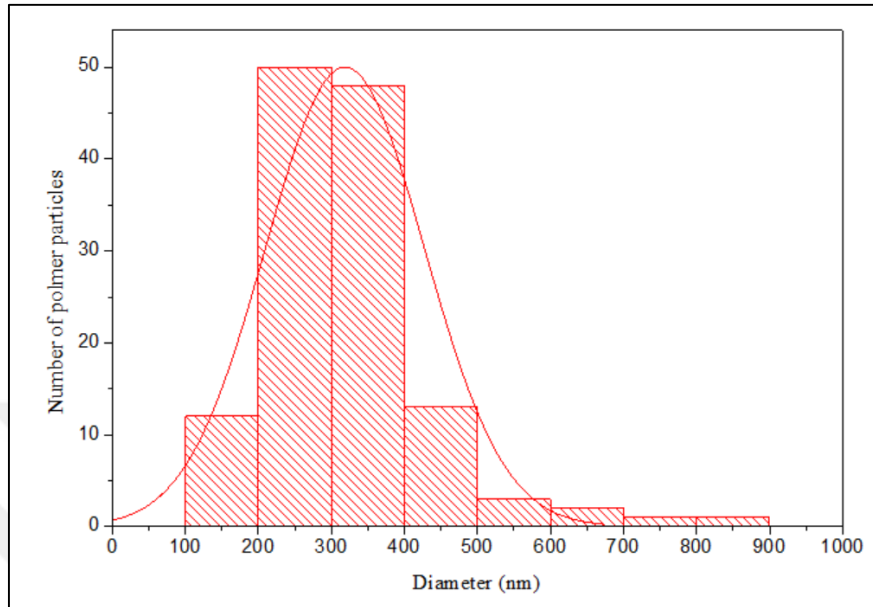
Figure 5.34. Size distribution of crosslinked polymer nanoparticles with MNP's

5.4. BIOCOMPATIBILTY STUDIES OF CROSSLINKED POLYMER NANOPARTICLES

Venkatesh et al [135] reported SDS to be toxic and that it affects the survival of aquatic animals such as fishes, microbes like yeasts and bacteria. Singer and Tjeerdema [136] reported that SDS is known to cause harmful effects on humans and animals, which consume water contaminated with it. Lindberg et. al [137] reported that repeated exposures of SDS causes skin irritation and hyperplasia in guinea pigs. Therefore, biocompatible study was performed for synthesized crosslinked polymer nanoparticles using SDS. Firstly, the crosslinked polymer nanoparticles were washed 3 times with water to remove residual SDS and then dried crosslinked polymer nanoparticles were suspended in dimethyl sulfoxide (DMSO). This solution was diluted with cell media for various nanoparticle solution concentrations (0.1%, 0.05%, 0.02%, 0.01%, 0.005%, 0.001%) and were treated with HUVECs and tested by MTS assay in order to determine the biocompatibility of the crosslinked polymer nanoparticles. MTS measurements were performed for 24, 48 and 72 hours.

Accoarding to Figure 5.35, NC refers the control cells that were grown in the cell media that does not contain crosslinked polymer NPs with SDS. Figure 5.35 refers crosslinked polymer nanoparticles with SDS cell viability for 0.1% containing sample. Control samples that contain some amount of DMSO in their medium were used as negative control since these polymer particles are suspended in DMSO. It is clearly seen that approximately 75% of cells survived at the end of 72 hours comparing to negative control which was grown in cell medium. Therefore, crosslinked polymer nanoparticles with SDS showed relatively non toxic effect for HUVEC cells.
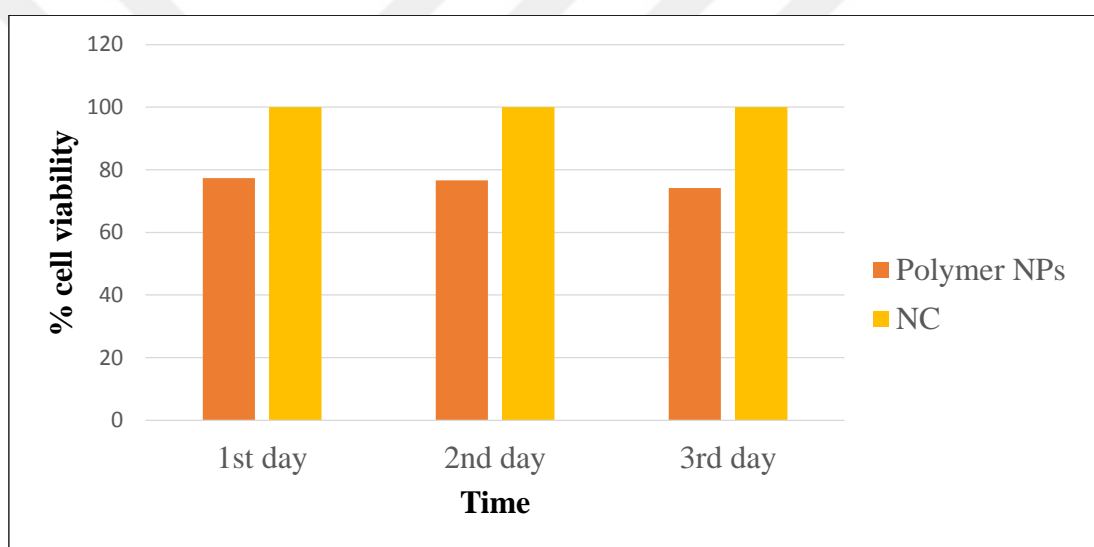
Figure 5.35. Cytotoxicity for 0.1% containing crosslinked polymer NPs with SDS

5.5. DEGRADATION RESULTS

Crosslinked polymer nanoparticles with and without magnetite were prepared as described in Section 4.6 for degradation studies. The synthesized crosslinked particles were divided into 4 almost equal amounts (~ 0.15 g) and 10 mL PBS at pH 7.4 was added to each sample. For pH measurements, the pH values were recorded daily for the first 5 days and then weekly. The average pH values are given in Table A.1 in Appendix A.

During degradation studies, acidic medium occurred due to the hydrolysis of polymer (PPF) that leads to the formation of fumaric acid therefore, pH decreased over time. pH profiles for the crosslinked polymer nanoparticles with and without magnetite are given in Figure 5.36.

According to Figure 5.36, pH value of crosslinked polymer nanoparticles without MNP's started at 7.17 and after 6 weeks the pH value was recorded nearly as 4.5 due to release of fumaric acid during the degradation of PPF. For crosslinked polymer nanoparticles with MNP's pH values started at 6.84 and decreased to about 4.
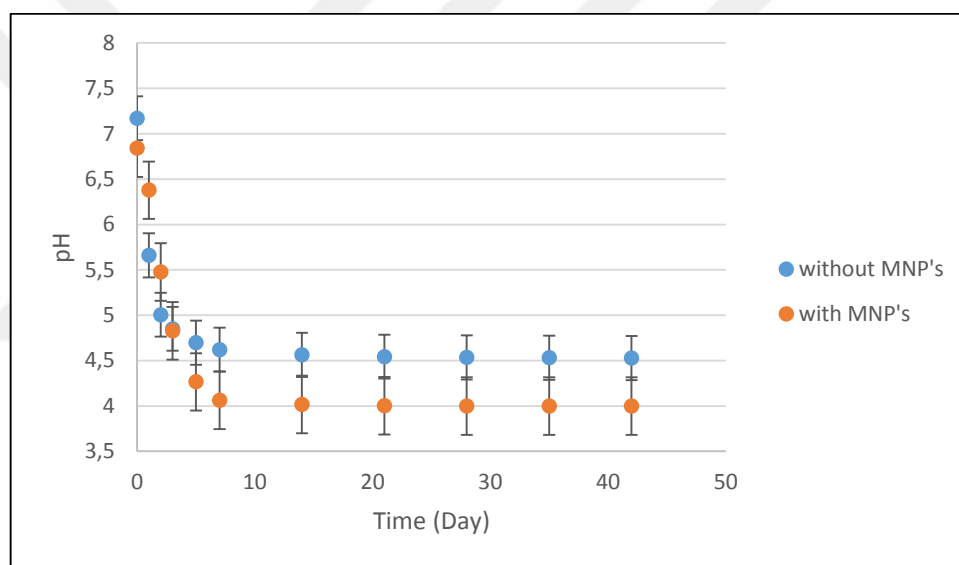
Figure 5.36. pH versus Time graphs of crosslinked polymer nanoparticles with and without MNP's

Weight loss is another method to follow the degradation of polymers. The percentages of weight loss are calculated from weight loss measurements of the crosslinked polymer nanoparticles with and without MNP's. Weight loss values of the both crosslinked polmer nanoparticles are given in Table A.2 in Appendix. The weight loss percentage versus time graph is shown in Figure 5.37. About 54% of the beads are found to degrade within 6 weeks.
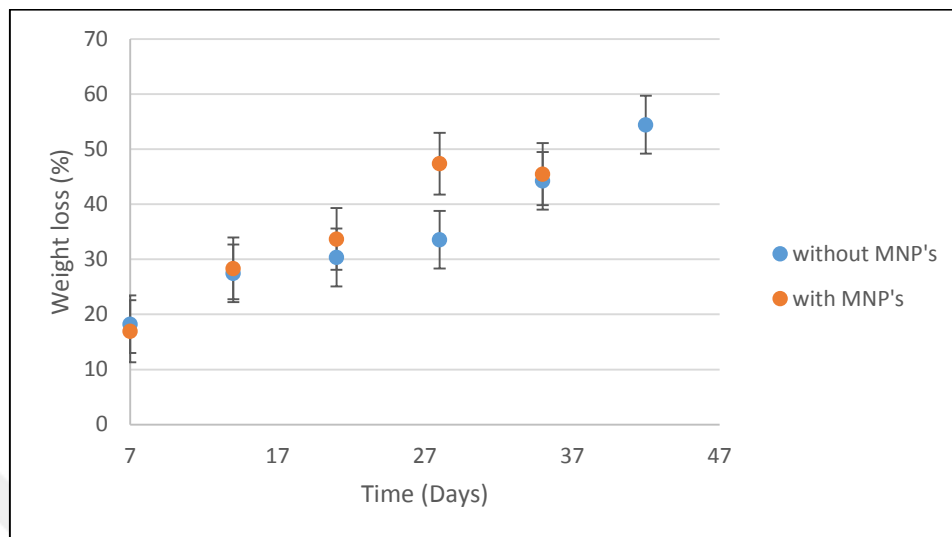
Figure 5.37. Weight Loss versus Time Graphs of crosslinked polymer nanoparticles with and without MNP's

Both pH and weight loss measurements show that the addition MNP's to PPF nanoparticles increases the degradation rate in PBS buffer solution.

Timmer et al. [138] examined the effect of crosslinking density, medium pH, and the change in weight on the in vitro degradation of photo-crosslinked networks of PPF/PPF-DA (diacrylate) over a 52-week period. PPF/PPF-DA networks with the lower crosslinking density demonstrated the greatest degradation with a 17% mass loss. In our study, after synthesis of crosslinked PPF nanoparticles without MNP's, the cross-link density was calculated by swelling studies in THF. A relatively low cross-link density of approximately 70% was obtained. The addition MNP's to the crosslinked polymer nanoparticles showed further decrease in cross-link density (data not shown) which may explain the higher degradation rate of the PPF-MNP nanocomposites as compared to PPF nanoparticles.

5.6. HIGH PERFORMANCE LIQUID CHROMATOGRAPHY RESULTS

High Performance Liquid Chromatography (HPLC) was used to determine the amount of paclitaxel released from crosslinked polymer nanoparticles with and without magnetite.

Three parallel series were studied to investigate drug release from crosslinked polymer nanoparticles with and without magnetite. First of all, the amounts of nonencapsulated drug were measured by HPLC from which the encapsulated amounts are calculated. The amounts of the nonencapsulated paclitaxel are tabulated in Table A.3 in Appendix A.

The amounts of released drug in the receiving medium (i.e. PBS buffer at pH 7.4) were measured through 30 days using HPLC. The amounts of the released paclitaxel are given in Table A.4 in Appendix A.

Fonseca et al. [139] studied that PLGA nanospheres loaded with Paclitaxel were prepared by adding an organic solution of PLGA and Paclitaxel in acetone to an aqueous poloxamer 188 solution. PTX release showed fast initial release during the first 24 h followed by a slower and continuous release over the next 9 days. Bernabeu et al. [140] studied Paclitaxel-loaded PCL–TPGS nanoparticles. PTX-loaded NPs were prepared using PCL–TPGS by emulsion-solvent evaporation using an ultrasonicator as homogenizer. The amount of drug released from the NPs in the first 24 h was approximately 20%. After 96 h, the PTX release was approximately 45%. In our work, at 4 days, 5% of drug was released from the crossliked PPF/VP nanoparticles by photo initiated miniemulsion polymerization technique.

The paclitaxel release profiles of crosslinked polymer nanoparticles with and without magnetite are shown in Figure 5.38. At the end of 22 days all the encapsulated drug is found to be released. The obtained system can be preferred if long release times without initial burst is required.
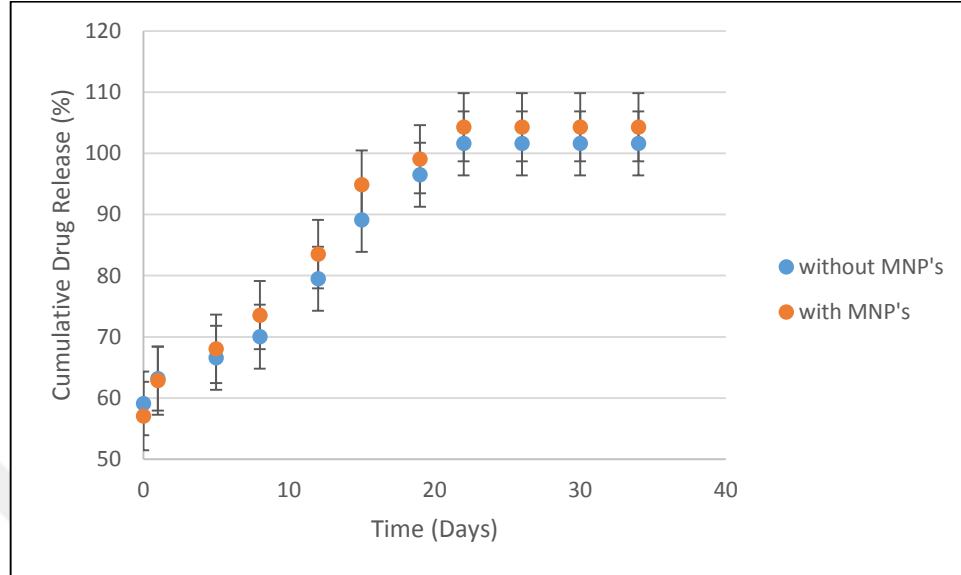
Figure 5.38. Cumulative paclitaxel released (%) vs. time graph of paclitaxel in crosslinked polymer nanoparticles with and without magnetite

Comparing the release profiles, the drug release appears to be similar in the presence of magnetic nanoparticles with the empty ones. Comparing the degradation profiles and drug release, it is clear that the drug is released before the degradation of the polymer. Only about 35% of the polymer bead has degraded when all the drug is released. Therefore, the drug release mechanism can be suggested to be predominantly diffusion controlled rather than degradation, although degradation controlled drug release is very likely to concurrently take place.

6. CONCLUSION AND FUTURE WORK

6.1. CONCLUSION

In this project, the aim is to develop a new drug delivey system. Polypropylene fumarate (PPF) which is a biocompatible polymer is used to produce biodegradable nanoparticles to be used as drug carriers and magnetic nanoparticles are embedded in these NPs to target a localized disease site within the body. In this project, PPF was crosslinked with vinylpyrrolidone (VP) using two methods. Firstly, PPF was crosslinked with VP at 90 ℃ to obtain crosslinked polymer particles. The size and morphology of obtained crosslinked polymer particles were determined using SEM. In synthesis of crosslinked polymer nanoparticles at 90 ℃, the desired size and morphology could not be obtained. Furthermore, high temperature synthesis is not suitable for drug applications. Therefore, this method discoutinued. For further experiments photo initiated miniemulsion polymerization method was developed.

In photo initiated miniemulsion polymerization method, crosslinked polymer nanoparticles were formed using UV irradiation. In this method, two different surfactants were used. Firstly, crosslinked polymer particles were produced using Tween80 as the surfactant. Oleic acid coated MNP's were incorporated in crosslinked polymer particles to obtain magnetic crosslinked polymer particles. The size and morphology of obtained crosslinked polymer particles using Tween80 were determined by SEM. SEM images showed that the average size of beads were approximately 100-150 μm. To obtain crosslinked polymer particles in the desired size range (i.e.<500 nm) crosslinked polymer nanoparticles were synthesized using SDS as the surfactant.

Crosslinked polymer nanoparticles using SDS were synthesized using magnetic bar and homogenizer. When magnetic bar was used, obtained particles had an average size of 20-40 μm. To obtain even smaller particles homogenizer was used instead of using magnetic bar. Crosslinked polymer nanoparticles with desired size were obtained using homognizer at 10000 rpm 5 minutes.

SEM images showed that the size of the beads was approximately 500 nm. For these particles, FTIR spectra showed that crosslinking between PPF and VP is successful.

Magnetic nanoparticles were incorporated into crosslinked polymer nanoparticles. Magnetic nanoparticles were synthesized by coprecipitation and partial oxidation method. For crosslinked polymer nanoparticles with MNP's that are synthesized by co precipitation method, FTIR analysis showed the crosslinking of PPF with VP. However, the morphology of the particles was unsatisfactory. Different parameters were used to obtained crosslinked polymer nanoparticles with MNP's in the desired morphlogy and size range. However, when the magnetite concentration is increased, the morphology of the obtained particles worsened. To overcome this problem, synthesized magnetic nanoparticles by partial oxidation method are used to obtain polymeric beads with higher magnetic properties even at low magnetite concentrations.

For crosslinked polymer nanoparticles with MNP's that are synthesized by partial oxidation method, different methods were used based on the addition of MNP's. When dissolved magnetite was added while organic and aqueous solution were homogenized the obtained beads were more identifiable. In addition, when these beads were washed with water and freezed using liquid nitrogen, desired shaped beads were obtained.

Degradation of these polymer particles with and without MNP's were investigated with pH and weight change measurements. In degradation studies, due to release of fumaric acid during the degradation of PPF pH decreased over time. About 50% of the beads are found to degrade within 6 weeks.

Finally, crosslinked polymer nanoparticles with and without MNP's were loaded with Paclitaxel. The amount of drug release from particles was determined by HPLC. These crosslinked polymer nanoparticles released all the encapsulated drug in less than one month and the presence of magnetite was shown not to have a significant effect on the drug release profile.

Biocompatible study was performed for synthesized crosslinked polymer nanoparticles using SDS. Synthesized crosslinked polymer nanoparticles were shown to be non toxic, proving that these particles can indeed be used as drug delivery systems in the body.

In summary, PPF and VP were crosslinked to synthesize polymer nanoparticles using photo initiated miniemulsion polymerization method. These polymer nanoparticles were embedded with magnetite nanoparticles and a model anti cancer drug paclitaxel was incorporated in the polymer matrix to obtain a magnetic drug delivery vehicle. All the encapsulated drug was to shown to be released from the polymeric carrier and based on degradation studies, the drug relase mechanism was suggested to be diffusion controlled. This work shows that photo initiated miniemulsion polymerization is a viable method to obtain polymer nanoparticles in the presence of magnetic nanoparticles encapsulating a drug in situ. This new delivery vehicle can be used to target a variety of drugs of interest due to the magnetic properties of the drug delivery system.

6.2. FUTURE WORK

In this work, we have shown that PPF can be cross liked with VP in UV initiated emulsion polymerization to obtain nanoparticles of desirable sizes. These nanoparticles can be synthesized in the presence of pre-synthesized magnetic nanoparticles to obtain magnetic polymer nanoparticles which can also be used to encapsulate an anti-cancer drug, namely paclitaxel. Drug release and degradation profiles are also investigated. However, there are several areas where the reseach can fold in the future.

The cross link density of the obtained nanoparticles is quite low and these particles may benefit from higher cross linkig densities. Therefore, in the synthesis the PPF and VP ratio, along with the amount of initiator and duration of UV exposure can be altered to obtain particles with different crosslinking densities. Upon determination of cross-link densities by sweeling studies, degradation and drug release profiles from these nanoparticles can be explored to obtain systems with a range of drug release profiles.

For crosslinked polymer nanoparticles with and without MNP's, the crosslinking density will be repeated and the crossliking density can be increased.

Although not included in this report, these particles showed promise to be used in targeted drug delivery. Due to their magnetic properties, which should be revealed by magnetization studies using vibrating sample magnetometer, these particles can be further explored in targeted drug delivery. If required higher amounts of magnetite doping in the polymer nanoparticle can also be investigated.

REFERENCES

1. S. Lv, M. Li, Z. Tang, W. Song, H. Sun, H. Liu, and X. Chen, Doxorubicin-Loaded Amphiphilic Polypeptide-Based Nanoparticles As An Efficient Drug Delivery System For Cancer Therapy. *Acta Biomaterialia*, 12:9330-9342, 2013.

2. K. Cho, X. Wang, S. Nie, and D.M. Shin, Therapeutic Nanoparticles For Drug Delivery In Cancer. *Clinical Cancer Research*, 5:1310-1316, 2008.

3. G. Soni and K.S. Yadav, Applications of Nanoparticles In Treatment and Diagnosis of Leukemia. *Materials Science and Engineering: C*:156-164, 2015.

4. D. Bhowmik, H. Gopinath, B.P. Kumar, S. Duraivel, and K.S. Kumar, Controlled Release Drug Delivery Systems. *The Pharma Innovation*, 10, 2012.

5. O.C. Farokhzad and R. Langer, Impact of Nanotechnology On Drug Delivery. *ACS Nano*, 1:16-20, 2009.

6. J.M. Chan, L. Zhang, K.P. Yuet, G. Liao, J.-W. Rhee, R. Langer, and O.C. Farokhzad, PLGA–Lecithin–PEG Core–Shell Nanoparticles For Controlled Drug Delivery. *Biomaterials*, 8:1627-1634, 2009.

7. R.A. Petros and J.M. Desimone, Strategies In The Design of Nanoparticles For Therapeutic Applications. *Nature Reviews Drug Discovery*, 8:615-627, 2010.

8. J.H. Lee and Y. Yeo, Controlled Drug Release From Pharmaceutical Nanocarriers. *Chemical Engineering Science*:75-84, 2015.

9.   A. Bangham, M.M. Standish, and J. Watkins, Diffusion of Univalent Ions Across The Lamellae Of Swollen Phospholipids. *Journal Of Molecular Biology*, 38-227, 1965.

10.   D.C. Drummond, O. Meyer, K. Hong, D.B. Kirpotin, and D. Papahadjopoulos, Optimizing Liposomes For Delivery of Chemotherapeutic Agents To Solid Tumors. *Pharmacological Reviews*, 4:691-744, 1999.

11.   S.K. Sahoo and V. Labhasetwar, Nanotech Approaches To Drug Delivery and Imaging. *Drug Discovery Today*, 24:1112-1120, 2003.

12.   O.M. Koo, I. Rubinstein, and H. Onyuksel, Role of Nanotechnology In Targeted Drug Delivery And Imaging: A Concise Review. *Nanomedicine: Nanotechnology, Biology and Medicine*, 3:193-212, 2005.

13.   J.V. Natarajan, C. Nugraha, X.W. Ng, and S. Venkatraman, Sustained-Release From Nanocarriers: A Review. *Journal of Controlled Release*:122-138, 2014.

14.   B. Mishra, B.B. Patel, and S. Tiwari, Colloidal Nanocarriers: A Review On Formulation Technology, Types and Applications Toward Targeted Drug Delivery. *Nanomedicine: Nanotechnology, Biology and Medicine*, 1:9-24, 2010.

15.   Y. Barenholz, Doxil-The First FDA-Approved Nano-Drug: Lessons Learned. *Journal of Controlled Release*, 2:117-134, 2012.

16.   V.P. Torchilin, Recent Advances With Liposomes As Pharmaceutical Carriers. *Nature Reviews Drug Discovery*, 2:145-160, 2005.

17.   K. Kono, T. Ozawa, T. Yoshida, F. Ozaki, Y. Ishizaka, K. Maruyama, C. Kojima, A. Harada, and S. Aoshima, Highly Temperature-Sensitive Liposomes Based On A Thermosensitive Block Copolymer For Tumor-Specific Chemotherapy. *Biomaterials*, 27:7096-7105, 2010.

18. A. Schroeder, R. Honen, K. Turjeman, A. Gabizon, J. Kost, And Y. Barenholz, Ultrasound Triggered Release of Cisplatin From Liposomes In Murine Tumors. *Journal Of Controlled Release*, 1:63-68, 2009.

19. S. Simões, J.N. Moreira, C. Fonseca, N. Düzgüneş, and M.C.P. De Lima, On The Formulation of Ph-Sensitive Liposomes With Long Circulation Times. *Advanced Drug Delivery Reviews*, 7:947-965, 2004.

20. V.P. Torchilin, Multifunctional Nanocarriers. *Advanced Drug Delivery Reviews*:302-315, 2012.

21. J. Panyam and V. Labhasetwar, Biodegradable Nanoparticles For Drug and Gene Delivery To Cells And Tissue. *Advanced Drug Delivery Reviews*, 3:329-347, 2003.

22. J. Panyam, M.M. Dali, S.K. Sahoo, W. Ma, S.S. Chakravarthi, G.L. Amidon, R.J. Levy, and V. Labhasetwar, Polymer Degradation and In Vitro Release of A Model Protein From Poly (D, L-Lactide-Co-Glycolide) Nano-And Microparticles. *Journal of Controlled Release*, 1:173-187, 2003.

23. E. Pérez-Herrero and A. Fernández-Medarde, Advanced Targeted Therapies In Cancer: Drug Nanocarriers, The Future Of Chemotherapy. *European Journal of Pharmaceutics and Biopharmaceutics*:52-79, 2015.

24. G.S. Kwon and T. Okano, Polymeric Micelles As New Drug Carriers. *Advanced Drug Delivery Reviews*, 2:107-116, 1996.

25. M.C. Jones, H. Gao, And J.C. Leroux, Reverse Polymeric Micelles For Pharmaceutical Applications. *Journal of Controlled Release*, 3:208-215, 2008.

26. S. Ganta, H. Devalapally, A. Shahiwala, and M. Amiji, A Review of Stimuli-Responsive Nanocarriers For Drug and Gene Delivery. *Journal of Controlled Release*, 3:187-204, 2008.

27. B.K. Nanjwade, H.M. Bechra, G.K. Derkar, F. Manvi, and V.K. Nanjwade, Dendrimers: Emerging Polymers For Drug-Delivery Systems. *European Journal of Pharmaceutical Sciences*, 3:185-196, 2009.

28. Y. Cheng, J. Wang, T. Rao, X. He, and T. Xu, Pharmaceutical Applications of Dendrimers: Promising Nanocarriers For Drug Delivery. *Frontiers In Bioscience: A Journal And Virtual Library*:1447-1471, 2007.

29. J.B. Wolinsky and M.W. Grinstaff, Therapeutic and Diagnostic Applications of Dendrimers For Cancer Treatment. *Advanced Drug Delivery Reviews*, 9:1037-1055, 2008.

30. M.K. Khan, S.S. Nigavekar, L.D. Minc, M.S. Kariapper, B.M. Nair, W.G. Lesniak, and L.P. Balogh, In Vivo Biodistribution of Dendrimers and Dendrimer Nanocomposites-Implications For Cancer Imaging and Therapy. *Technology In Cancer Research and Treatment*, 6:603-613, 2005.

31. G.A. Hughes, Nanostructure-Mediated Drug Delivery. *Nanomedicine: Nanotechnology, Biology And Medicine*, 1:22-30.

32. M. Liu And J.M. Fréchet, Designing Dendrimers For Drug Delivery. *Pharmaceutical Science and Technology Today*, 10:393-401, 1999.

33. R. Singh And J.W. Lillard, Nanoparticle-Based Targeted Drug Delivery. *Experimental and Molecular Pathology*, 3:215-223, 2009.

34. W.B. Turnbull and J.F. Stoddart, Design and Synthesis of Glycodendrimers. *Reviews In Molecular Biotechnology*, 3–4:231-255, 2002.

35. J. Kreuter, *Colloidal Drug Delivery Systems*, Vol 66 CRC Press, 1994.

36. K. Park, G.Y. Lee, Y.S. Kim, M. Yu, R.W. Park, I.S. Kim, S.Y. Kim, and Y. Byun, Heparin–Deoxycholic Acid Chemical Conjugate As An Anticancer Drug Carrier And Its Antitumor Activity. *Journal Of Controlled Release*, 3:300-306, 2006.

37. C.M.J. Hu, S. Aryal, and L. Zhang, Nanoparticle-Assisted Combination Therapies For Effective Cancer Treatment. *Therapeutic Delivery*, 2:323-334, 2010.

38. L. Brannon-Peppas and J.O. Blanchette, Nanoparticle and Targeted Systems For Cancer Therapy. *Advanced Drug Delivery Reviews*, 11:1649-1659, 2004.

39. X. Wang, Y. Wang, Z.G. Chen, and D.M. Shin, Advances of Cancer Therapy By Nanotechnology. *Cancer Research and Treatment*, 1:1-11, 2009.

40. J.A. Hubbell, Biomaterials In Tissue Engineering. *Bio/Technology (Nature Publishing Company)*, 6:565-576, 1995.

41. R. Thomson, M. Wake, M.J. Yaszemski, and A. Mikos. Biodegradable Polymer Scaffolds To Regenerate Organs. In, *Biopolymers Ii*. Pages 245-274. Springer, 1995.

42. P.A. Gunatillake and R. Adhikari, Biodegradable Synthetic Polymers For Tissue Engineering. *Eur Cell Mater*, 1:1-16, 2003.

43. E.P. Herrero, M.J. Alonso, and N. Csaba, Polymer-Based Oral Peptide Nanomedicines. *Therapeutic Delivery*, 5:657-668, 2012.

44. C.C. Lee, J.A. Mackay, J.M. Fréchet, and F.C. Szoka, Designing Dendrimers For Biological Applications. *Nature Biotechnology*, 12:1517-1526, 2005.

45.   A. Kumari, S.K. Yadav, and S.C. Yadav, Biodegradable Polymeric Nanoparticles Based Drug Delivery Systems. *Colloids and Surfaces B: Biointerfaces*, 1:1-18, 2010.

46.   S. Galindo-Rodriguez, E. Allémann, H. Fessi, and E. Doelker, Physicochemical Parameters Associated With Nanoparticle Formation In The Salting-Out, Emulsification-Diffusion, and Nanoprecipitation Methods. *Pharmaceutical Research*, 8:1428-1439, 2004.

47.   J.P. Rao and K.E. Geckeler, Polymer Nanoparticles: Preparation Techniques and Size-Control Parameters. *Progress In Polymer Science*, 7:887-913, 2011.

48.   F. Masood, Polymeric Nanoparticles For Targeted Drug Delivery System For Cancer Therapy. *Materials Science And Engineering: C*:569-578, 2016.

49.   E. Allemann, R. Gurny, and E. Doelker, Drug-Loaded Nanoparticles: Preparation Methods and Drug Targeting Issues. *European Journal of Pharmaceutics and Biopharmaceutics*, 5:173-191, 1993.

50.   N. Anton, J.P. Benoit, and P. Saulnier, Design and Production of Nanoparticles Formulated From Nano-Emulsion Templates-A Review. *Journal of Controlled Release*, 3:185-199, 2008.

51.   C.P. Reis, R.J. Neufeld, A.J. Ribeiro, and F. Veiga, Nanoencapsulation I. Methods For Preparation of Drug-Loaded Polymeric Nanoparticles. *Nanomedicine: Nanotechnology, Biology And Medicine*, 1:8-21, 2006.

52.   D. Quintanar-Guerrero, E. Allémann, H. Fessi, and E. Doelker, Preparation Techniques And Mechanisms of Formation of Biodegradable Nanoparticles From Preformed Polymers. *Drug Development And Industrial Pharmacy*, 12:1113-1128, 1998.

53.   E. Allémann, R. Gurny, and E. Doelker, Preparation of Aqueous Polymeric Nanodispersions by A Reversible Salting-Out Process: Influence of Process Parameters On Particle Size. *International Journal of Pharmaceutics*, 1:247-253, 1992.

54.   V. Mittal, *Miniemulsion Polymerization Technology*, Vol 34 John Wiley and Sons, 2011.

55.   S.C. Thickett and R.G. Gilbert, Emulsion Polymerization: State of The Art In Kinetics And Mechanisms. *Polymer*, 24:6965-6991, 2007.

56.   K. Landfester. Miniemulsions For Nanoparticle Synthesis. In, *Colloid Chemistry II*. Pages 75-123. Springer, 2003.

57.   J.C. Salamone, *Concise Polymeric Materials Encyclopedia*, Vol 1 CRC Press, 1998.

58.   K.E. Uhrich, S.M. Cannizzaro, R.S. Langer, and K.M. Shakesheff, Polymeric Systems For Controlled Drug Release. *Chemical Reviews*, 11:3181-3198, 1999.

59.   W.B. Liechty, D.R. Kryscio, B.V. Slaughter, and N.A. Peppas, Polymers For Drug Delivery Systems. *Annual Review of Chemical and Biomolecular Engineering*:149, 2010.

60.   R. Langer, New Methods of Drug Delivery. *Science*, 4976:1527-1533, 1990.

61.   E. Cauchetier, M. Deniau, H. Fessi, A. Astier, and M. Paul, Atovaquone-Loaded Nanocapsules: Influence of The Nature of The Polymer On Their In Vitro Characteristics. *International Journal of Pharmaceutics*, 1:273-281, 2003.

62.   Y. Fu And W.J. Kao, Drug Release Kinetics and Transport Mechanisms of Non-Degradable and Degradable Polymeric Delivery Systems. *Expert Opinion On Drug Delivery*, 4:429-444, 2010.

63. R. Langer and N. Peppas, Chemical and Physical Structure of Polymers As Carriers For Controlled Release of Bioactive Agents: A Review. *Journal of Macromolecular Science-Reviews In Macromolecular Chemistry and Physics*, 1:61-126, 1983.

64. W.L. Webber, F. Lago, C. Thanos, and E. Mathiowitz, Characterization of Soluble, Salt-Loaded, Degradable PLGA Films and Their Release of Tetracycline. *Journal of Biomedical Materials Research*, 1:18-29, 1998.

65. N.A. Peppas, P. Bures, W. Leobandung, and H. Ichikawa, Hydrogels In Pharmaceutical Formulations. *European Journal of Pharmaceutics and Biopharmaceutics*, 1:27-46, 2000.

66. S. Herrlich, S. Spieth, S. Messner, and R. Zengerle, Osmotic Micropumps For Drug Delivery. *Advanced Drug Delivery Reviews*, 14:1617-1627, 2012.

67. R.A. Keraliya, C. Patel, P. Patel, V. Keraliya, T.G. Soni, R.C. Patel, and M. Patel, Osmotic Drug Delivery System As A Part Of Modified Release Dosage Form. *ISRN Pharmaceutics*, 2012.

68. M. Prabaharan, J.J. Grailer, S. Pilla, D.A. Steeber, and S. Gong, Amphiphilic Multi-Arm-Block Copolymer Conjugated With Doxorubicin Via Ph-Sensitive Hydrazone Bond For Tumor-Targeted Drug Delivery. *Biomaterials*, 29:5757-5766, 2009.

69. H.S. Yoo and T.G. Park, Biodegradable Polymeric Micelles Composed of Doxorubicin Conjugated PLGA–PEG Block Copolymer. *Journal of Controlled Release*, 1–2:63-70, 2001.

70. F.V. Burkersroda, L. Schedl, and A. Göpferich, Why Degradable Polymers Undergo Surface Erosion or Bulk Erosion. *Biomaterials*, 21:4221-4231, 2002.

71. E. Marin, M.I. Briceño, and C. Caballero-George, Critical Evaluation of Biodegradable Polymers Used In Nanodrugs. *International Journal of Nanomedicine*:3071, 2013.

72. W.C. Lee And I. Chu, Preparation and Degradation Behavior of Polyanhydrides Nanoparticles. *Journal Of Biomedical Materials Research Part B: Applied Biomaterials*, 1:138-146, 2008.

73. S. Fredenberg, M. Wahlgren, M. Reslow, and A. Axelsson, The Mechanisms of Drug Release In Poly (Lactic-Co-Glycolic Acid)-Based Drug Delivery Systems-A Review. *International Journal of Pharmaceutics*, 1:34-52, 2011.

74. A. Atala, *Synthetic Biodegradable Polymer Scaffolds*: Springer Science and Business Media, 1997.

75. J.P. Fisher, T.A. Holland, D. Dean, and A.G. Mikos, Photoinitiated Cross-Linking of The Biodegradable Polyester Poly (Propylene Fumarate). Part II. In Vitro Degradation. *Biomacromolecules*, 5:1335-1342, 2003.

76. M.D. Timmer, C.G. Ambrose, and A.G. Mikos, In Vitro Degradation of Polymeric Networks of Poly (Propylene Fumarate) and The Crosslinking Macromer Poly (Propylene Fumarate)-Diacrylate. *Biomaterials*, 4:571-577, 2003.

77. M.D. Timmer, C.G. Ambrose, and A.G. Mikos, Evaluation of Thermal-and Photo-Crosslinked Biodegradable Poly (Propylene Fumarate)-Based Networks. *Journal of Biomedical Materials Research Part A*, 4:811-818, 2003.

78. F.K. Kasper, K. Tanahashi, J.P. Fisher, and A.G. Mikos, Synthesis of Poly (Propylene Fumarate). *Nature Protocols*, 4:518-525, 2009.

79. B. Baroli, Photopolymerization of Biomaterials: Issues and Potentialities In Drug Delivery, Tissue Engineering, and Cell Encapsulation Applications. *Journal of Chemical Technology and Biotechnology*, 4:491-499, 2006.

80. C. Esen and G. Schweiger, Preparation of Monodisperse Polymer Particles by Photopolymerization. *Journal of Colloid and Interface Science*, 1:276-280, 1996.

81. Z. Gao, E.A. Grulke, and A.K. Ray, Synthesis of Monodisperse Polymer Microspheres by Photopolymerization of Microdroplets. *Colloid and Polymer Science*, 8:847-854, 2007.

82. K. Park, *Controlled Drug Delivery: Challenges and Strategies*: Amer Chemical Society, 1997.

83. M.N. Cooke, J.P. Fisher, D. Dean, C. Rimnac, and A.G. Mikos, Use of Stereolithography To Manufacture Critical-Sized 3D Biodegradable Scaffolds For Bone Ingrowth. *Journal of Biomedical Materials Research Part B: Applied Biomaterials*, 2:65-69, 2003.

84. I. Gatlik, P. Rzadek, G. Gescheidt, G. Rist, B. Hellrung, J. Wirz, K. Dietliker, G. Hug, M. Kunz, and J.P. Wolf, Structure-Reactivity Relationships In Radical Reactions: A Novel Method For The Simultaneous Determination of Absolute Rate Constants And Structural Features. *Journal of The American Chemical Society*, 36:8332-8336, 1999.

85. C. Decker, K. Zahouily, D. Decker, T. Nguyen, and T. Viet, Performance Analysis of Acylphosphine Oxides In Photoinitiated Polymerization. *Polymer*, 18:7551-7560, 2001.

86. S. Jockusch and N.J. Turro, Phosphinoyl Radicals: Structure and Reactivity. A Laser Flash Photolysis and Time-Resolved ESR Investigation. *Journal of The American Chemical Society*, 45:11773-11777, 1998.

87. J.P. Fisher, M.D. Timmer, T.A. Holland, D. Dean, P.S. Engel, and A.G. Mikos, Photoinitiated Cross-Linking of The Biodegradable Polyester Poly (Propylene Fumarate). Part I. Determination of Network Structure. *Biomacromolecules*, 5:1327-1334, 2003.

88.   M. Salarian, W.Z. Xu, M.C. Biesinger, and P.A. Charpentier, Synthesis and Characterization of Novel Tio 2-Poly (Propylene Fumarate) Nanocomposites For Bone Cementation. *Journal of Materials Chemistry B*, 32:5145-5156, 2014.

89.   R.J. Farn, *Chemistry and Technology of Surfactants*: John Wiley and Sons, 2008.

90.   B. Kronberg and B. Lindman, *"Surfactants and Polymers In Aqueous Solution"*. 2003, John Wiley and Sons Ltd., Chichester.

91.   J.L. Salager, Surfactants Types and Uses. *Fire P Booket-E300-Attaching Aid In Surfactant Science and Engineering In English. Merida Venezuela*:3, 2002.

92.   C.J. Thoman, T.D. Habeeb, M. Huhn, M. Korpusik, and D.F. Slish, Use of Polysorbate 80 (Tween 80) As A Phase-Transfer Catalyst. *The Journal of Organic Chemistry*, 18:4476-4478, 1989.

93.   M. Yokoyama, Drug Targeting With Nano-Sized Carrier Systems. *Journal of Artificial Organs*, 2:77-84, 2005.

94.   U. Häfeli, Magnetically Modulated Therapeutic Systems. *International Journal of Pharmaceutics*, 1:19-24, 2004.

95.   J. Dobson, Magnetic Nanoparticles For Drug Delivery. *Drug Development Research*, 1:55-60, 2006.

96.   C.W. Chen, *Magnetism and Metallurgy of Soft Magnetic Materials*: Courier Corporation, 2013.

97.   A.S. Teja and P.Y. Koh, Synthesis, Properties, and Applications of Magnetic Iron Oxide Nanoparticles. *Progress In Crystal Growth And Characterization of Materials*, 1:22-45, 2009.

98.   S.V.E. Vonsovskii and R. Hardin, Magnetism. 1974.

99.   K.J. Klabunde and R. Richards, *Nanoscale Materials In Chemistry*: Wiley Online Library, 2009.

100.   E.P. Wohlfarth, *Ferromagnetic Materials: A Handbook On The Properties of Magnetically Ordered Substances*, Vol 2 Elsevier, 1980.

101.   W. Wu, Q. He, and C. Jiang, Magnetic Iron Oxide Nanoparticles: Synthesis and Surface Functionalization Strategies. *Cheminform*, 24:I, 2009.

102.   T. Indira and P. Lakshmi, Magnetic Nanoparticles-A Review. *Internatinal Journal Pharmaceutical Sciences and Nanotechnology*, 3:1035-1042, 2010.

103.   G.T. Burstein, The Iron Oxides: Structure, Properties, Reactions, Occurrence and Uses: R. M. Cornell and U. Schwertmann. 573 Pp. VCH, Weinheim and New York, 1996. ISBN: 3-527-28576-8. *Corrosion Science*, 8:1499-1500, 1997.

104.   U. Khan, A. Akbar, U. Ahmad, S. Riaz, and S. Naseem, Magnetic Behavior of Iron Oxide Thin Films For Biomedical Applications. *Materials Today: Proceedings*, 10, Part B:5421-5425, 2015.

105.   S.C. Mcbain, H.H. Yiu, and J. Dobson, Magnetic Nanoparticles For Gene and Drug Delivery. *International Journal of Nanomedicine*, 2:169, 2008.

106.   D. Chełminiak, M. Ziegler-Borowska, and H. Kaczmarek, Synthesis of Magnetite Nanoparticles Coated With Poly(Acrylic Acid) by Photopolymerization. *Materials Letters*:464-467, 2016.

107.   M.C. Mascolo, Y. Pei, and T.A. Ring, Room Temperature Co-Precipitation Synthesis of Magnetite Nanoparticles In A Large Ph Window With Different Bases. *Materials*, 12:5549-5567, 2013.

108. K. Petcharoen and A. Sirivat, Synthesis and Characterization of Magnetite Nanoparticles Via The Chemical Co-Precipitation Method. *Materials Science and Engineering: B*, 5:421-427, 2012.

109. G.F. Goya, Handling The Particle Size and Distribution of Fe_3O_4 Nanoparticles Through Ball Milling. *Solid State Communications*, 12:783-787, 2004.

110. A. Biswas, I.S. Bayer, A.S. Biris, T. Wang, E. Dervishi, and F. Faupel, Advances In Top–Down And Bottom–Up Surface Nanofabrication: Techniques, Applications and Future Prospects. *Advances In Colloid and Interface Science*, 1:2-27, 2012.

111. T. Sugimoto, *Fine Particles: Synthesis, Characterization, and Mechanisms of Growth*, Vol. 92 CRC Press, 2000.

112. B. Domènech, A. Alonso, D.N. Muraviev, J. Macanás, J. Bastos-Arrieta, and M. Muñoz, *Bifunctional Polymer-Metal Nanocomposite Ion Exchange Materials*: INTECH Open Access Publisher, 2012.

113. A.H. Lu, E.E.L. Salabas, and F. Schüth, Magnetic Nanoparticles: Synthesis, Protection, Functionalization, and Application. *Angewandte Chemie International Edition*, 8:1222-1244, 2007.

114. S. Laurent, D. Forge, M. Port, A. Roch, C. Robic, L. Vander Elst, and R.N. Muller, Magnetic Iron Oxide Nanoparticles: Synthesis, Stabilization, Vectorization, Physicochemical Characterizations, and Biological Applications. *Chemical Reviews*, 6:2064-2110, 2008.

115. L. Laconte, N. Nitin, and G. Bao, Magnetic Nanoparticle Probes. *Materials Today*, 5:32-38, 2005.

116. N. Wu, L. Fu, M. Su, M. Aslam, K.C. Wong, and V.P. Dravid, Interaction of Fatty Acid Monolayers With Cobalt Nanoparticles. *Nano Letters*, 2:383-386, 2004.

117. G. Kataby, M. Cojocaru, R. Prozorov, and A. Gedanken, Coating Carboxylic Acids On Amorphous Iron Nanoparticles. *Langmuir*, 5:1703-1708, 1999.

118. P. Velusamy, S. Chia-Hung, A. Shritama, G.V. Kumar, V. Jeyanthi, and K. Pandian, Synthesis of Oleic Acid Coated Iron Oxide Nanoparticles and Its Role In Anti-Biofilm Activity Against Clinical Isolates of Bacterial Pathogens. *Journal of The Taiwan Institute of Chemical Engineers*, 2015.

119. M. Faraji, Y. Yamini, and M. Rezaee, Magnetic Nanoparticles: Synthesis, Stabilization, Functionalization, Characterization, and Applications. *Journal of The Iranian Chemical Society*, 1:1-37, 2010.

120. C. Solans, P. Izquierdo, J. Nolla, N. Azemar, and M. Garcia-Celma, Nano-Emulsions. *Current Opinion In Colloid and Interface Science*, 3:102-110, 2005.

121. J. Vidal-Vidal, J. Rivas, and M. Lopez-Quintela, Synthesis of Monodisperse Maghemite Nanoparticles by The Microemulsion Method. *Colloids and Surfaces A: Physicochemical And Engineering Aspects*, 1:44-51, 2006.

122. S. Sun and H. Zeng, Size-Controlled Synthesis of Magnetite Nanoparticles. *Journal of The American Chemical Society*, 28:8204-8205, 2002.

123. S.G. Kwon, Y. Piao, J. Park, S. Angappane, Y. Jo, N.M. Hwang, J.G. Park, and T. Hyeon, Kinetics of Monodisperse Iron Oxide Nanocrystal Formation by "Heating-Up" Process. *Journal of The American Chemical Society*, 41:12571-12584, 2007.

124. M.V. Barbosa, L.O. Monteiro, G. Carneiro, A.R. Malagutti, J.M. Vilela, M.S. Andrade, M.C. Oliveira, A.D. Carvalho-Junior, and E.A. Leite, Experimental Design of A Liposomal Lipid System: A Potential Strategy For Paclitaxel-Based Breast Cancer Treatment. *Colloids and Surfaces B: Biointerfaces*:553-561, 2015.

125. A.K. Singla, A. Garg, and D. Aggarwal, Paclitaxel and Its Formulations. *International Journal of Pharmaceutics*, 1:179-192, 2002.

126. D. Wu, Y. Zheng, X. Hu, Z. Fan, and X. Jing, Anti-Tumor Activity of Folate Targeted Biodegradable Polymer–Paclitaxel Conjugate Micelles On EMT-6 Breast Cancer Model. *Materials Science and Engineering: C*:68-75, 2015.

127. R.J. Hamilton and P.A. Sewell, *Introduction To High Performance Liquid Chromatography*: Springer, 1982.

128. S.L. Flegler, J.W. Heckman, K.L. Klomparens, K.L. Klomparens, and K.L. Klomparens, *Scanning and Transmission Electron Microscopy: An Introduction*: WH Freeman New York, 1993.

129. F.M. Mirabella, *Internal Reflection Spectroscopy: Theory and Applications*, Vol. 15 CRC Press, 1992.

130. B.A. Miller-Chou and J.L. Koenig, A Review of Polymer Dissolution. *Progress In Polymer Science*, 8:1223-1270, 2003.

131. P. Vineeth, P. Vadaparthi, K. Kumar, B.D.J. Babu, A.V. Raoc, and K.S. Babu, Influence of Organic Solvents On Nanoparticle Formation and Surfactants On Release Behaviour In-Vitro Using Costunolide As Model Anticancer Agent.

132. A.V. Fuchs and G.D. Will, Photo-Initiated Miniemulsion Polymerization As A Route To The Synthesis of Gold Nanoparticle Encapsulated Latexes. *Polymer*, 10:2119-2124, 2010.

133. K. Landfester and M. Antonietti, The Polymerization of Acrylonitrile In Miniemulsions:"Crumpled Latex Particles" or Polymer Nanocrystals. *Macromolecular Rapid Communications*, 12:820-824, 2000.

134.   V.E. Diz, G. Leyva, R.D. Zysler, J. Awruch, and L.E. Dicelio, Photophysics of An Octasubstituted Zinc(II) Phthalocyanine Incorporated Into Solid Polymeric Magnetic and Non-Magnetic PLGA–PVA Nanoparticles. *Journal of Photochemistry and Photobiology A: Chemistry*:44-51, 2016.

135.   V. Chaturvedi and A. Kumar, Toxicity of Sodium Dodecyl Sulfate In Fishes and Animals. A Review. *Internatinal Journal of Applied Biolgy Pharmaceutical Technology*:630-633, 2010.

136.   M.M. Singer and R.S. Tjeerdema. Fate and Effects of The Surfactant Sodium Dodecyl Sulfate. In, *Reviews of Environmental Contamination and Toxicology*. Pages 95-149. Springer, 1993.

137.   M. Lindberg, B. Forslind, S. Sagström, and G. Roomans, Elemental Changes In Guinea Pig Epidermis At Repeated Exposure To Sodium Lauryl Sulfate. *Acta Dermato-Venereologica*, 6:428-431, 1992.

138.   M.D. Timmer, C.G. Ambrose, and A.G. Mikos, In Vitro Degradation of Polymeric Networks of Poly(Propylene Fumarate) and The Crosslinking Macromer Poly(Propylene Fumarate)-Diacrylate. *Biomaterials*, 4:571-577, 2003.

139.   C. Fonseca, S. Simoes, and R. Gaspar, Paclitaxel-Loaded PLGA Nanoparticles: Preparation, Physicochemical Characterization and In Vitro Anti-Tumoral Activity. *Journal of Controlled Release*, 2:273-286, 2002.

140.   E. Bernabeu, G. Helguera, M.J. Legaspi, L. Gonzalez, C. Hocht, C. Taira, and D.A. Chiappetta, Paclitaxel-Loaded PCL-TPGS Nanoparticles: In Vitro and In Vivo Performance Compared With Abraxane. *Colloids and Surfaces B: Biointerfaces*:43-50, 2014.

APPENDIX A: EXPERIMENTAL DATAS FOR CROSSLINKED POLYMER NANOPARTICLES

Table A.1 Average pH measurements for crosslinked polymer nanoparticles

Time (Day)	Without MNPs	With MNPs
0	7.17	6.84
1	5.66	6.37
2	5.00	5.47
3	4.85	4.82
5	4.69	4.26
7	4.62	4.06
14	4.56	4.01
21	4.54	4.00
28	4.53	3.99
35	4.53	3.99
42	4.53	3.99

Table A.2 Percentage of Weight Loss for crosslinked polymer nanoparticles

Time (Day)	Without MNPs (%)	With MNPs (%)
7	18.57	16.95
14	27.47	28.35
21	30.33	33.70
28	33.56	47.36
35	44.24	45.48
42	54.43	

Table A.3 Cumulative amount of the nonencapsulated paclitaxel from crosslinked polymer nanoparticles

	Cumulative amount of nonencapsulated paclitaxel (mg)
Supernatant	1.06
1. Washing	1.43
2. Washing	1.77
3. Washing	2.12

Table A.4 Cumulative amount of the released paclitaxel from crosslinked polymer
nanoparticles

Time (Day)	Cumulative amount of released paclitaxel (mg)
0	2.21
1	2.36
5	2.49
8	2.61
12	2.97
15	3.33
19	3.60
22	3.80
26	3.8
30	3.8

Table A.5 Cumulative amount of the nonencapsulated paclitaxel from crosslinked polymer
nanoparticles with MNPs

	Cumulative amount of nonencapsulated paclitaxel (mg)
Supernatant	0.90
1. Washing	1.30
2. Washing	1.61
3. Washing	1.92

Table A.6 Cumulative amount of the released paclitaxel from crosslinked polymer nanoparticles with MNPs

Time (Day)	Cumulative amount of released paclitaxel (mg)
0	2.17
1	2.39
5	2.59
8	2.8
12	3.19
15	3.62
19	3.78
22	3.98
26	3.98
30	3.98

APPENDIX B: PACLITAXEL SCAN FOR CROSSLINKED POLYMER NANOPARTICLES
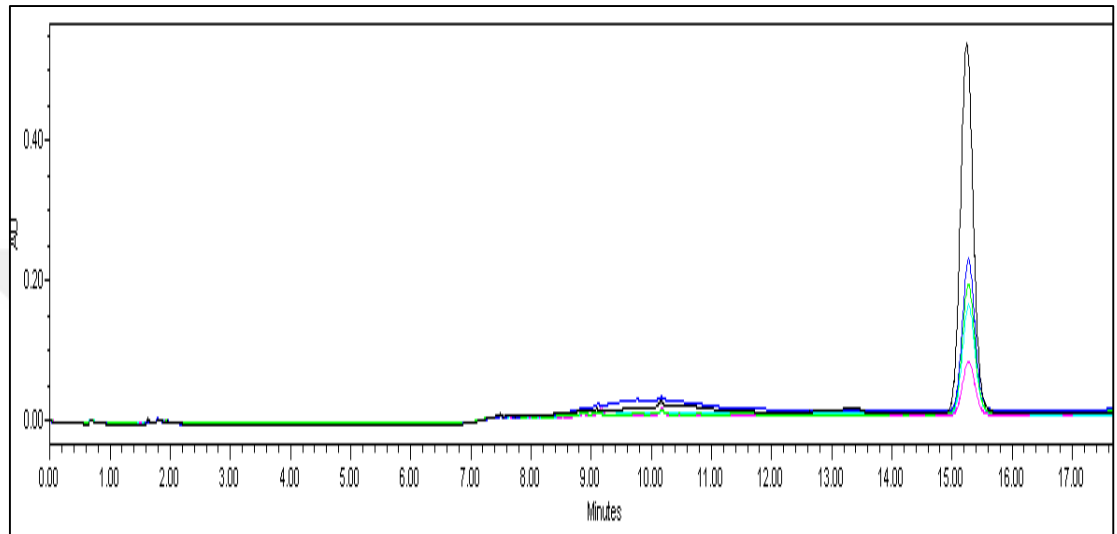
Figure B.1 Standard curve of Paxlitaxel
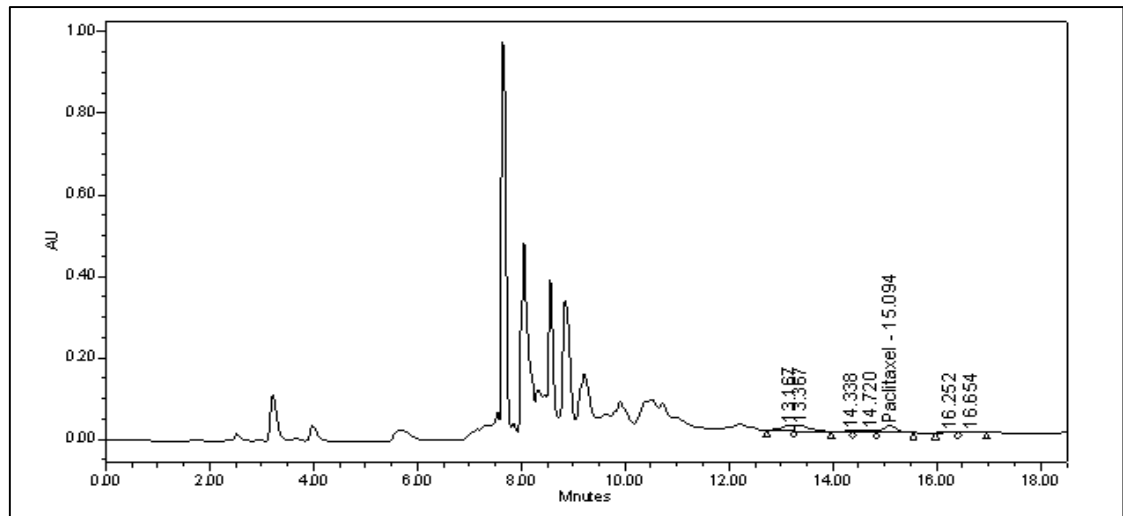
Figure B.2 Paclitaxel scan Suparnatant for crosslinked polymer nanoparticles without MNPs
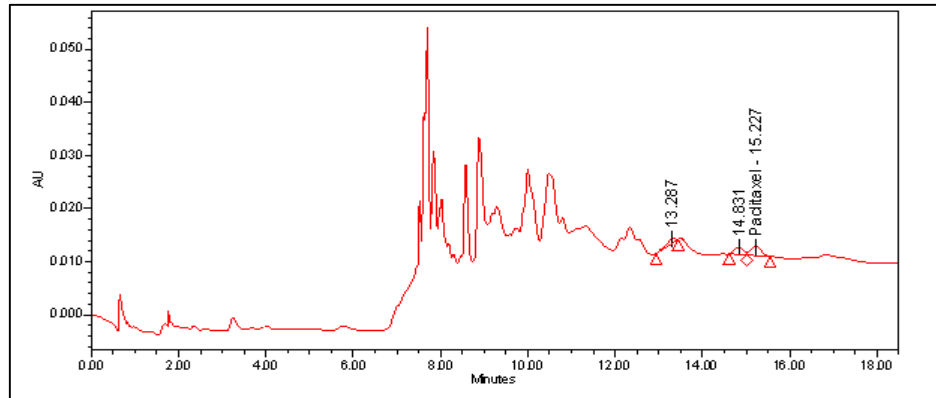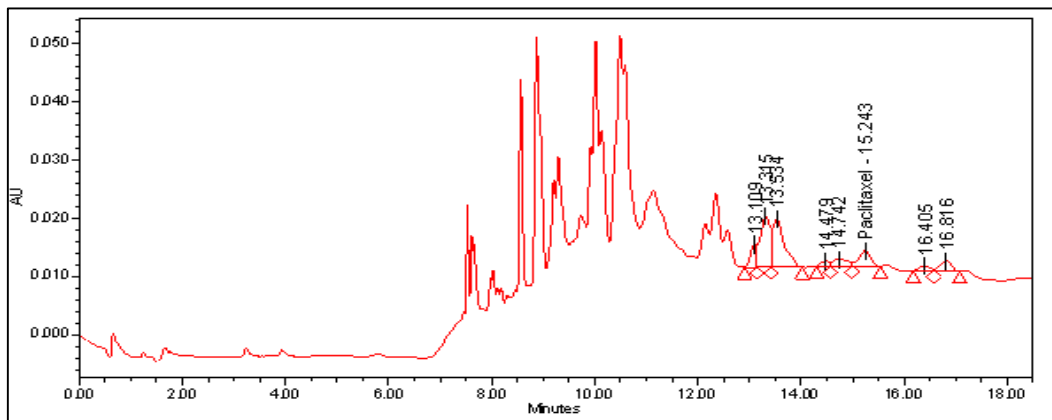
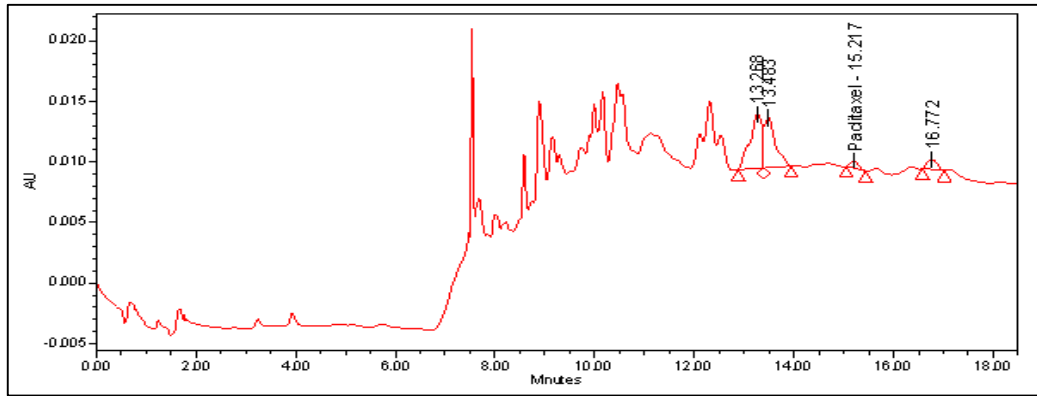Figure B.3 Paclitaxel scan first washing for crosslinked polymer nanoparticles without MNPs
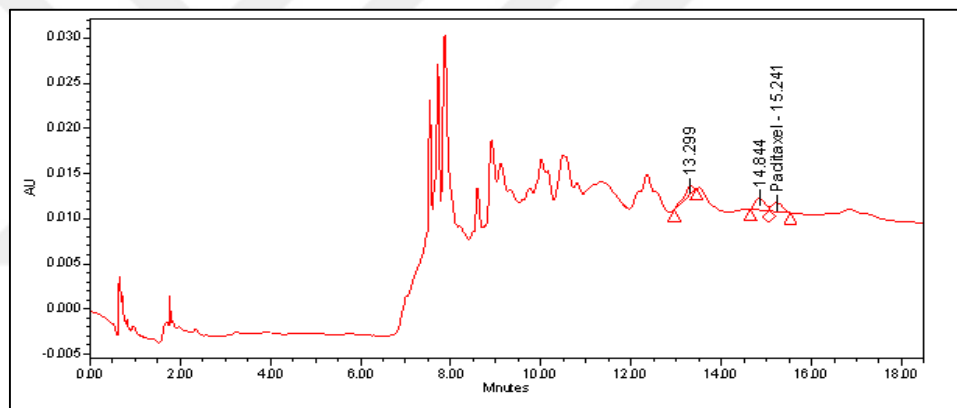
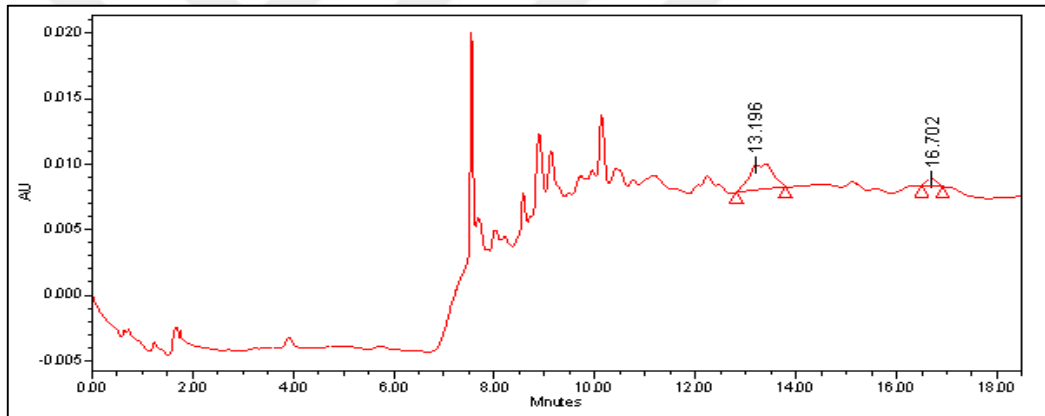Figure B.4 Paclitaxel scan second washing for crosslinked polymer nanoparticles without MNPs
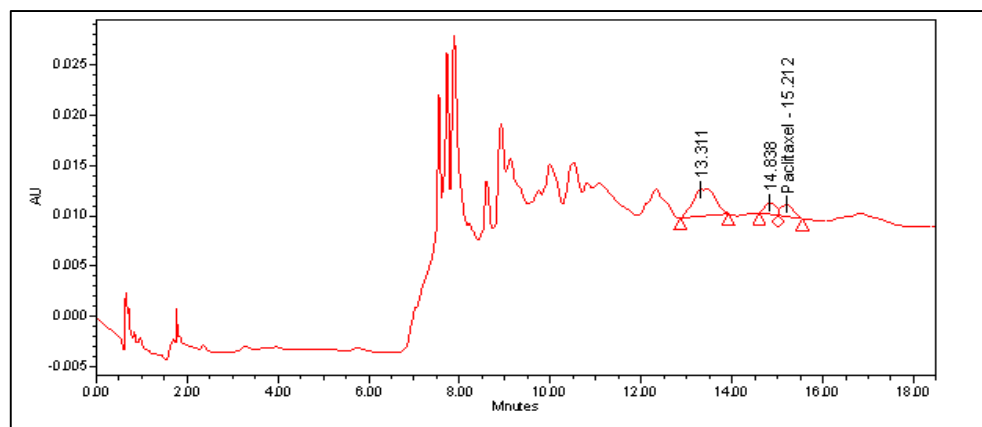
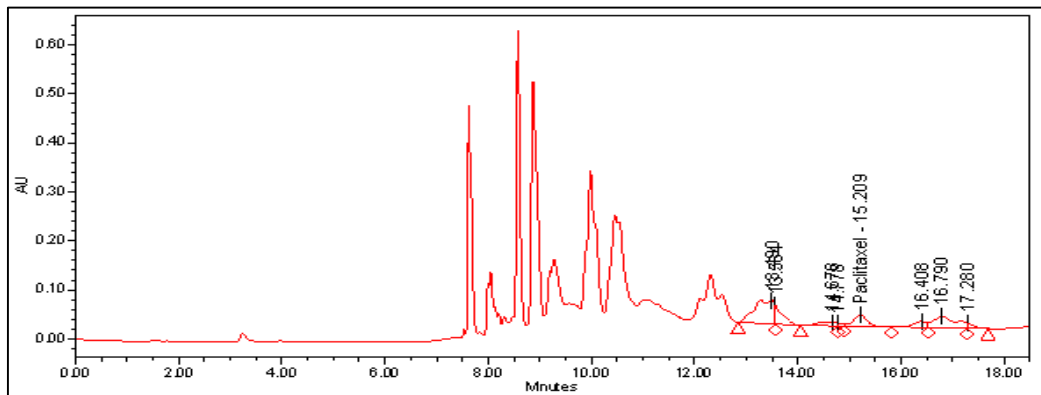Figure B.5 Paclitaxel scan third washing for crosslinked polymer nanoparticles without MNPs
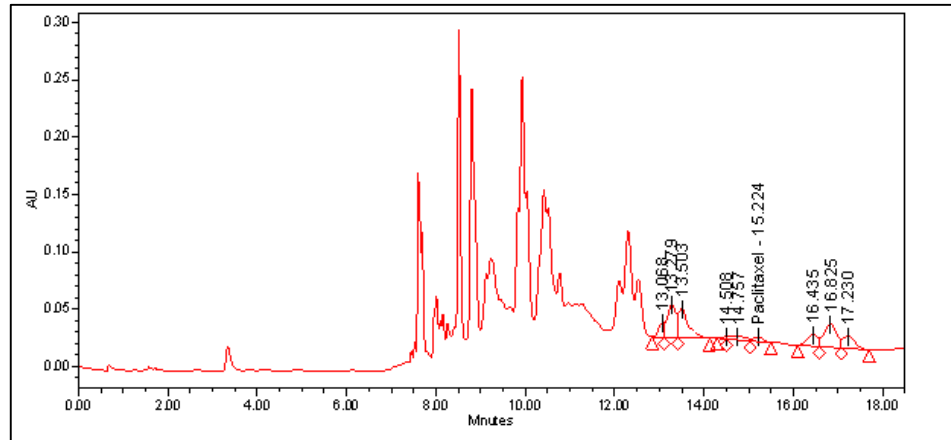
Figure B.6 Paclitaxel scan t:0 for crosslinked polymer nanoparticles without MNPs
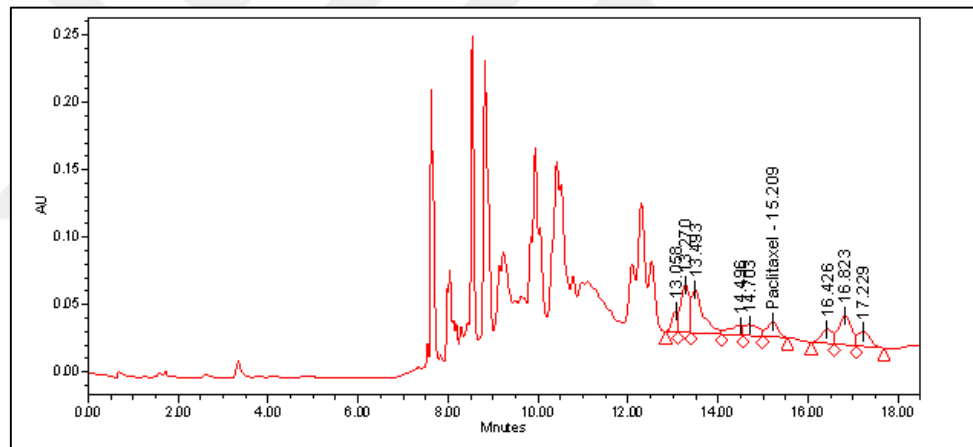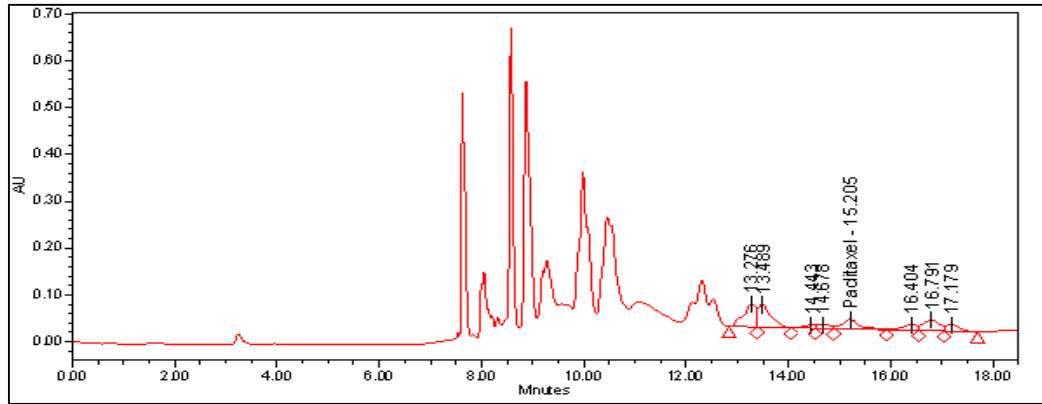

Figure B.7 Paclitaxel scan 1. Day for crosslinked polymer nanoparticles without MNPs
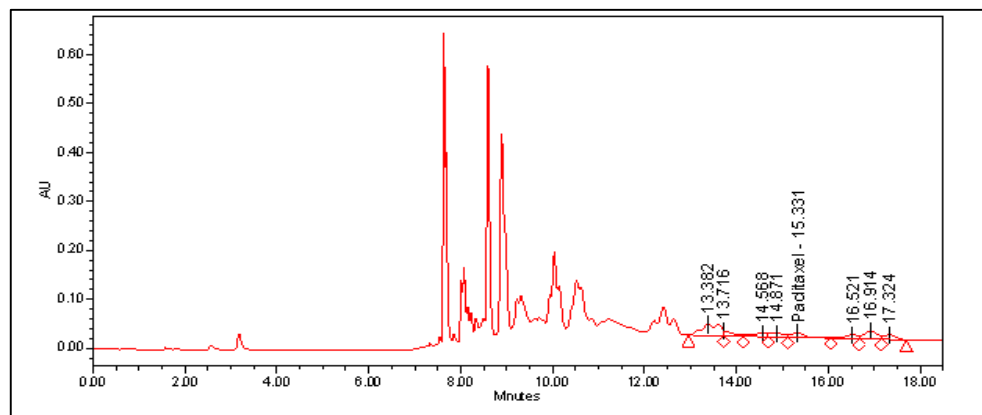
Figure B.8 Paclitaxel scan 5. Day for crosslinked polymer nanoparticles without MNPs
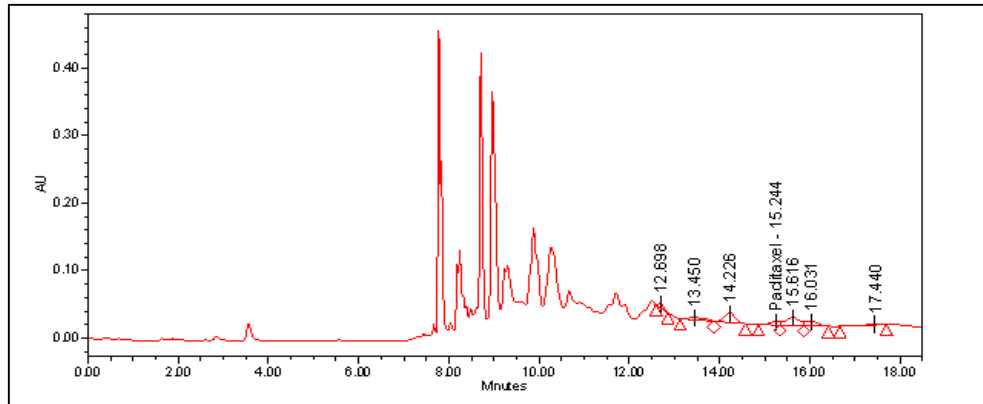
Figure B.9 Paclitaxel scan 8. Day for crosslinked polymer nanoparticles without MNPs
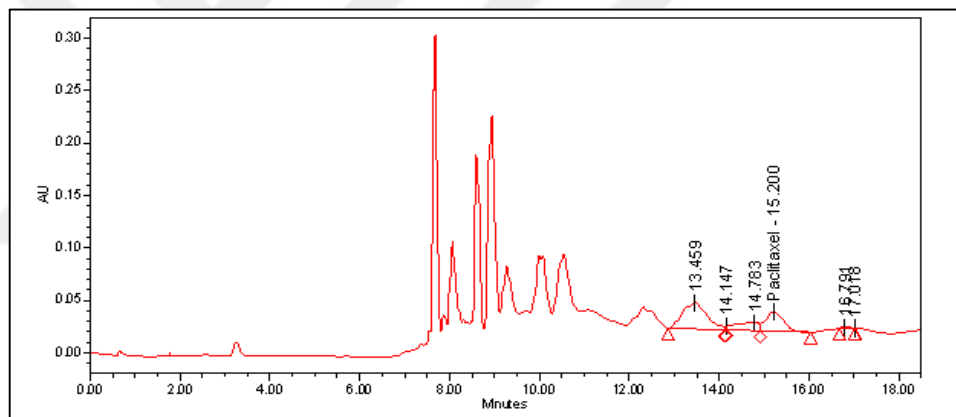
Figure B.10 Paclitaxel scan 12. Day for crosslinked polymer nanoparticles without MNPs
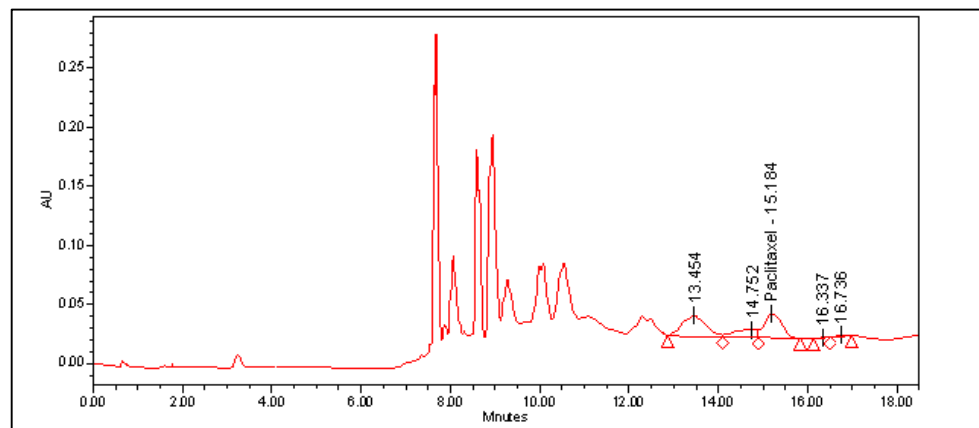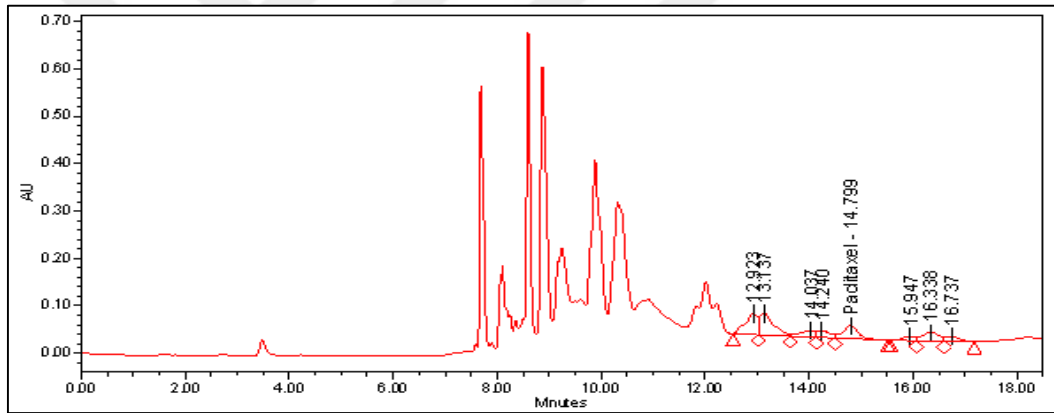

Figure B.11 Paclitaxel scan 15. Day for crosslinked polymer nanoparticles without MNPs
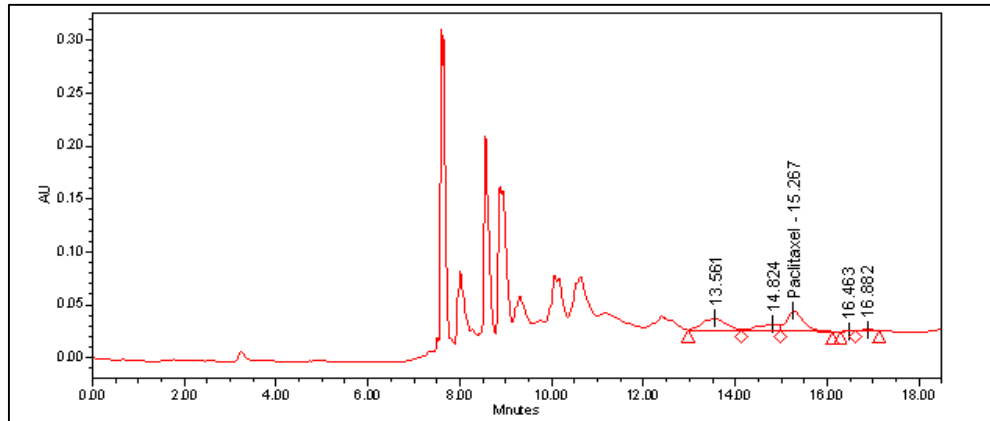
Figure B.12 Paclitaxel scan 19. Day for crosslinked polymer nanoparticles without MNPs
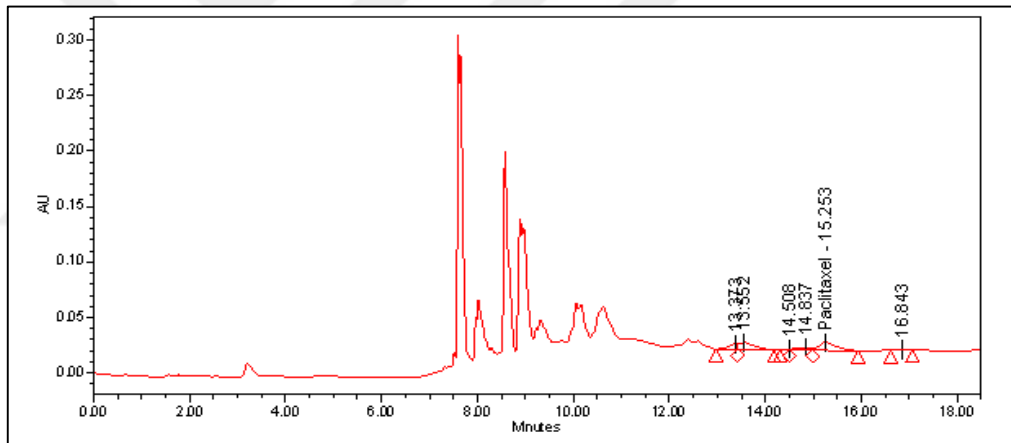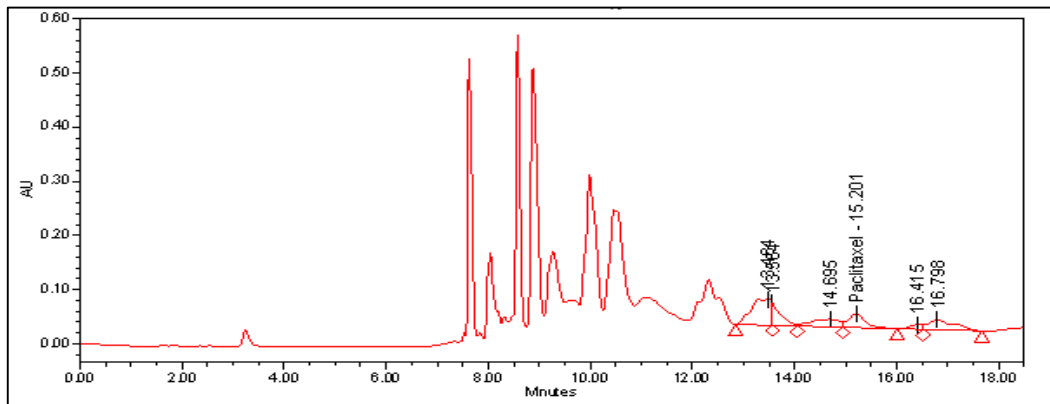

Figure B.13 Paclitaxel scan 22. Day for crosslinked polymer nanoparticles without MNPs
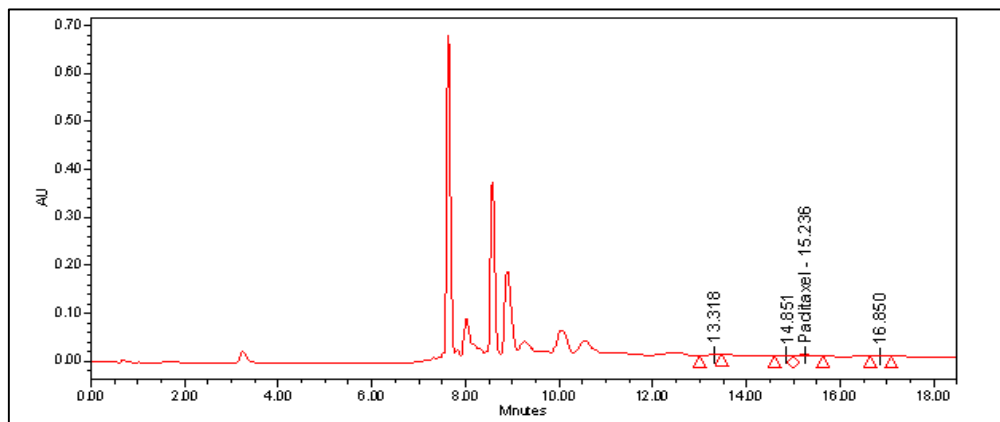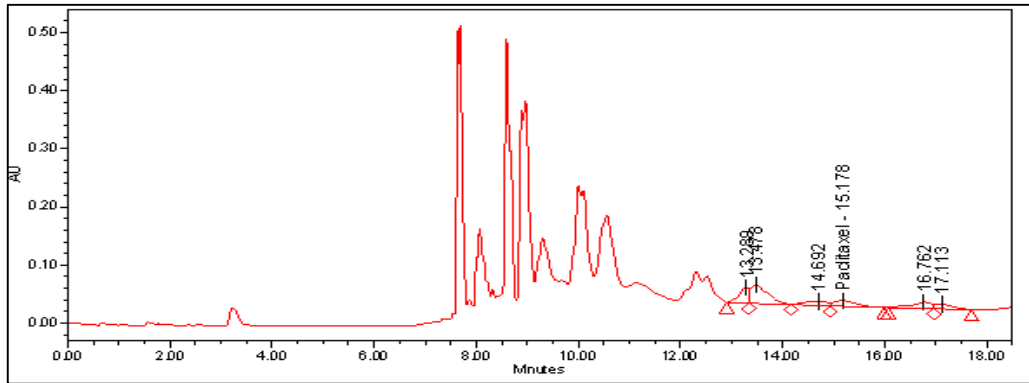

Figure B.14 Paclitaxel scan 26. Day for crosslinked polymer nanoparticles without MNPs
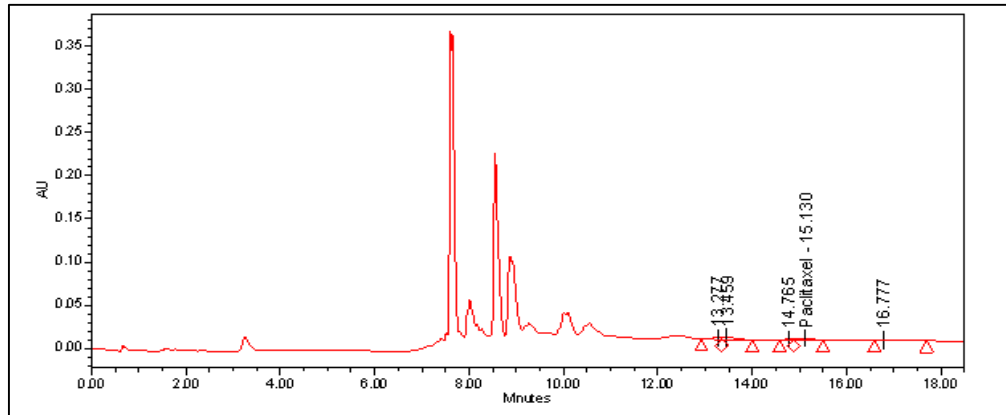
Figure B.15 Paclitaxel scan 30. Day for crosslinked polymer nanoparticles without MNPs
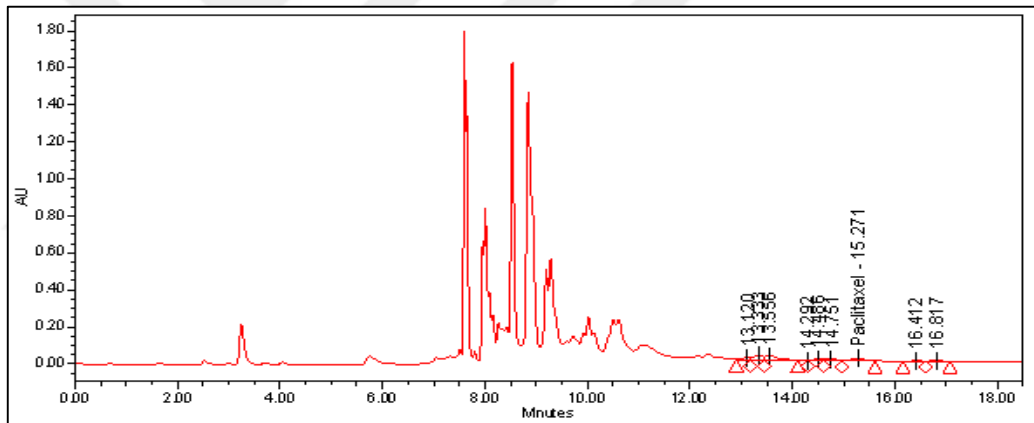
Figure B.16 Paclitaxel scan Suparnatant for crosslinked polymer nanoparticles with MNPs

Figure B.17 Paclitaxel scan first washing for crosslinked polymer nanoparticles with MNPs

Figure B.18 Paclitaxel scan second washing for crosslinked polymer nanoparticles with MNPs

Figure B.19 Paclitaxel scan third washing for crosslinked polymer nanoparticles with MNPs

Figure B.20 Paclitaxel scan t:0 for crosslinked polymer nanoparticles with MNPs

Figure B.21 Paclitaxel scan 1. Day for crosslinked polymer nanoparticles with MNPs

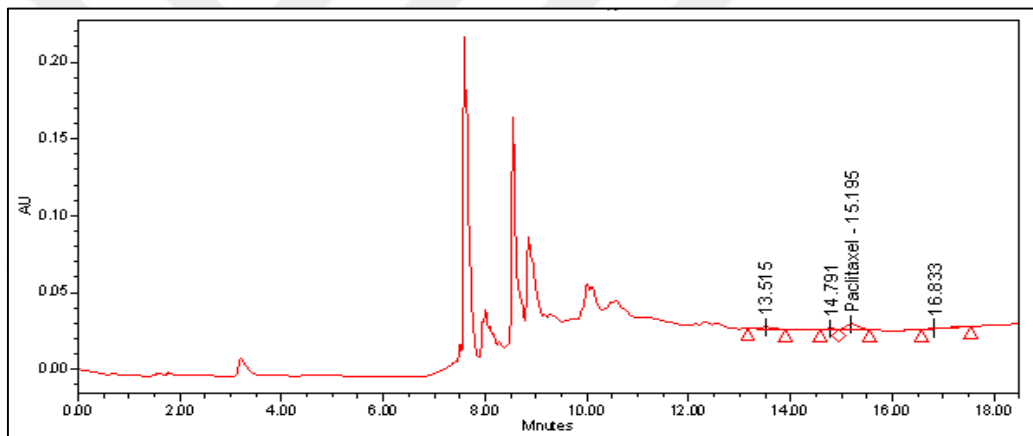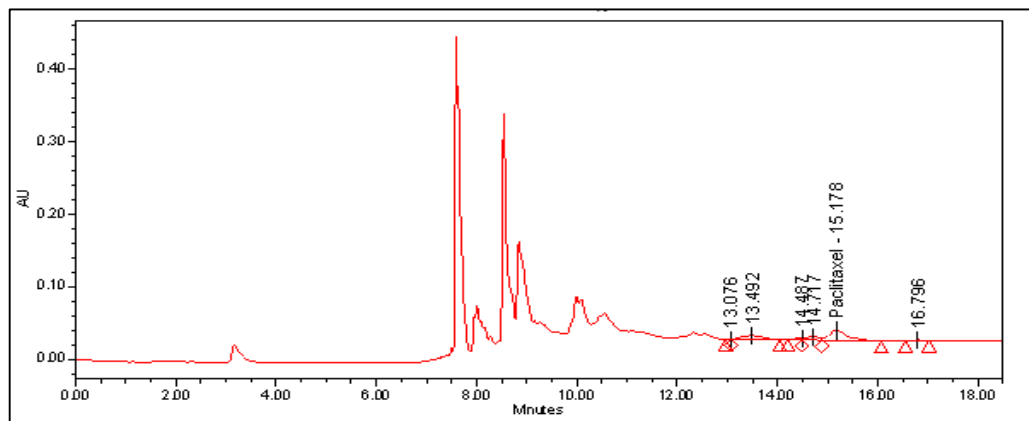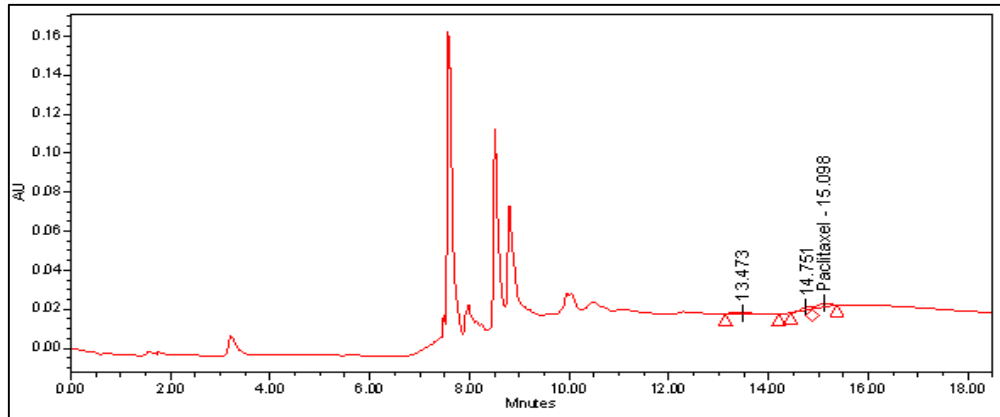Figure B.22 Paclitaxel scan 5. Day for crosslinked polymer nanoparticles with MNPs

Figure B.23 Paclitaxel scan 8. Day for crosslinked polymer nanoparticles with MNPs

Figure B.24 Paclitaxel scan 12. Day for crosslinked polymer nanoparticles with MNPs

Figure B.25 Paclitaxel scan 15. Day for crosslinked polymer nanoparticles with MNPs

Figure B.26 Paclitaxel scan 19. Day for crosslinked polymer nanoparticles with MNPs

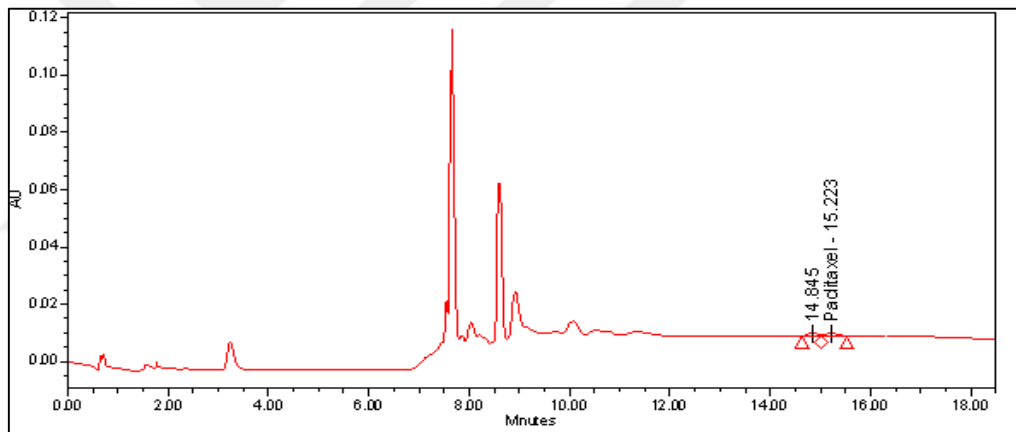Figure B.27 Paclitaxel scan 22. Day for crosslinked polymer nanoparticles with MNPs

Figure B.28 Paclitaxel scan 26. Day for crosslinked polymer nanoparticles with MNPs
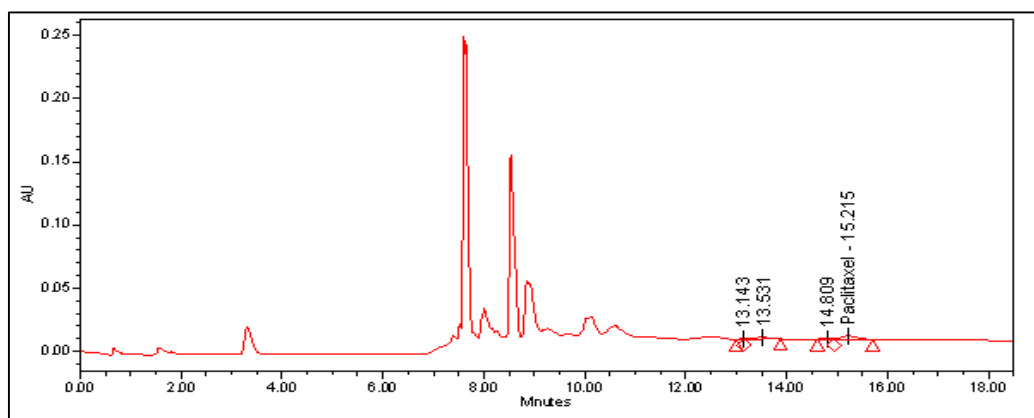

Figure B.29 Paclitaxel scan 30. Day for crosslinked polymer nanoparticles with MNPs